Universitat Politècnica de Catalunya, Barcelona, 15 – 19 April 2013

Numerical Simulation of Fast Transient Phenomena in Fluid-Structure Systems

A Short Course by F. Casadei
Retired from European Commission, Joint Research Centre
Institute for the Protection and Security of the Citizen
T.P. 480, I-21027 Ispra (VA), Italy.
E-mail: casadeifolco@gmail.com

1

Contents

2

Detailed contents (1/2)

- ALE description for structures
- Lagrangian contact:
  - Classical methods
  - Pinballs
  - SPH (for fluid-like materials)
- Meshless methods:
  - SPH for structures
  - DEM

3

Detailed contents (2/2)

- Spectral elements
- Spatial time step partitioning
- Domain decomposition
- Mesh adaptivity:
  - Application to solids
  - Application to fluids
  - FSI

4

ALE description of structures

Donea, Huerta, Casadei (early 1990s)

- Extend ALE formulation to materials with memory, namely, non-linear path-dependent materials

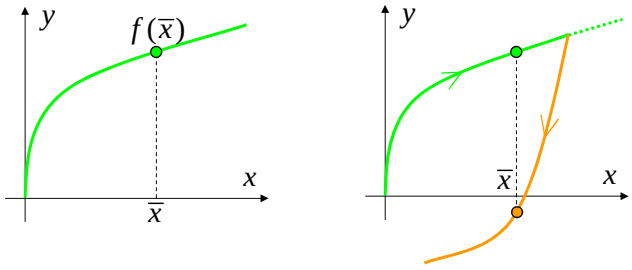

No memory Memory

5

ALE description of structures (2)

- Major extra difficulty w/r to Newtonian fluids: necessity to transport stresses and stress-related quantities across inter-element boundaries. Fields are usually discontinuous and evaluated only at Gauss Points
- Previous attempts had used implicit interpolation techniques: too expensive in the present explicit fast transient context
- Two distinct strategies, borrowed from the fluid dynamic experience: a) a Lax-Wendroff scheme based on nodal averaging and smoothing of the stress gradients, and b) a Godunov scheme inspired by methods often used for conservation laws in finite volumes
- Both techniques implemented in 2D quadrilateral finite elements using single-point as well as multiple-point spatial numerical integration

6

ALE description of structures (3)

- When ALE is applied to nonlinear path-dependent materials, three conservation equations basically similar to Euler equations are obtained and therefore the same techniques (time integration strategy, rezoning algorithms, treatment of boundary conditions, etc.) developed for the fluids can be directly applied, with the important exception, however, of the stress transport algorithm

- Time integration is achieved by same fractional step strategy seen above for fluids: 1) Lagrangian phase, in which it is assumed that the mesh follows the material particles and transport terms vanish; 2) Convective flux calculation (transport terms only)

- The time integration procedure still remains completely explicit and only an extra loop over the elements to deal with transport is required at each time step, compared with the Lagrangian case

7

Example 1 – Taylor bar impact

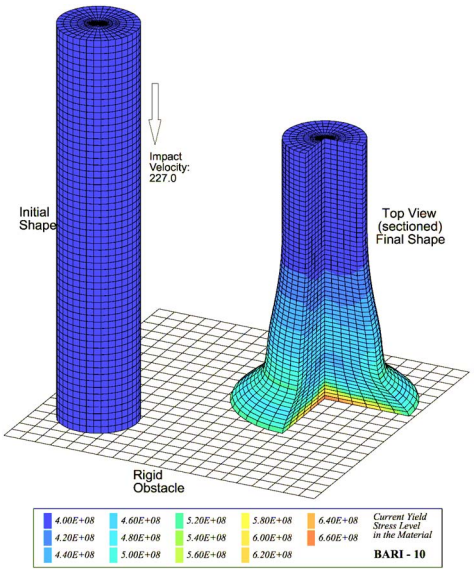

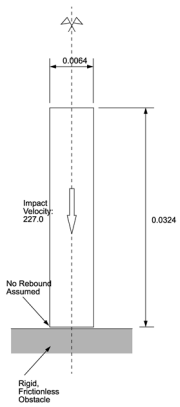

Material Data	
Density	8930
Young's Modulus	1.17×10^{11}
Yield Stress	4.0×10^{8}
Plastic Modulus	1.0×10^{8}
Poisson's Ratio	0.35

8

Example 1 – Taylor bar impact (2)

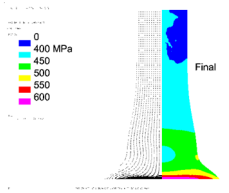

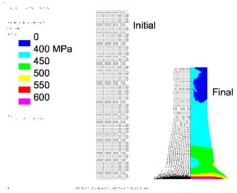

Reference solution: Lagrangian, 12 x 120 quadratic elements

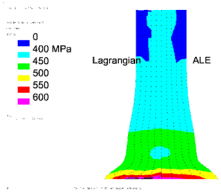

Comparison Lagrangian/ALE, 5 x 50 linear elements

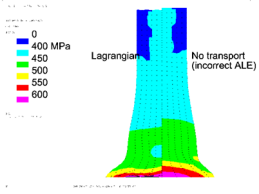

Effect of transport terms

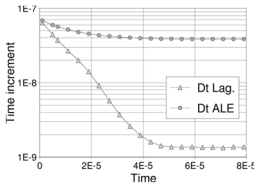

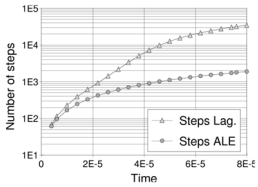

Formulation effects on time increment

9

Example 1 – Taylor bar impact (3)

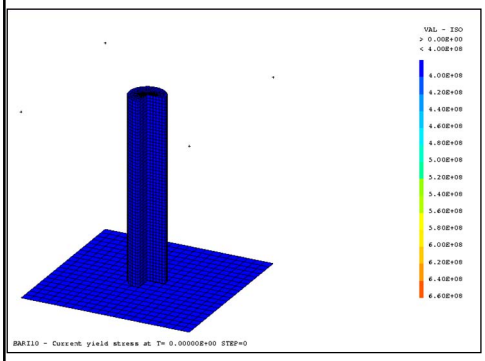

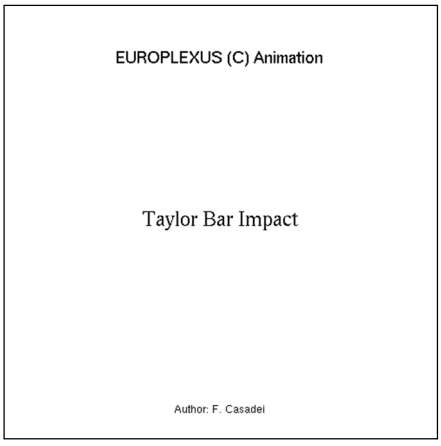

BARI10: ALE solution, 6 x 60 linear elements, Lax-Wendroff stress transport

10

Example 2 – Bar pulling

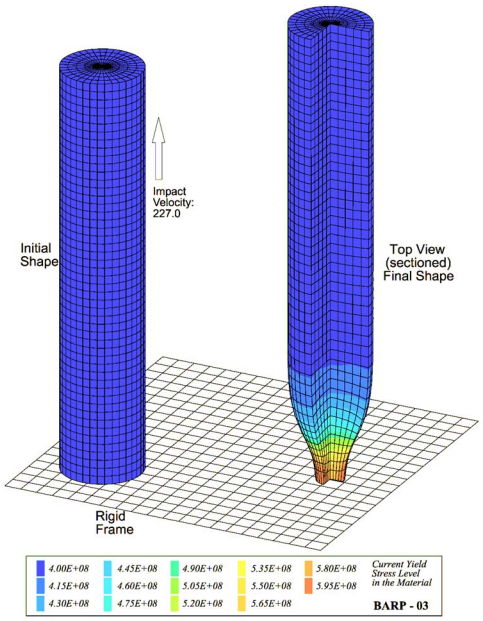

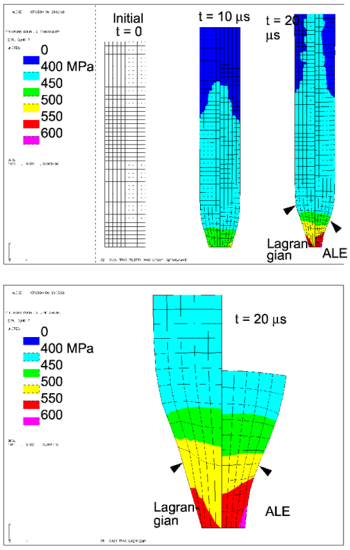

Comparison Lagrangian/ALE, 5 x 50 linear elements

11

Example 3 – Coining

Material Data	
Density	8930
Young's Modulus	$2.\times10^{11}$
Yield Stress	2.5×10^{8}
Plastic Modulus	$1.\times10^{9}$
Poisson's Ratio	0.3

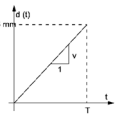

Punching Time T [ms]	Punching Velocity v [m/s]
40.00	0.15
2.00	3.00
0.10	60.00
0.02	300.00

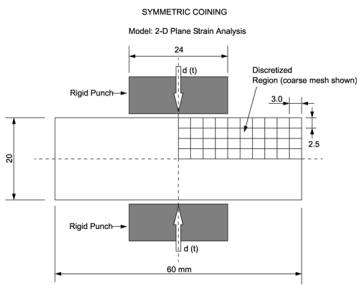

Bilateral, Plane strain

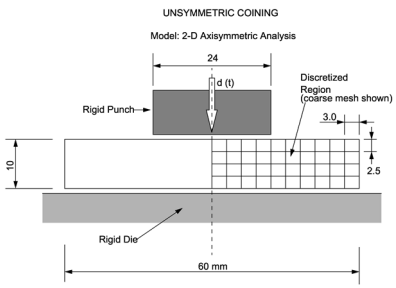

Unilateral, Axisymmetric

12

Example 3 – Coining (2)

Influence of punch velocity:

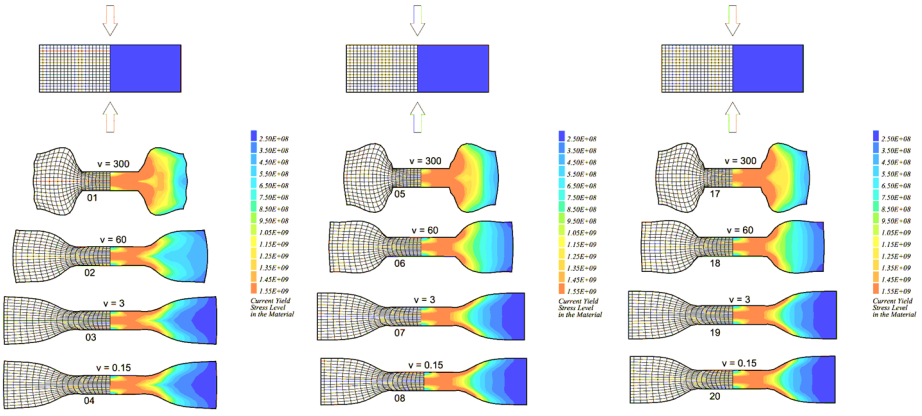

Lax-Wendroff
2 x 2

Godunov "B"
2 x 2

Godunov "A"
2 x 2

13

Example 3 – Coining (3)

Influence of punch velocity:

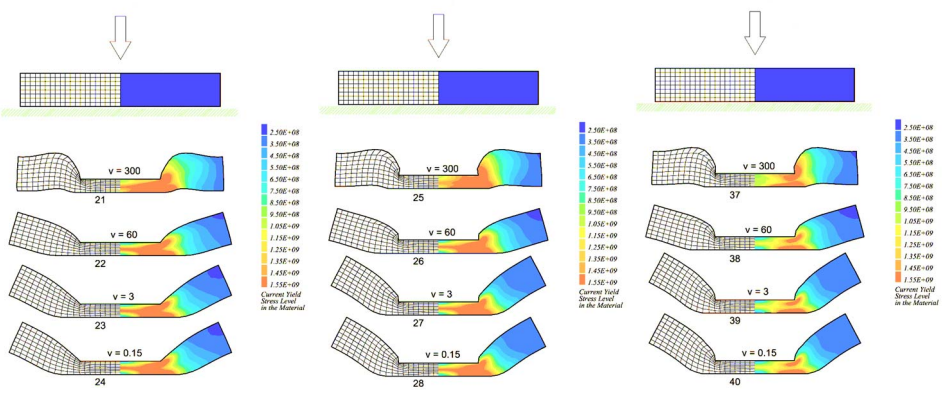

Lax-Wendroff
2 x 2

Godunov "B"
2 x 2

Godunov "A"
2 x 2

14

Example 3 – Coining (4)

Initial:

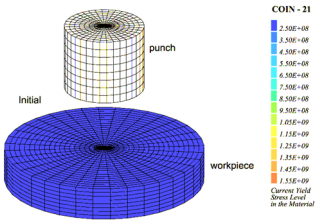

Unilateral, 2 x 2

L-W, v = 300

Final:

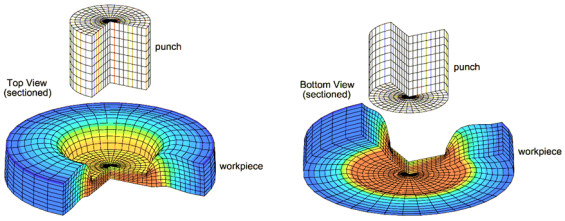

15

Example 3 – Coining (5)

Bilateral, 2 x 2

GDV "B", v = 300

Bilateral,
Plane strain (**COIN05**)

Unilateral, 2 x 2

GDV "B", v = 300

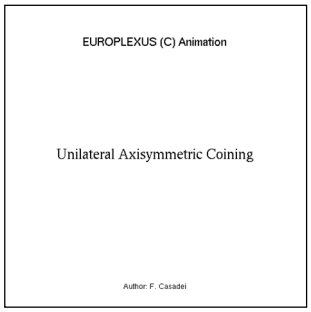

Unilateral,
Axisymmetric (**COIN25**)

16

Lagrangian contact

- Non-permanent FSI

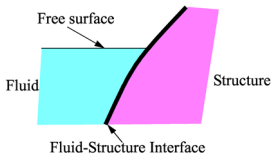

- Contact-impact between solids

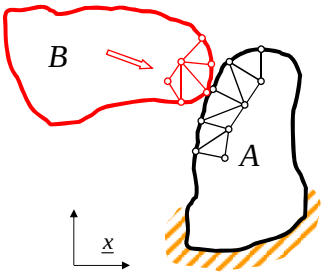

17

A contact-impact example (crash)

18

Example : tube crash

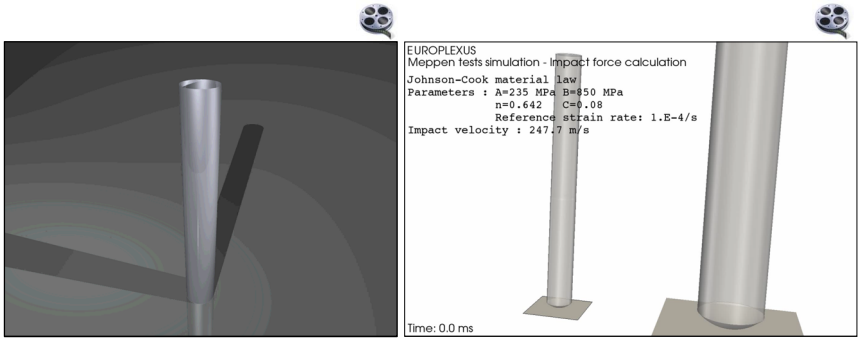

19

Example : container drop

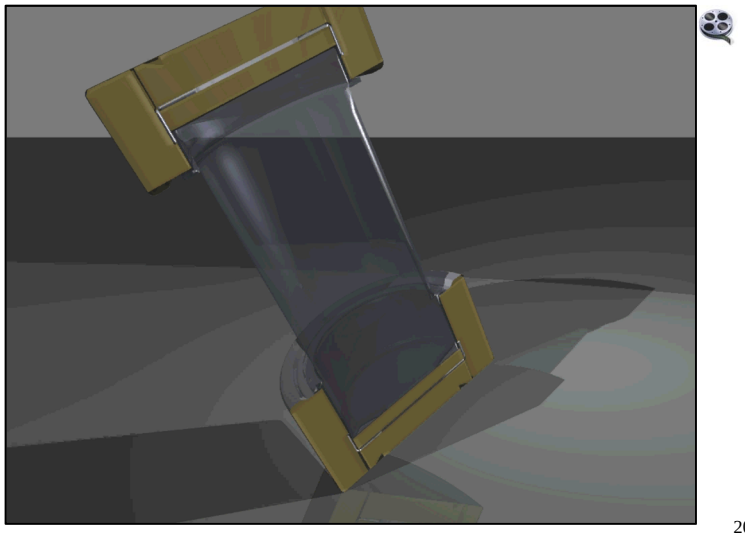

20

Contact-Impact Classification

- Slow, e.g. metal forming
  - Slow loading, smooth contact, friction
- Fast, e.g. impact or crash test
  - Fast loading, friction not too important
  - Large deformations, but typically no fragments
- Very fast, e.g. perforation
  - Complete failure, fragmentation

21

Examples of “Slow” Transient Contact

- A - Deep drawing of an elasto-plastic strip (no friction)

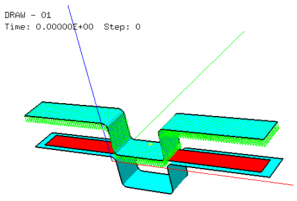

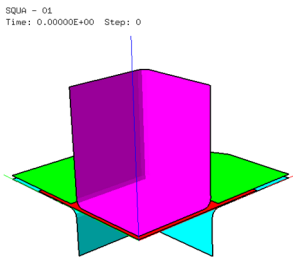

- B - Deep drawing of a square box (with friction)

22

Example 6a – Deep drawing A

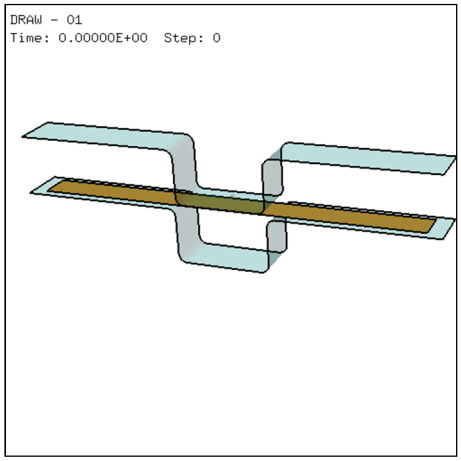

Deformation

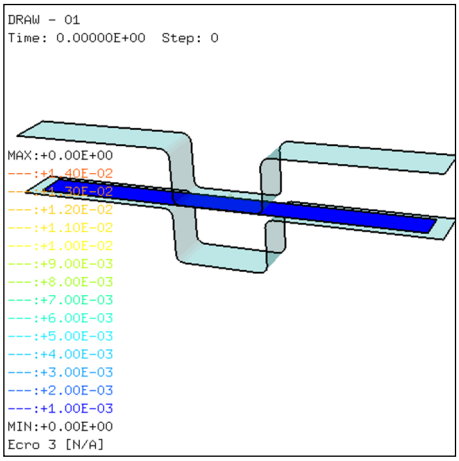

Plastic strain

23

Example 6a – Deep drawing A (2)

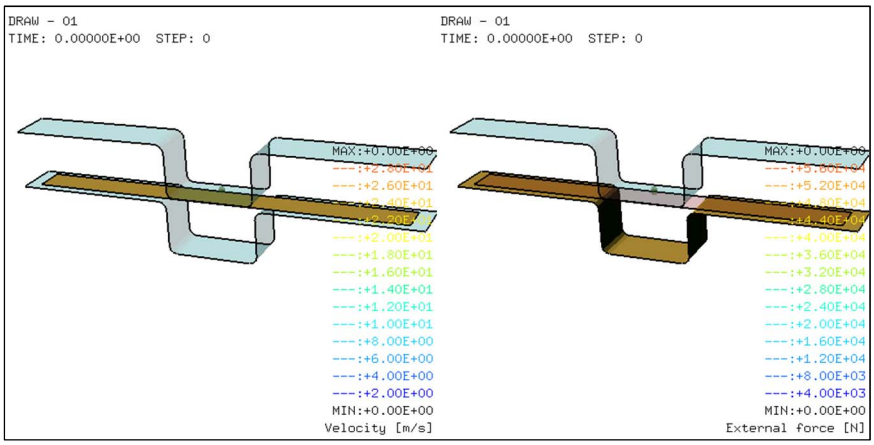

Velocities

Force on the die

24

Example 6b – Deep drawing B

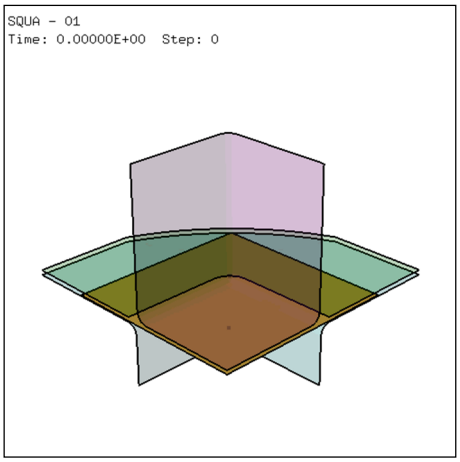

Deformation

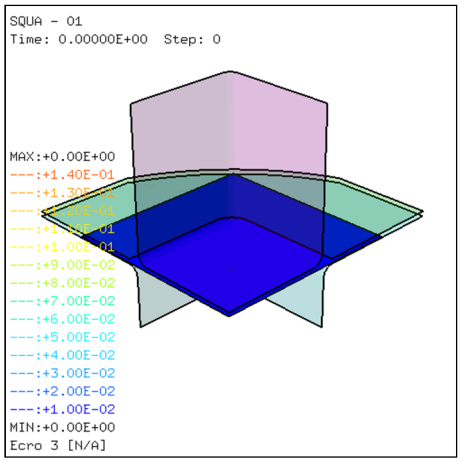

Plastic strain

25

Examples of Fast Transient Impact

- Crash of a metallic tube (self-contact)
  [Courtesy of CEA]

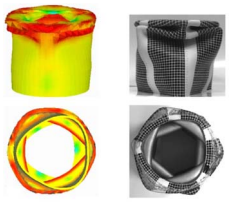

- Bird strike on jet fan by the SPH method
  [Courtesy of Snecma/CEA]

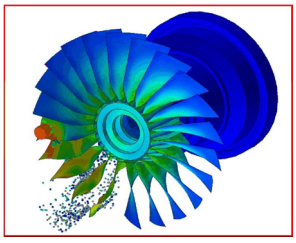

26

Tube Crash [Courtesy of CEA]

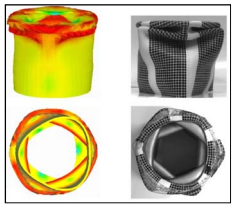

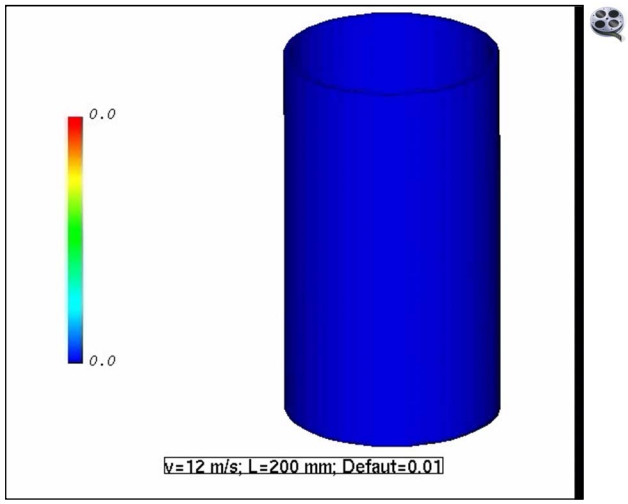

27

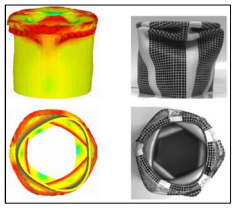

Tube Crash (2)

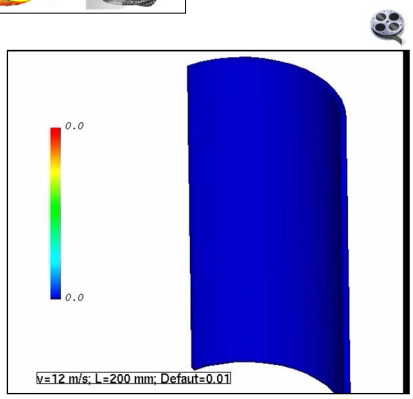

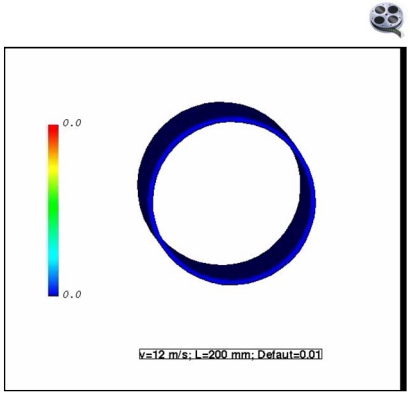

28

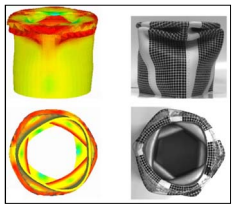

Tube Crash (3)

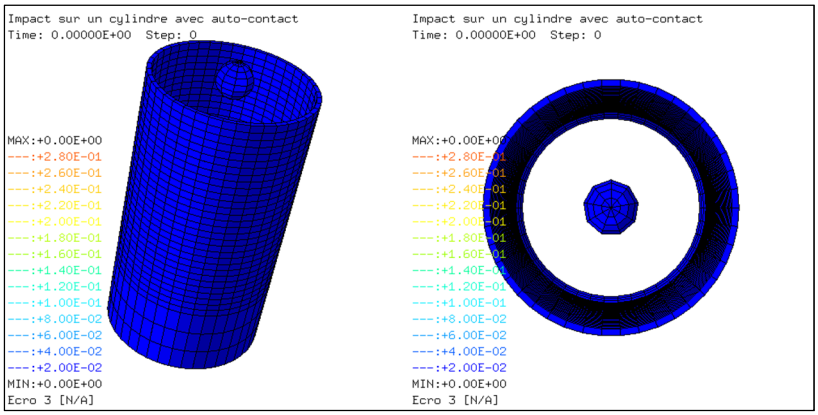

Plastic strain

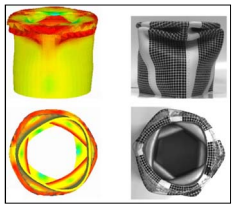

Tube Crash (4)

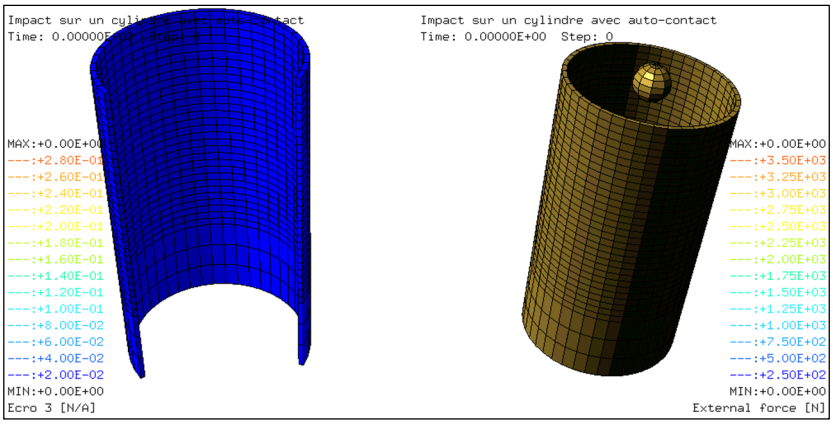

Plastic strain *External forces*

Conventional contact-impact methods

- Slide-line (2D) or slide-surface (3D) [Hallquist, Benson, mid-'80s]
  - "Slave" nodes
  - "Master" surfaces
  - Contact detected as node-through-surface penetration

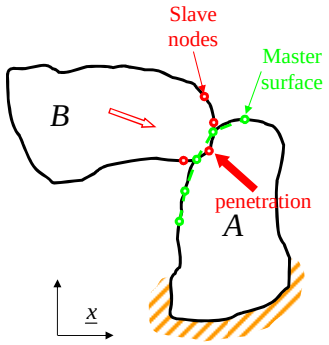

31

Components of Contact-Impact Methods

Contact-impact algorithms usually consist of two main components:

- Contact detection module, e.g. penetration detector (~heavy geometrical computations)
- Contact enforcement technique, e.g. penalty, Lagrange multipliers, …

32

Some Drawbacks of Conventional Techniques

- Lack of symmetry (master/slave)
- Geometrically complex (contact detection)
- Complicated input data
- Ambiguous contact cases:

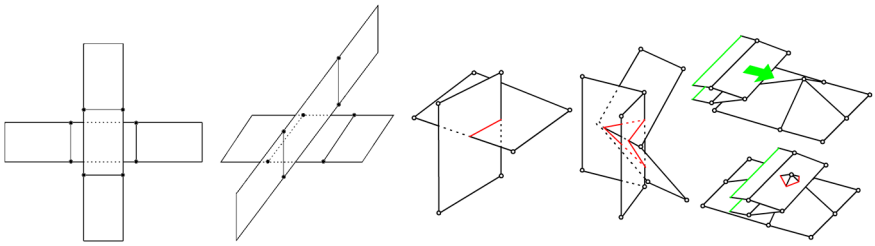

Surface-to-surface Edge-to-surface Edge-to-edge …

33

The Basic Pinball Method

[Belytschko & Neal, 1991]

- Embed a sphere (pinball) in each element

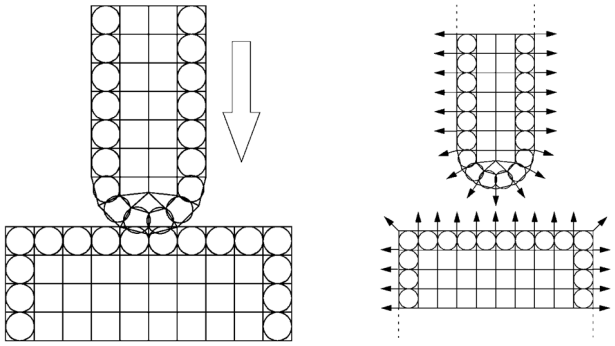

34

The Basic Pinball Method (2)

- Contact occurs between elements when:

$$d_{12} < (R_1 + R_2)$$

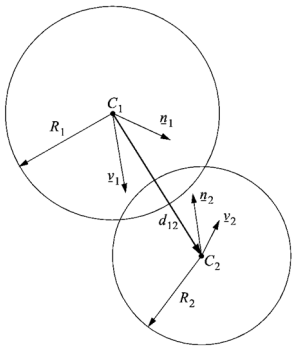

35

Shortcomings

- Slender or distorted continuum elements

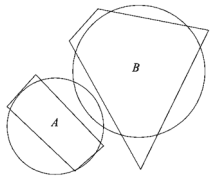

- Zero-thickness beam/shell elements

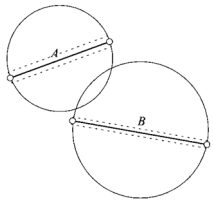

36

The Hierarchic Pinball Method

[Belytschko & Yeh, 1993]

- Embed a parent pinball in each element
- Recursively generate descendent pinballs as long as contact holds

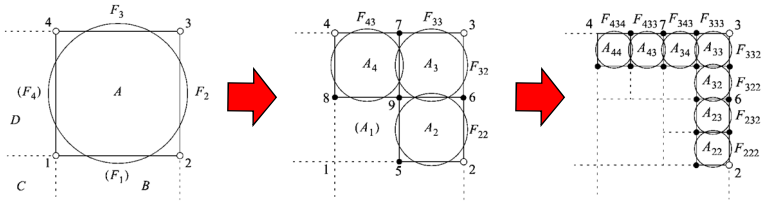

Level 0 (parent) Level 1 Level 2

37

Hierarchic Pinball Method (2)

- Hierarchy stops when:
  - Continuum: min size or max level is reached
  - Shells: size equals physical element thickness

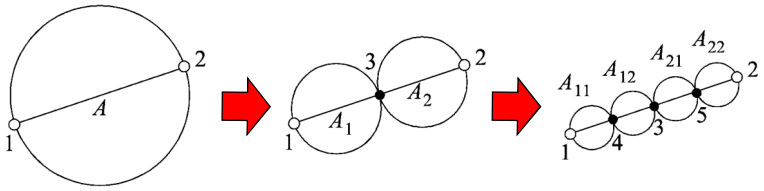

Level 0 (parent) Level 1 Level 2

38

Contact Force Computation

- Constraints on velocities:

$$\mathbf{v}_A \cdot \hat{\mathbf{n}} - \mathbf{v}_B \cdot \hat{\mathbf{n}} \leq 0$$

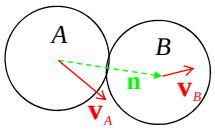

- By expanding the velocities:

$$\left[\sum_{i=1}^{n_A} N_{Ai}(A)\mathbf{v}_{Ai}\right]\cdot\hat{\mathbf{n}} - \left[\sum_{i=1}^{n_B} N_{Bi}(B)\mathbf{v}_{Bi}\right]\cdot\hat{\mathbf{n}} \leq 0$$

- These inequalities are of the generic form:

$$\boxed{\mathbf{Cv} \leq \mathbf{b}}$$

39

Example – Bar impact

- (See Part 1)

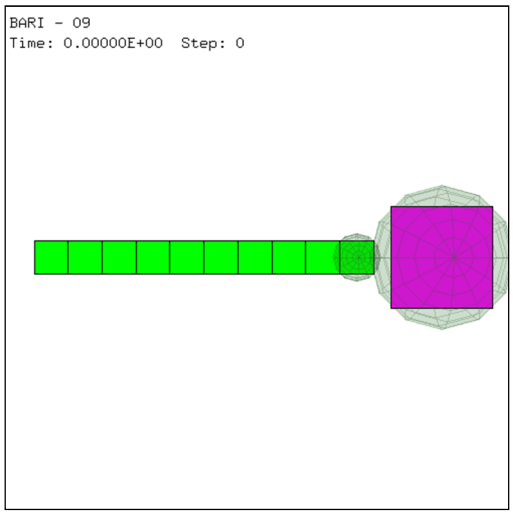

40

Example 7 – Cable impact

- A cable is fixed at one end and has a concentrated mass at the other end. The mass has an initial velocity. In its motion, the cable impacts on a second cable fixed at both extremities.
- Cables have <u>no resistance to bending or compression</u> (only to traction).

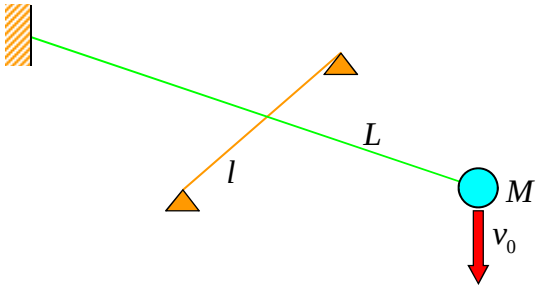

$L = 10$
$l = 2$
$M = 100$
$v_0 = -100$

41

Example 7 – Cable impact (2)

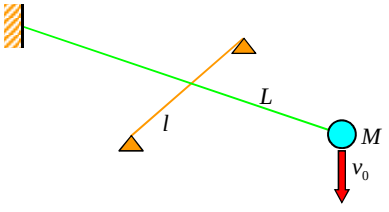

WRAP06

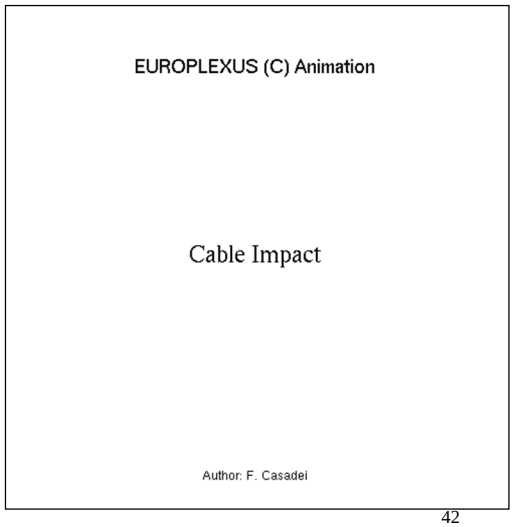

42

Example 7b – Indentation

- A rigid spherical indenter is pushed at constant speed of 10 m/s into a ductile block of material

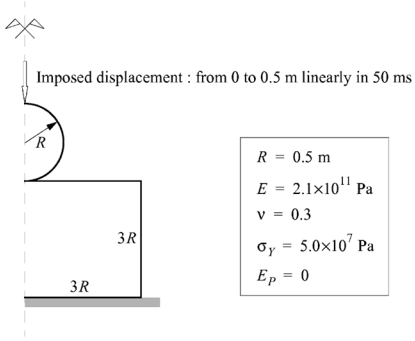

- Compute the indentation force as a function of displacement
  - 2D axisymmetric solution
  - 3D solution(s)

43

Example 7b – Indentation (2)

- 2D axisymmetric solution:

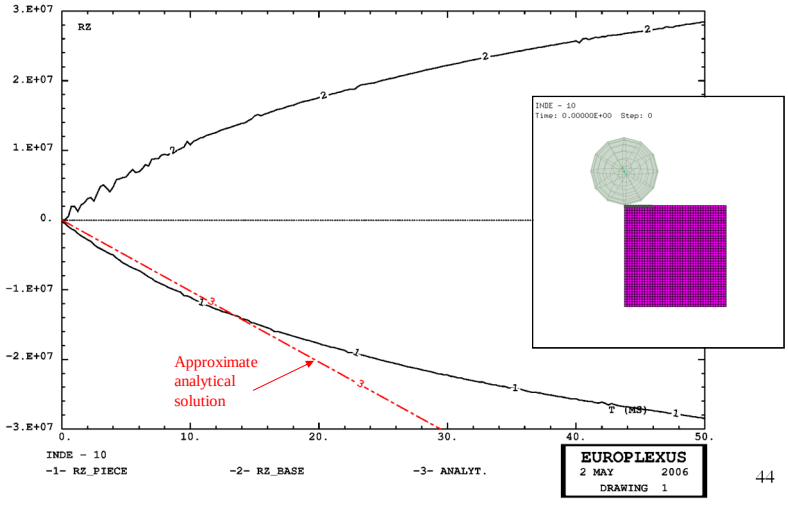

44

Example 7b – Indentation (3)

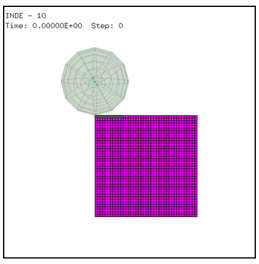

- 2D axisymmetric solution:

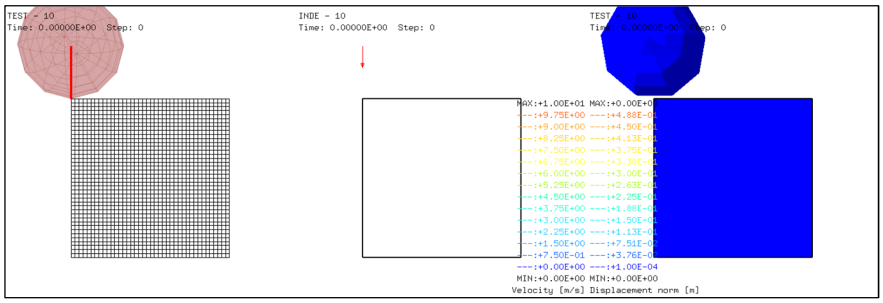

Contact and deformations | Velocities | Displacement norm

45

Example 7b – Indentation (4)

- 3D hexahedra-only solution:

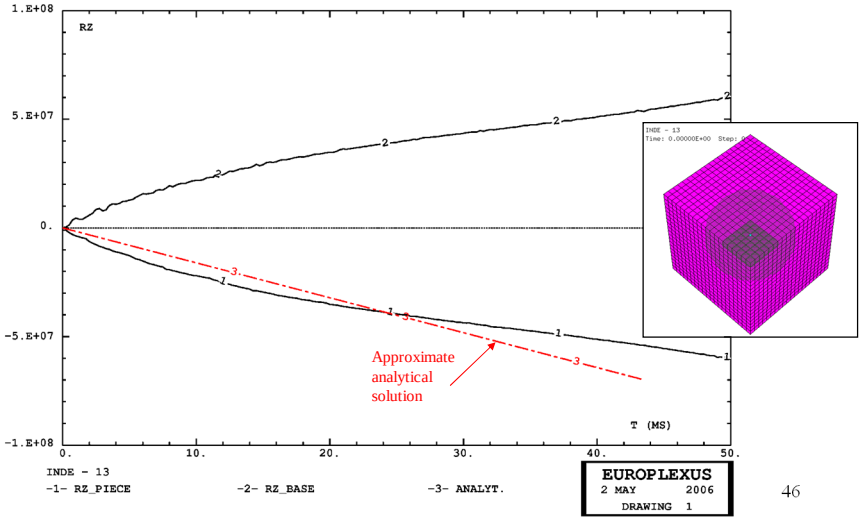

46

Example 7b – Indentation (5)

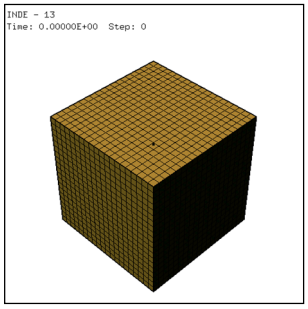

- 3D hexahedra-only solution:

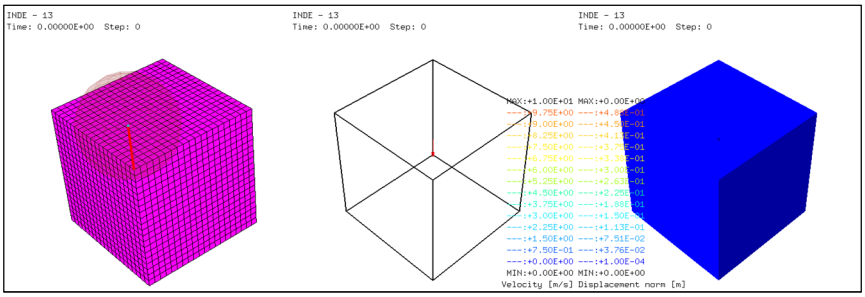

Contact and deformations | Velocities | Displacement norm

47

Example 7b – Indentation (6)

- 3D symmetric mesh solution:

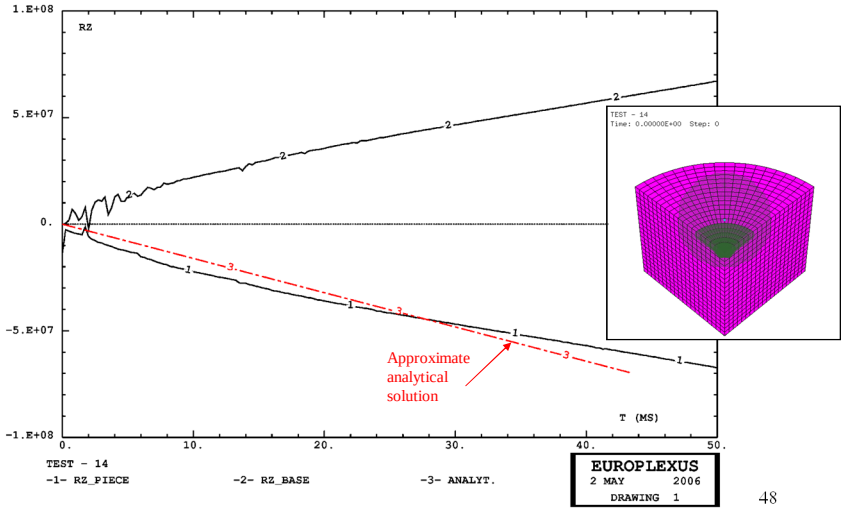

48

Example 7b – Indentation (7)

- 3D symmetric mesh solution:

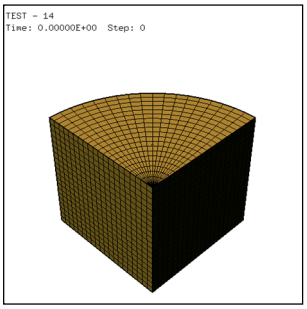

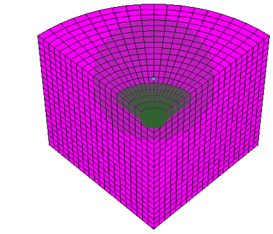

Initial mesh and pinballs

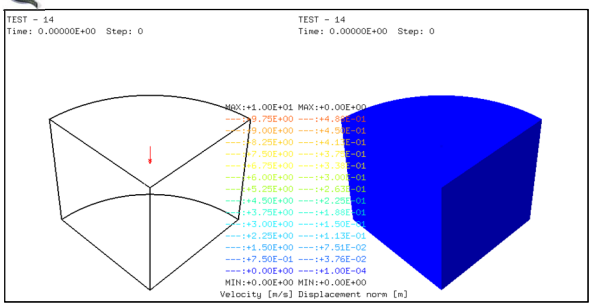

Velocities Displacement norm

49

Example 7b – Indentation (8)

- Comparison of 3D solutions:

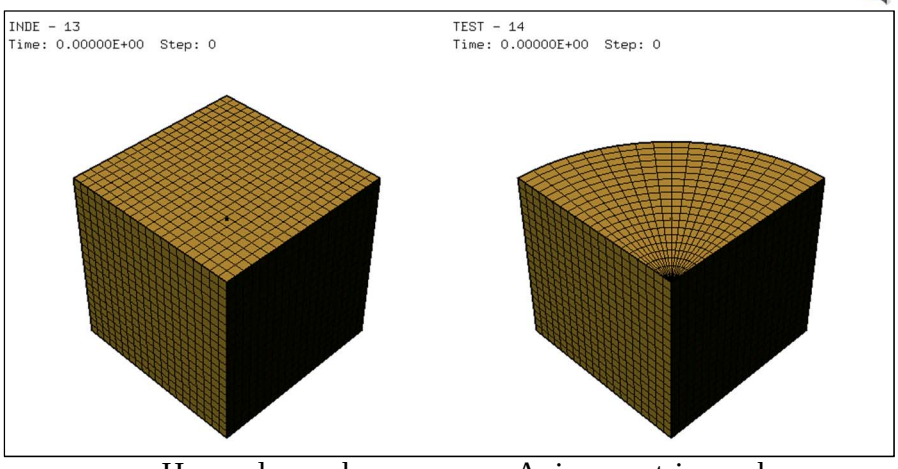

Hex-only mesh Axisymmetric mesh

50

Example 7b – Indentation (9)

- Comparison of all solutions:

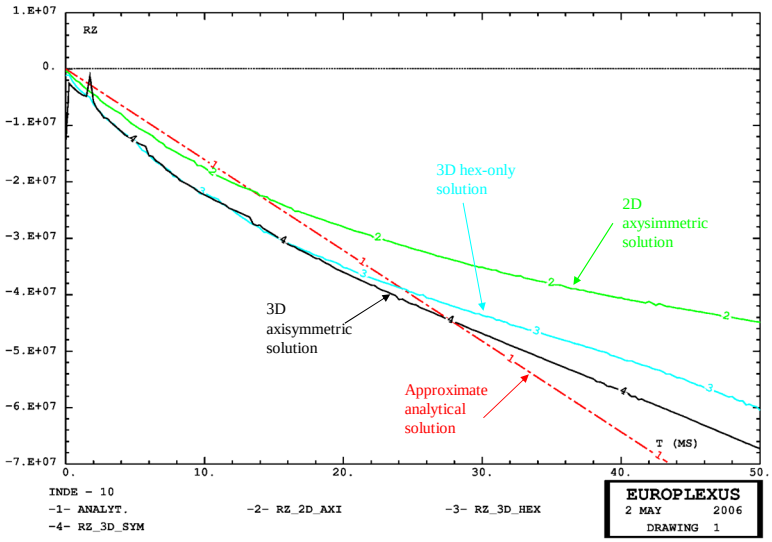

51

Example 7c – Plate perforation (Courtesy of CEA)

- A tough cylindrical projectile impacts a ductile circular plate at the initial velocity of 100 m/s and completely perforates it

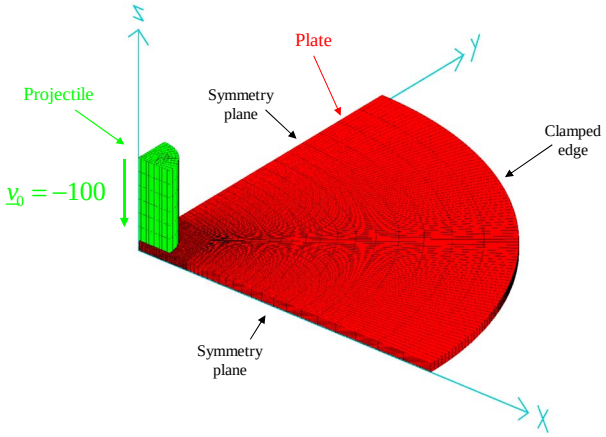

52

Example 7c – Plate perforation (2)

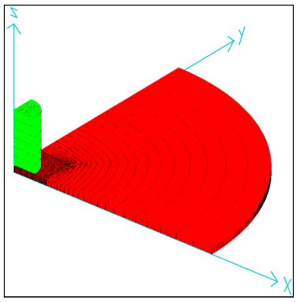

53

Example 7d – Falling Rock Catcher

- A falling rock catcher of 6 m by 3 m is hit by a spherical rock of 0.6 m diameter and a mass of 283 kg, at a speed of 100 km/h (28.3 m/s) and with an inclination of 45 degrees:

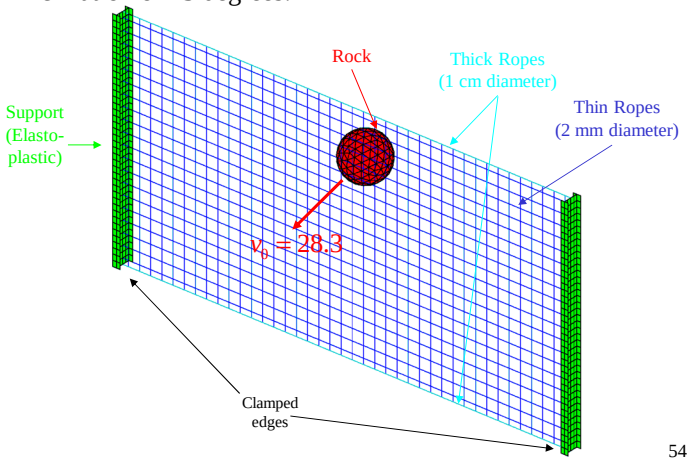

54

Example 7d – Falling Rock Catcher (2)

- Two solutions are presented, one with a ductile cable material (rupture strain 50%) and one with a fragile cable material (rupture strain 5%):

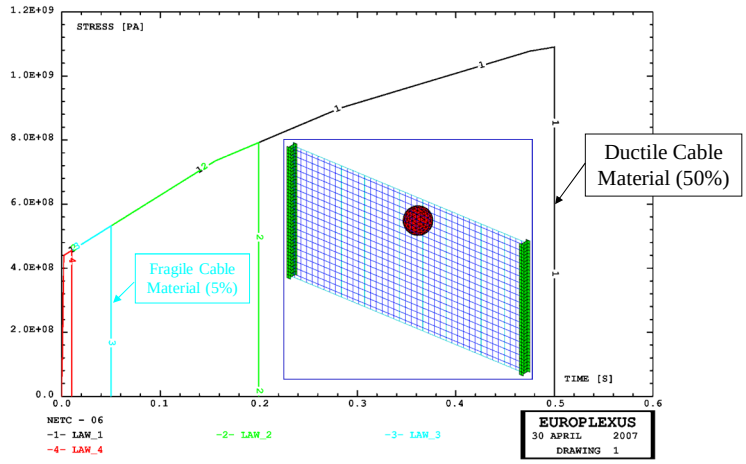

55

Example 7d – Falling Rock Catcher (3)

- View of pinballs used for contact calculations:

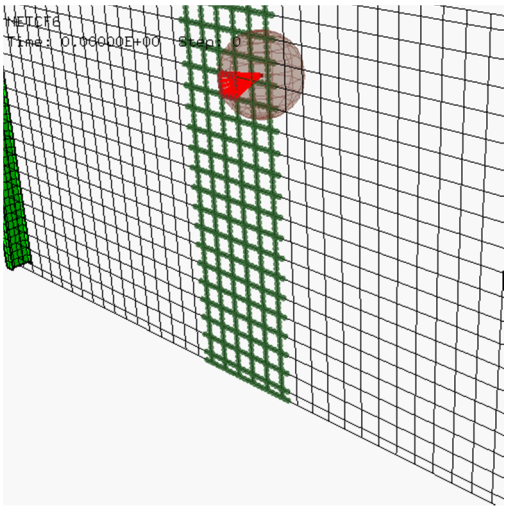

56

Example 7d – Falling Rock Catcher (4)

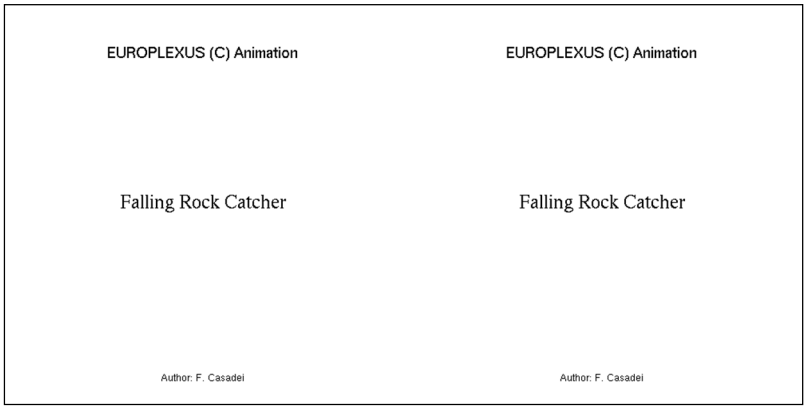

Ductile Fragile

57

Example: impact tests of car crash absorbers

Test set-up for car crash absorbers

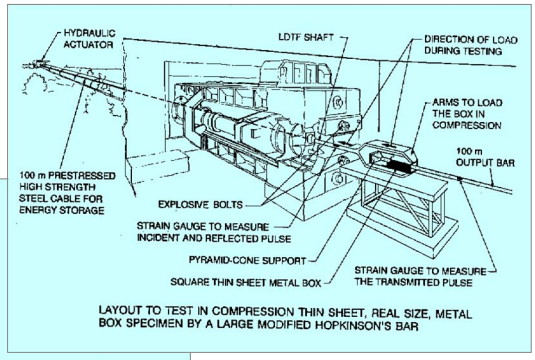

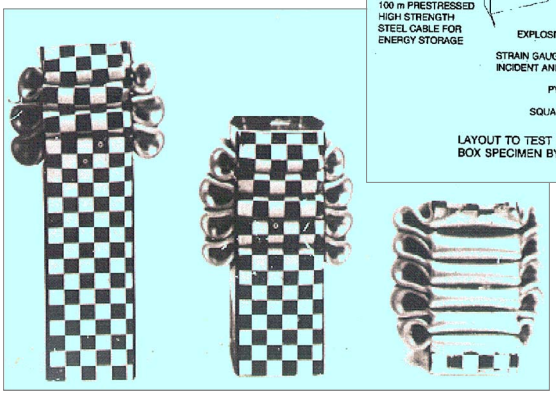

Car absorbers after crash tests

58

Tube Crash by the Pinball method

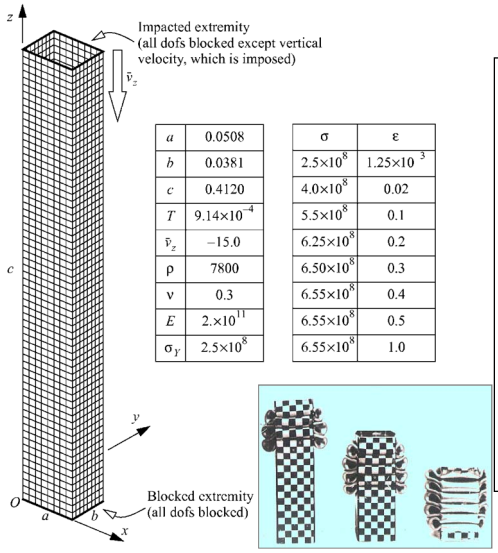

a	0.0508
b	0.0381
c	0.4120
T	9.14×10^{-4}
$\bar{v}_z$	−15.0
ρ	7800
ν	0.3
E	$2.\times10^{11}$
σ_y	2.5×10^{8}

σ	ε
2.5×10^{8}	1.25×10^{-3}
4.0×10^{8}	0.02
5.5×10^{8}	0.1
6.25×10^{8}	0.2
6.50×10^{8}	0.3
6.55×10^{8}	0.4
6.55×10^{8}	0.5
6.55×10^{8}	1.0

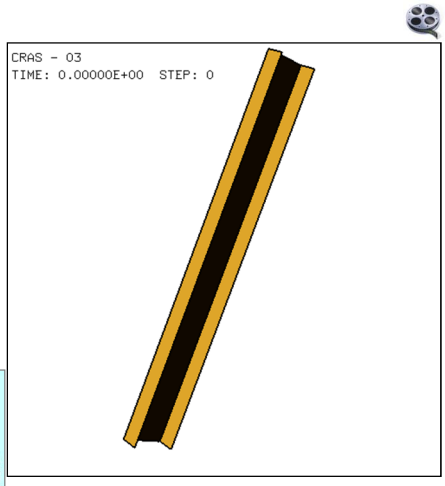

59

Tube Crash by the Pinball method (2)

- To speed up contact search, use bucket-sort algorithm:

Brute force	20.4 h CPU
Fast search	2.8 h CPU

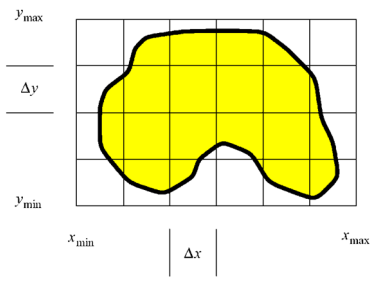

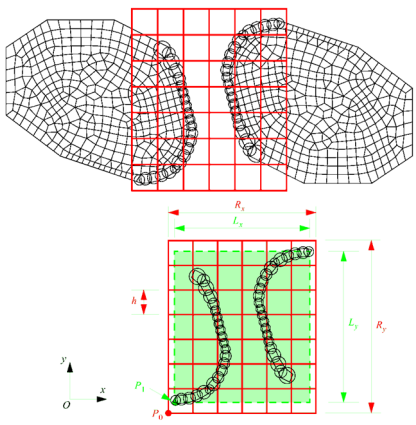

OPTI PINS …
GRID DPIN 1.5

60

Tube Crash by the Pinball method (3)

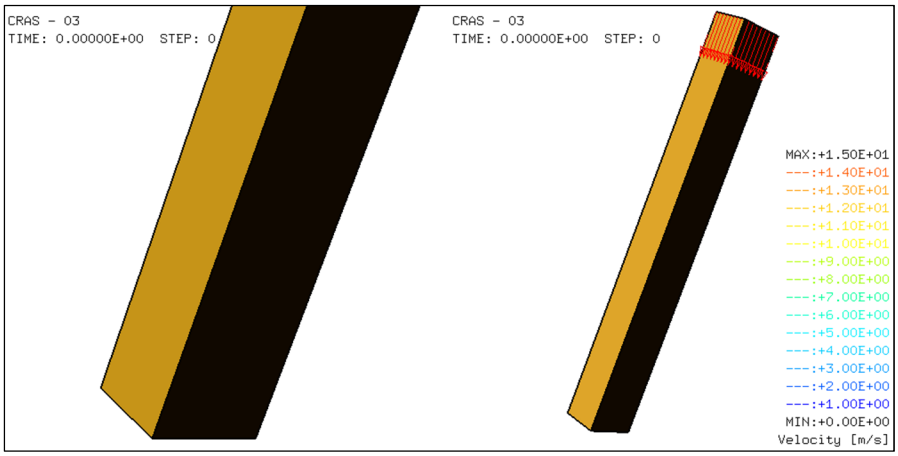

61

SPH (Courtesy of CEA / Snecma)

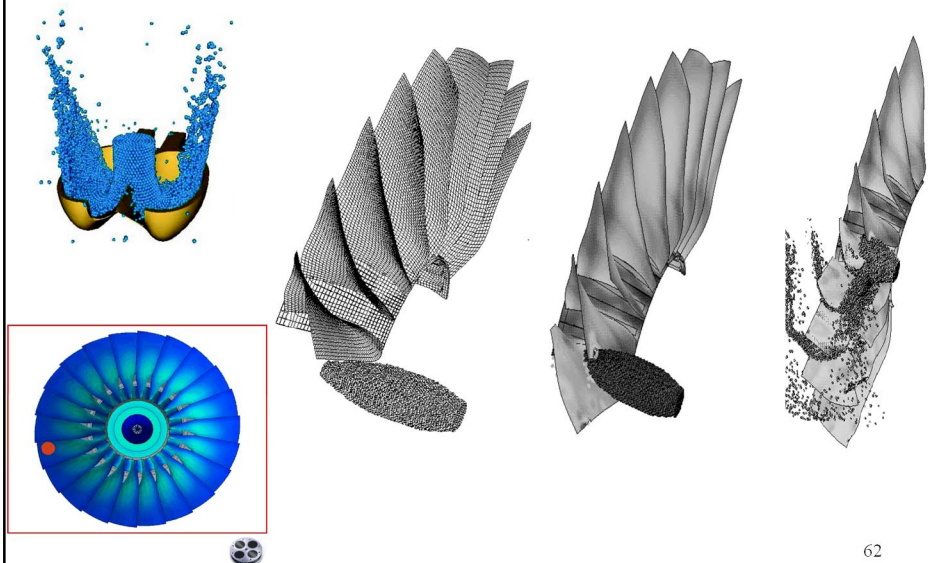

62

Smoothed Particles Hydrodynamics

(Courtesy H.Bung, CEA Saclay)

- Application domain: impact of a relatively soft body (~fluid) onto a structure, typically with fragmentation:
  - Aeronautics: bird strike
  - Nuclear: various applications (e.g. corium slug impact)
  - …
- Goal: verify behaviour of the structure (not so much of the impacting body)
- Advantages: it allows to overcome the limitations of classical FE-based methods in problems where a constant mesh topology becomes a serious drawback

63

Why a Particle-Based Method?

- FE Lagrangian formulation: the mesh follows the material
  - Well adapted for solid behaviour
  - Relatively easy treatment of B.C.s
  - Need to model only the real domain
- However: if deformations exceed a certain value, remeshing becomes necessary, else calculation stops
- FE Eulerian formulation: the mesh is fixed
  - Well adapted for fluid behaviour
  - No mesh distortions
  - More difficult treatment of B.C.s (e.g. free surface tracking)
  - In certain problems (e.g. rotating bodies) need to model more than the real domain
  - Longer and less accurate calculations due to transport terms

64

Why a Particle-Based Method? (2)

- ALE formulation: the mesh moves arbitrarily
  - Simple and elegant treatment of Fluid-Structure Interaction (permanent!)
  - Combines advantages of Lag./Eul. without respective drawbacks
  - Mesh rezoning has limitations (e.g. with fragmentation) and is difficult to do e.g. in the presence of rotating bodies
- SPH formulation: the mesh is made of particles (no standard connectivity)
  - Same advantages as the Lagrangian formulation: easy B.C.s and only the real domain is modelled
  - Without the associated drawbacks: the mesh does not "deform"
  - Recalculation of connectivity at each step is costly
  - More difficult representation of material laws
  - Relatively "young" method

65

SPH Formulation

- Developed in the '70s for astrophysical problems (Lucy, Gingold, Monaghan, 1977) involving the motion of compressible fluids in complex geometries
- It can be effectively coupled with standard FE to model impact phenomena with fragmentation
- The approach is Lagrangian and has the advantage of not using a mesh in the traditional sense, so that all problems related to excessive mesh distortions are avoided

66

SPH Formulation (2)

- Basic idea: represent a continuum by a (large) set of particles, whose motion is governed by the conservation laws of continuum mechanics
- The method is based upon the following identity for a function f:

$$f(\vec{r}) = \int f(\vec{r}') \cdot \delta(\vec{r} - \vec{r}') dV'$$

$\vec{r}$ = position vector δ = Dirac's distribution

f = scalar or vectorial field ($\rho, \underline{v}, ...$)

- One tries to approximate the former integral by a "regularization", i.e. to replace Dirac's function by a kernel function $W(\vec{r}, h)$, where h is the characteristic length

67

SPH Formulation (3)

- One can thus define an approximation $\langle f(\vec{r}) \rangle$ of the field as: $f(\vec{r})$

$$f(\vec{r}) \approx \langle f(\vec{r}) \rangle = \int f(\vec{r}) W(\vec{r} - \vec{r}', h) dV'$$

The kernel must satisfy the following properties:

- As the regularization length tends to 0, it tends to Dirac's distribution:

$$\lim_{h \to 0} W(\vec{r} - \vec{r}', h) = \delta(\vec{r} - \vec{r}')$$

- It is normalized:

$$\int W(\vec{r}, h) dV' = 1$$

- We use a cubic kernel (Monaghan's W4)

68

SPH Formulation (4)

- To write the equations of continuum mechanics under the form of a particle approximation, it is necessary to estimate the various fields (density, energy, etc.) and their spatial gradients (gradient, divergence, …).

- Then, for each term:

Term of dynamic conservation equation at point $\vec{r}$

↓

Multiply by $W(\vec{r}-\vec{r}')$

↓

Integrate over the fluid domain (special attention to boundaries!)

↓

Approximate the integrals by discrete summations

↓

Term of SPH equation at point $\vec{r}$

69

Slug impact [Courtesy of CEA Saclay]

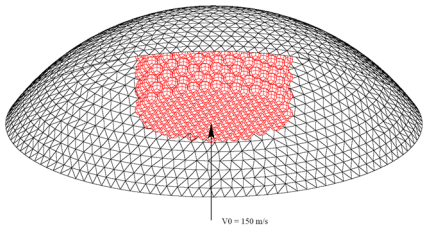

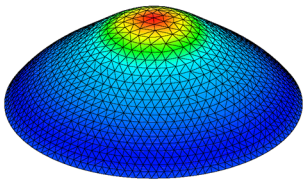

2648 triangular shells, 1180 particles

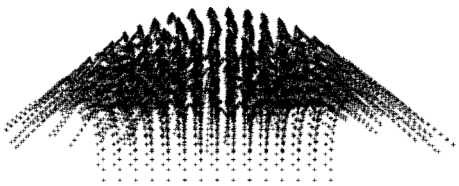

70

SPH impact [Courtesy of Samtech/Sonaca]

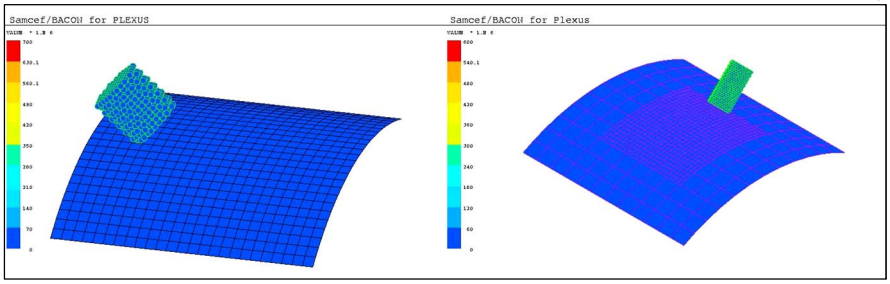

71

SPH impact [Courtesy of Samtech/Sonaca]

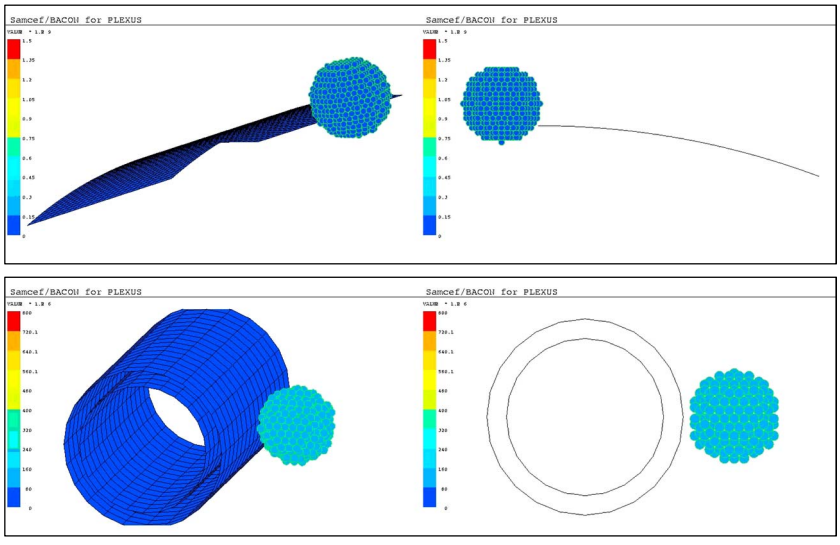

72

Bird Strike [Courtesy of Snecma/CEA]

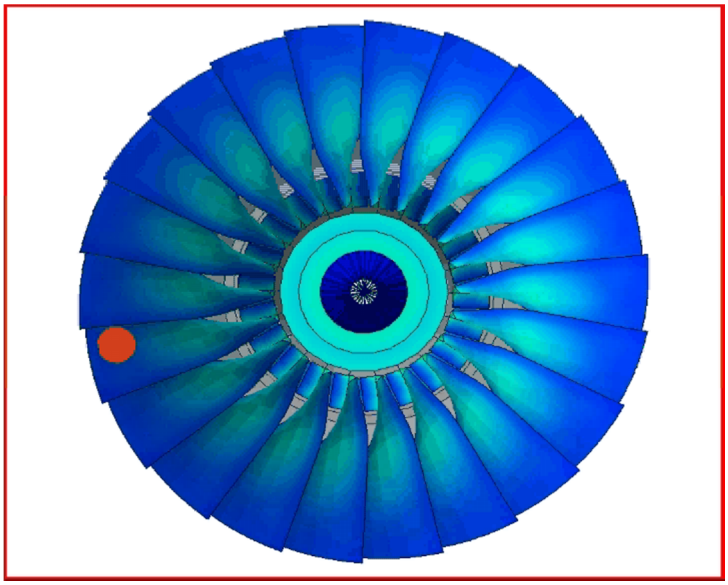

73

Bird Strike [Courtesy of Snecma/CEA]

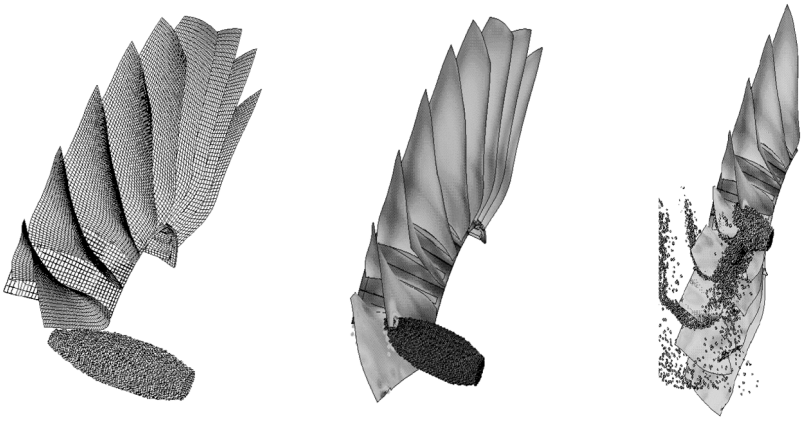

74

Example 8 – SPH impacts

(Courtesy of CEA and Samtech S.A.)

PRGL01:

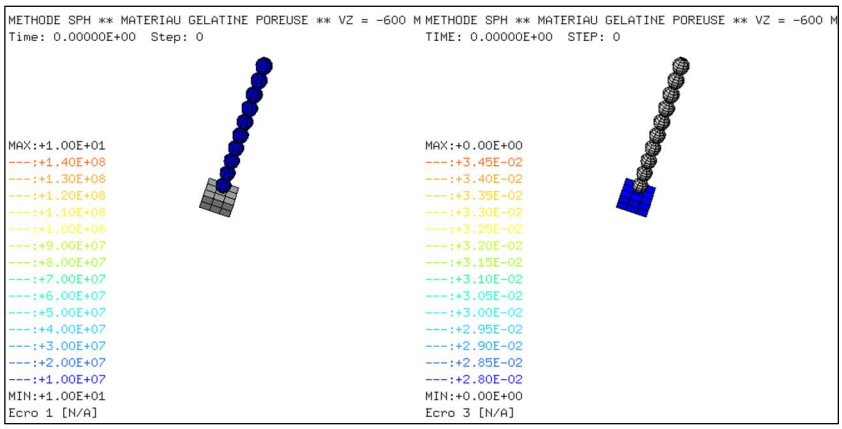

Absolute pressure in projectile Plastic strain in target

75

Example 8 – SPH impacts

(Courtesy of CEA and Samtech S.A.)

ROMA01:

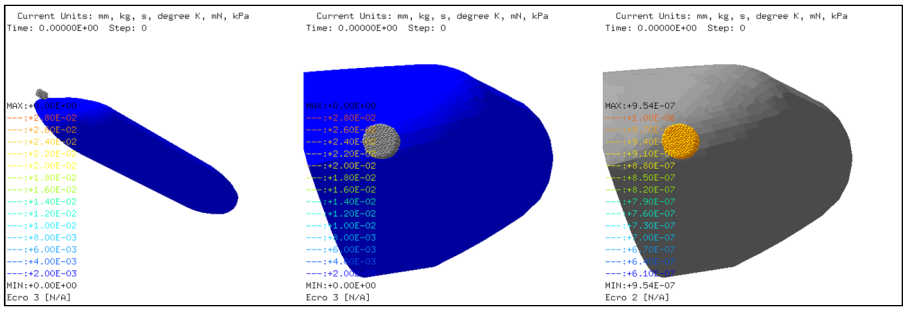

Plastic strain in structure Plastic strain in structure (zoom) Density in projectile

76

Example 8 – SPH impacts (2)

SONA01:

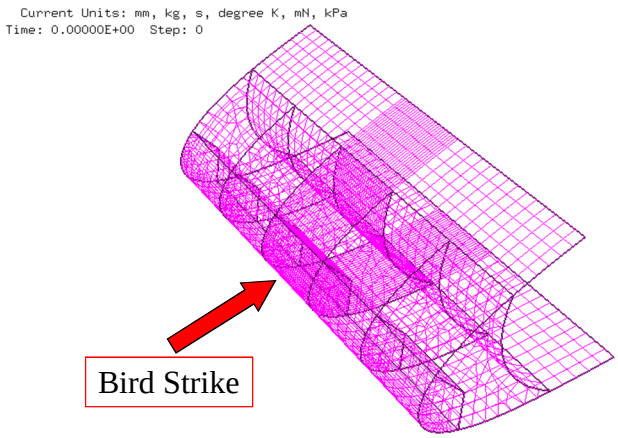

77

Example 8 – SPH impacts (3)

SONA01:

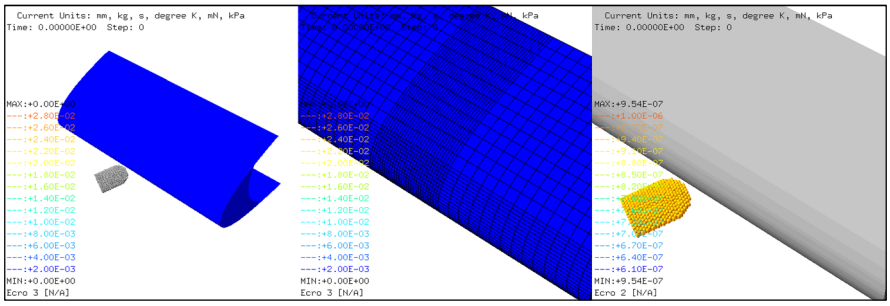

Plastic strain in structure | Plastic strain in structure (zoom) | Density in the projectile

78

SPH for structures

(Courtesy INSA-Lyon / EDF) Implemented in EUROPLEXUS by B. Maurel

Application of SPH to **structural mechanics:** 3 major difficulties

Lack of spatial **precision/convergence** :

⟶ Use Moving Least Square (**MLS**) functions

Instability in the presence of **traction** :

⟶ Use **Total Lagrangian** formulation

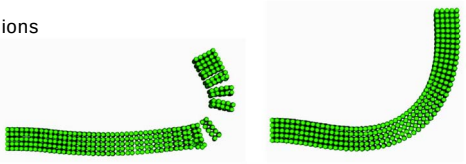

Classical SPH | Total Lagrangian

Zero-energy modes :

⟶ Introduce "**stress points**"

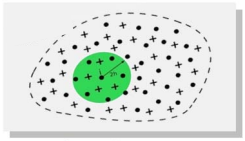

Introduce « Stress Points »

Traction instability

79

SPH for shells

(Courtesy INSA-Lyon / EDF)

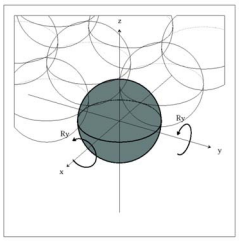

Rotational dofs added

- Challenge: use **just one layer** of spheres through the shell thickness

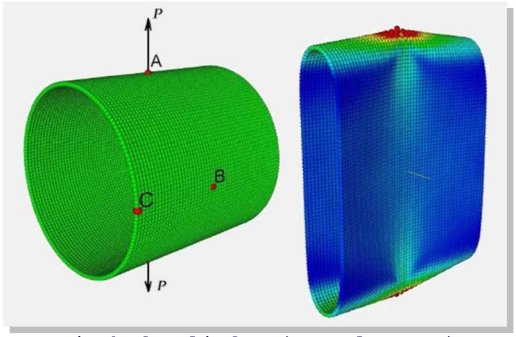

Pinched cylinder (Maurel, 2008)

80

SPH for shells

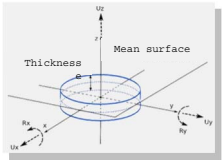

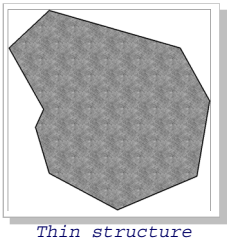

Thin structure

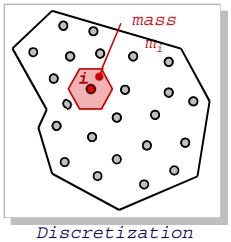

Discretization

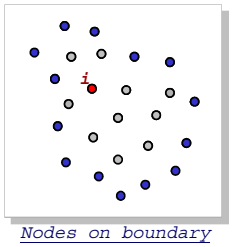

Nodes on boundary

SPH shell node

SPH Node

Boundary SPH node

« Stress Point »

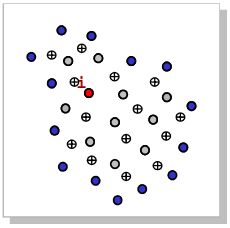

« Stress points »

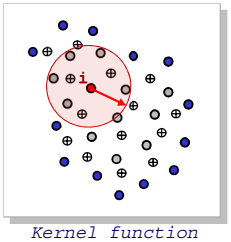

Kernel function domain

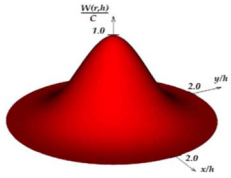

Cubic spline kernel W

81

SPH *vs.* FE

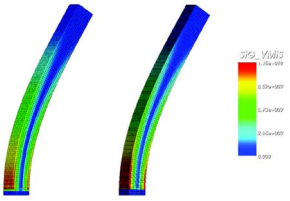

Solid bending

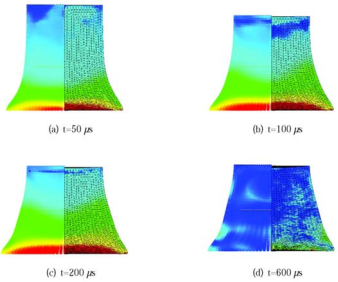

Solid impact

SPH

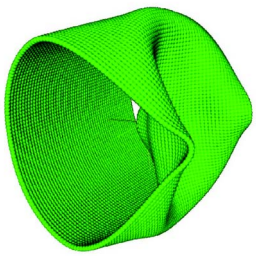

FE

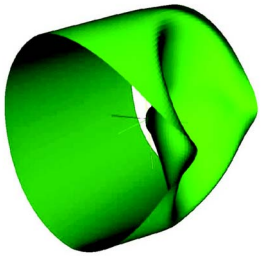

Shell impact

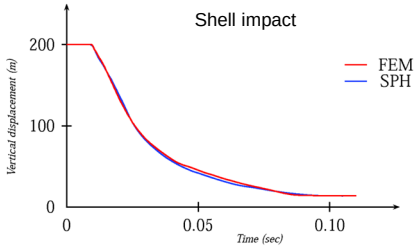

82

SPH : Lagrangian contact

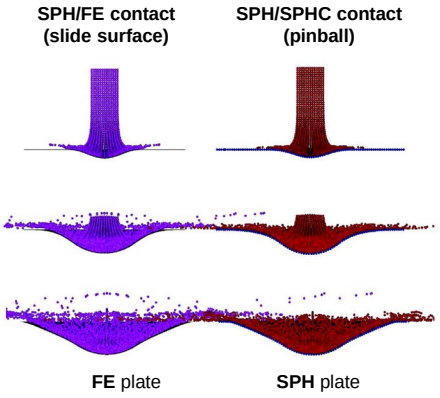

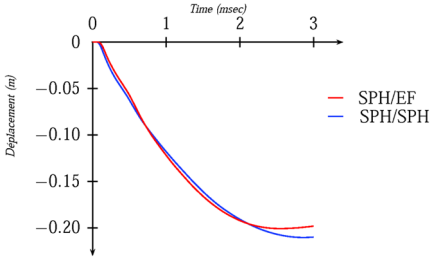

Water jet on plate

83

SPH facilitates treatment of rupture

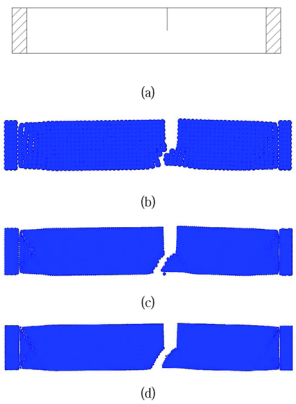

Specimen with crack

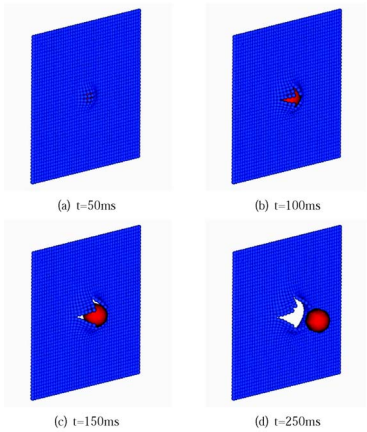

Shell perforation

84

Impact on Fluid-filled Tanks by SPH

(Courtesy of **F. Caleyron**, A. Combescure, V. Faucher, S. Potapov)
[INSA Lyon, CEA Saclay, EDF Clamart]

→ **Protection** of **citizens** and of **installations** against **plane crash**

→ Thermal effects due to **dispersion** and **combustion** of **fuel** within the structure

WTC 2: impact (9h03)

WTC 2: collapse (9h59)

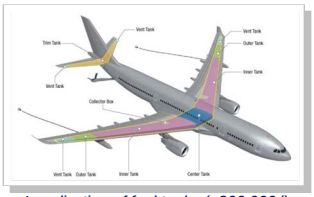

Localization of fuel tanks (~200 000 l)

→ Accounting for the presence of **fuel** **mandatory** in the analysis of **effects** of a plane crash

→ **Experiments** are difficult, expensive et dangerous: partial failure of CID project (NASA, 1984)

Dryden Flight Research Center EC84-31809 Photographed 1984
Remotely piloted Boeing 720 Controlled Impact Demonstration
aircraft following impact with iron cutter posts. NASA photo

85

SPH Failure Model

According to: Mécanique des Matériaux Solides, (***Lemaitre & Chaboche**, 2004)*:

« The theory of **damage** allows to foresee the **onset of a macroscopic crack** (*i.e.* at REV size).
The theory of **cracking** allows to foresee **its evolution** until complete failure of the structure »

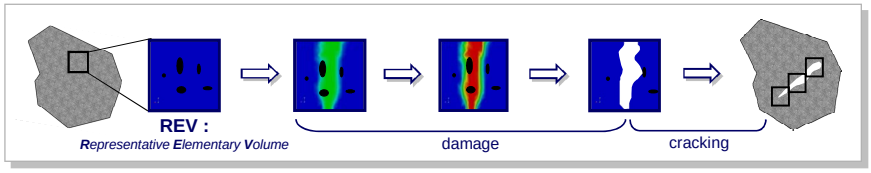

Philosophy of the method:

- **onset** of a crack when **critical damage** is reached in a REV
- **propagation** by cracking of **neighboring REVs**

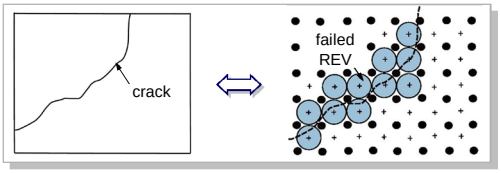

⇨ REV: - supported by « stress points »
- size given by spatial discretization

86

Damage – Cracking Transition

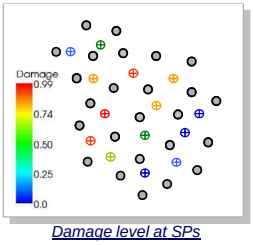

Damage level at SPs

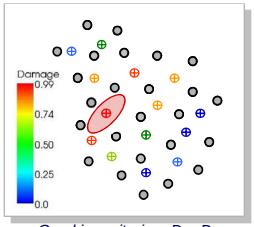

Cracking criterion: $D = D_c$

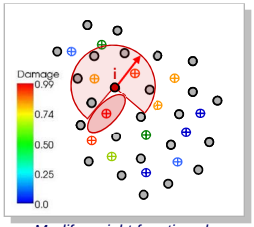

Modify weight functions by « visibility method »

SPH Node
Boundary SPH node
« Stress Point »

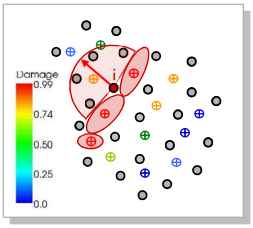

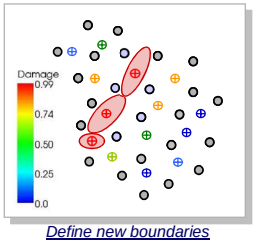

Define new boundaries

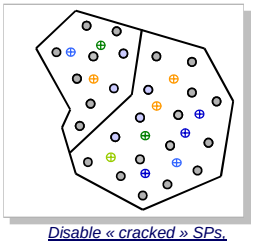

Disable « cracked » SPs, treat « fragments »

- Energy & mass are **conserved**
- **Simple** but **coarse** crack representation
- **Fine** SPH mesh is needed

87

Crack propagation in mixed mode

(John & Shah 1988)

- **Concrete:** linear elastic
- **Mazars** damage model
- **Loading:** impact
- Assume **plane stress**

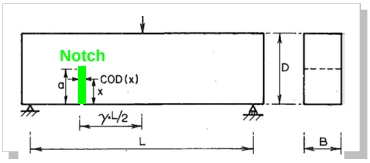

Scheme of experimental setup (John & Shah)

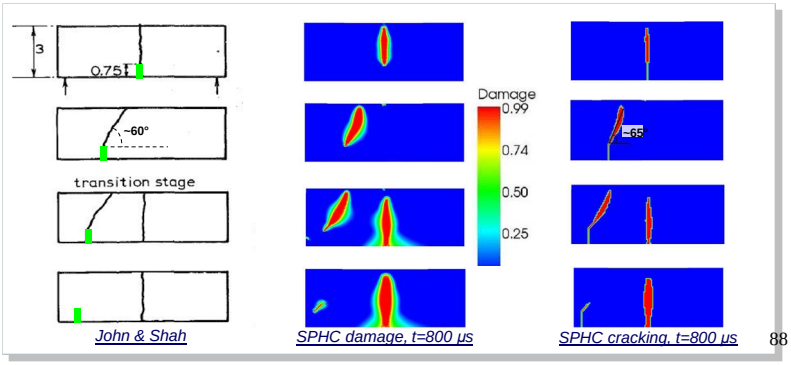

John & Shah | SPHC damage, t=800 µs | SPHC cracking, t=800 µs

88

Convergence study

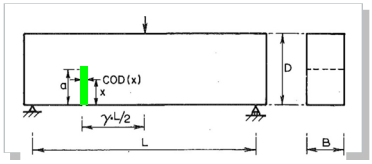

Scheme of experimental setup (John & Shah)

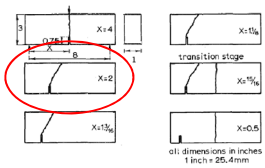

Experimental results

Mesh size →	10	5	3	2	1
D →	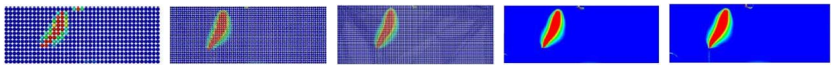				
L_{crack} →	20 +/- 10	20 +/- 5	15 +/-3	16 +/-2	17 +/-1

⇨ **Low dependency** upon mesh size: **localization limiter is effective**

Crack branching in 2D

(Belytsckho *et al.* 2006)

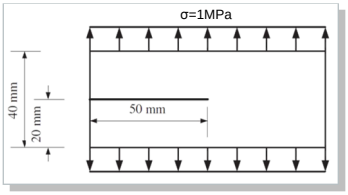

- Concrete: linear elastic, **Mazars** damage model
- **Loading:** traction ramp from 0 to σ
- **Plane stress**
- **Sensitivity** study to parameters τ_c and a

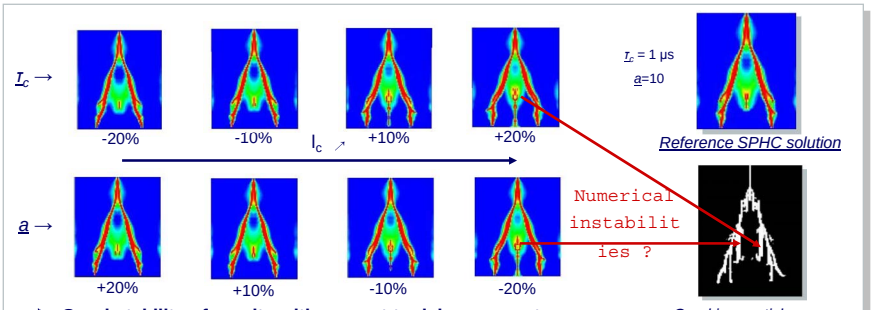

⇨ **Good stability of results with respect to delay parameter**

Petaling of a plate (Rusinek *et al.* 2009)

→ **Experimental conditions**

- Plates in mild steel ES
- Hemispherical projectile
- V_{imp}< 100 m/s
- Lubricated or dry contacy

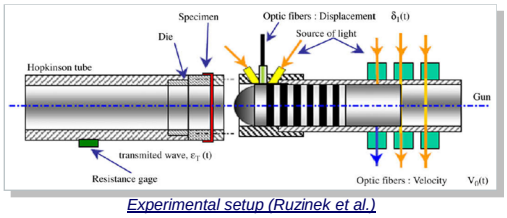

Experimental setup (Ruzinek et al.)

Dry contact (Rusinek et al.)

Lubricated contact (Ruzinek et al.)

⇨ The **petaling** mode depends upon **impact velocity** and upon **lubrication**

→ **Computational model**

- Steel: visco-plastic Johnson-Cook model with Lemaître & Chaboche damage model
- Spherical projectile: rigid
- Contact: pinball method

Petaling of a plate

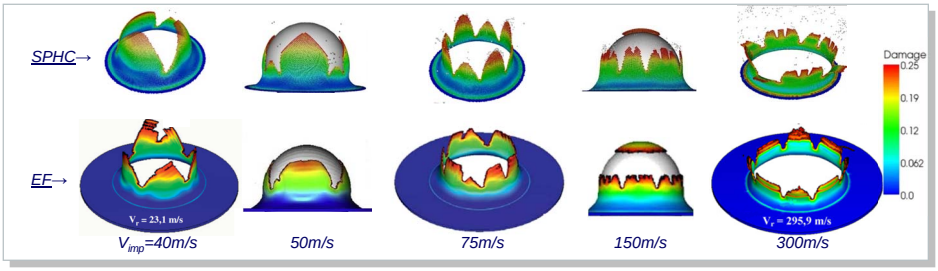

Comparison of SPHC (EuroPlexus) and EF (Ruzinek et al.) simulations

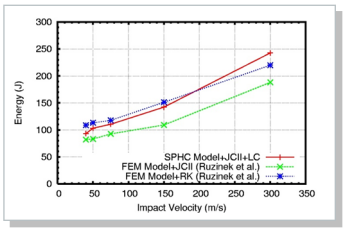

Kinetic energy « lost » by projectile

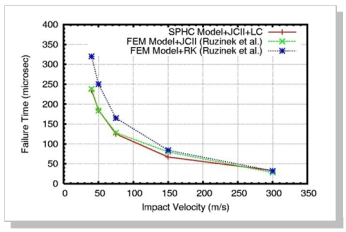

Time of plate rupture

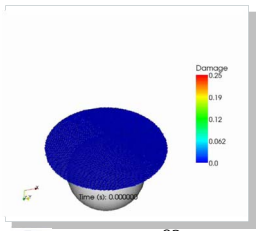

V_{imp}=300m/s

Fragmentation of a cylinder (Goto *et al.* 2008)

→ Experimental conditions

- Cylinder of AISI 1018 steel
- LX-17 explosive charge

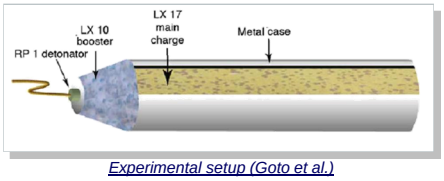

Experimental setup (Goto et al.)

→ Computational model

- Explosive: FEF, JWL equation of state
- Steel: SPHC, visco-plasticitic Johnson-Cook material, Lemaître & Chaboche damage model
- Contact: sliding surfaces

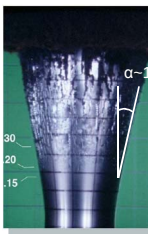

t=25 µs (Goto et al.)

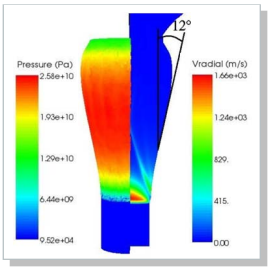

t=25 µs (SPHC)

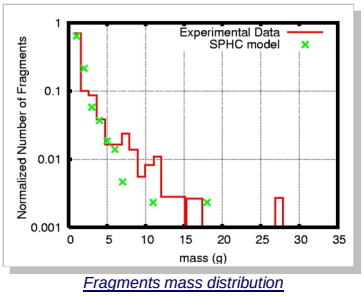

Fragments mass distribution

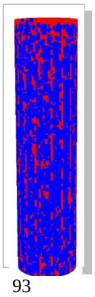

t=100 µs

SPH / SPHC Contact by Pinballs (Maurel 2008, Caleyron 2011)

→ **Fits naturally into SPH formulation**: 1 SPH particle = 1 « Pinball »

→ Treatment of a contact

- Compute the **normal** $\vec{n}$ **on contact**
  - Critical for effectiveness of the method: centres, mean, shell …
  - Choose the **normal to the shell**
  - Introduces a **pathological** case

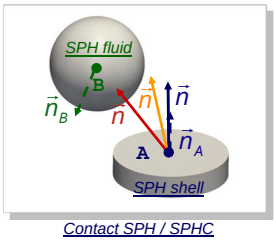

Contact SPH / SPHC

- Detect contact by **interpenetration sphere/cylinder**
- **Unilateral condition (inequality)** $(\vec{v}_A - \vec{v}_B)\cdot\vec{n} \le 0$
  - **Detection of rebound** by virtual configuration * w/out contact

$$d^*_{AB} > d_{AB} \ ?$$

  - Impenetrability **condition** $(\vec{v}_A^{\,n+3/2} - \vec{v}_B^{\,n+3/2})\cdot\vec{n}^{n+1} = 0 \Rightarrow \underline{\underline{C}}\,\vec{V} = \vec{0}$
- Contact force by **Lagrange multipliers** $\vec{F}_c = \underline{\underline{C}}^t\vec{\lambda}$

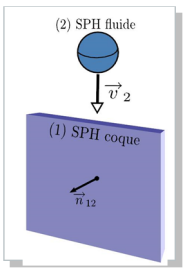

Pathological case

Perforation of a Tank (Timm 2003)

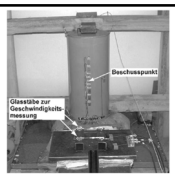

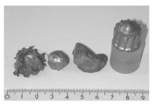

→ **Experiment**

- perforation of a cylinder
- empty ou full
- 300 m/s < V_{imp} < 730 m/s
- H/D & *e* variable

« Hydrodynamic ram » phenomenon

Empty (Timm, 2003) *Full (Timm, 2003)*

→ **Model**

- **Steel:** SPHC, visco-plasticity of JC, damage model of Lemaître & Chaboche, CT
- **Fluid:** SPH, perfect, slightly compressible
- **Impactor:** rigid
- **Contact:** « pinballs » method

⇨ Reproduction of the rupture mode

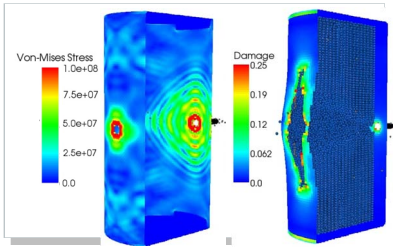

Empty (SPHC) *Full (SPHC)*

95

SPHC/FE Coupling ("Arlequin" Method, Ben Dhia 1998)

→ **Superposition zone**

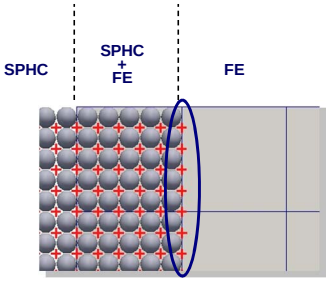

Additional « Stress Points »

→ **Empty tank:** equivalent SPH mesh sizes

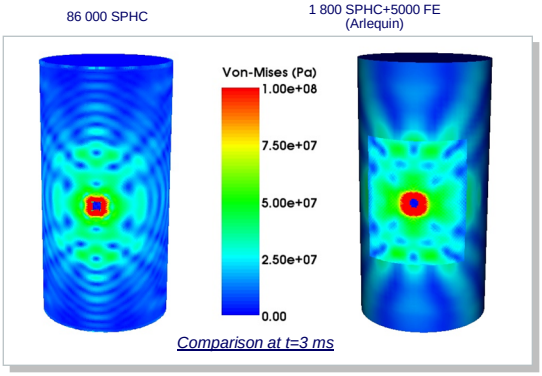

Comparison at t=3 ms

- CPU speed-up factor 5
- Exit velocities ~ equivalent
- Loss of resolution on high frequencies

96

SPHC/FE Coupling in Tank Perforation

→ **Full tank:** refined SPH mesh

19 000 SPHC +
104 000 SPH

31 800 SPHC+2200 FE
(Arlequin)

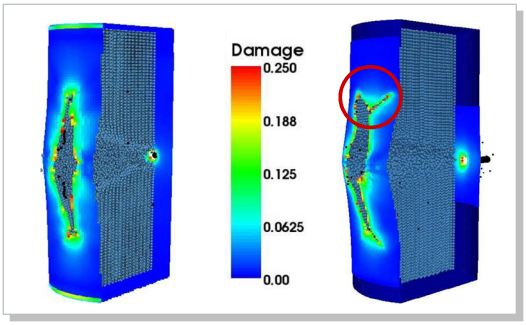

Comparison at t=1.8 ms

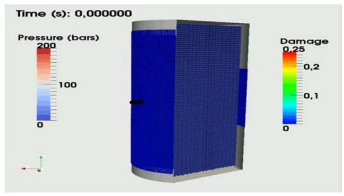

Tank rupture and fluid jet until 20 ms

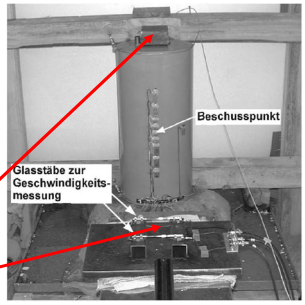

- The entire transient can be computed thks to coupling
- Exit velocities ~ equivalent
- Bifurcation of the crack (~ boundary conditions)

97

Plate Rupture / Jet Simulation (J. Fabis, ONERA Lille)

→ A **simple** but **representative** test of tank impact: **shock pressure on a plate**

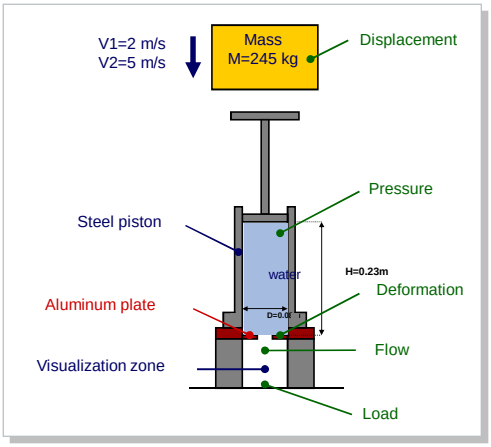

Scheme of the test rig

→ Specimens characteristics

- **Thickness:** 25 mm, 2 mm, 1 mm
- circular **hole**, **notch** U, I, X

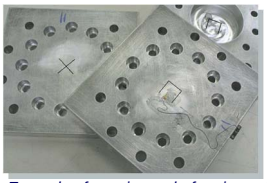

Example of specimens before impact

→ Physical phenomena

- **shock pressure** in the fluid
- **fluid jet**
- **deformation**, **cracking**, **rupture** depending on cases

98

Sample Test (courtesy J. Fabis, ONERA Lille)

A test

99

Plate with Circular Hole

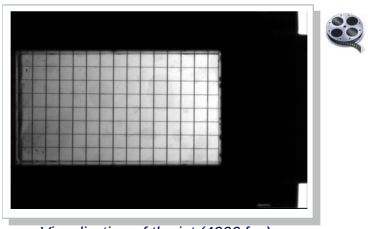

Visualization of the jet (4000 fps)

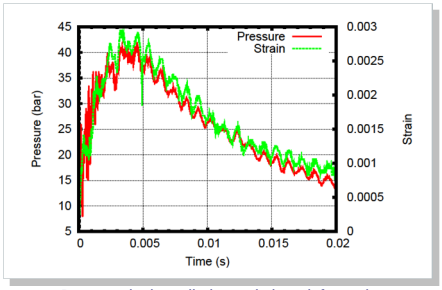

Pressure in the cylinder and plate deformation

→ **Observations**

- **periodic pattern** in the jet
- **pressure** peak then **sinusoidal decrease**
- similar variation of **deformation**

frequencies are reproducible for a given specimen

→ **Interpretation**

- **turbulent instability** (Plateau-Rayleigh)
- excitation frequency = **eigenmode of device**

⇨ strongly coupled **fluid-structure** oscillator

100

Types of Notches and Failure Modes

→ **U-Notch**

V_1=2 m/s

V_2=5 m/s

→ **X-Notch**

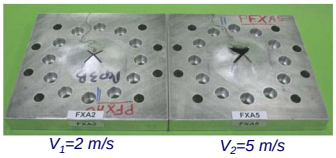

V_1=2 m/s V_2=5 m/s

zoom

→ **I-Notch**

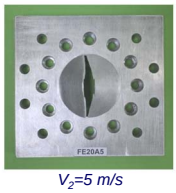

V_2=5 m/s

→ **Design Fault**

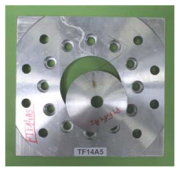

V_2=5 m/s

⇨ A variety of strongly non-linear phenomena in addition to FSI:

- **large deformations**
- **plasticity**
- **cracking**
- **full rupture**

101

Numerical Model

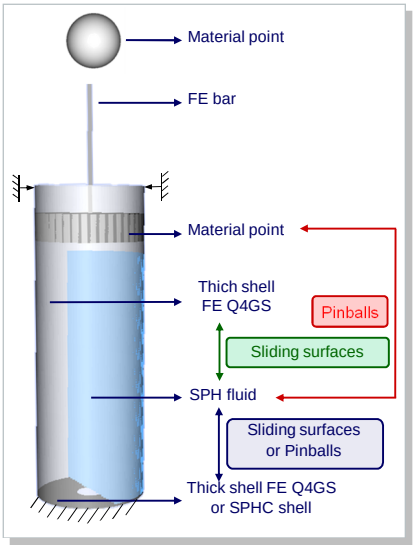

→ Explicit **representation** of the **device**

→ Model of the **structure**

- cylinder: - FE thick shell
  - APX: linear elastic
- plate: - FE thick shell **(+ SPHC if cracking)**
  - AL4G: élasto-plastic with damage

→ **Fluid model**

- SPH
- Water: slightly compressible, acoustic, perfect

→ **Fluid-structure interaction**

- FE-SPH: **sliding surface** without parasitic forces
- SPH-SPHC: **pinballs**

→ ~1 700 FE, ~112 000 SPH , ~15 000 SPHC

→ **parallel calculations** on 4 CPUs

102

Results for Thick Plate with Circular Hole

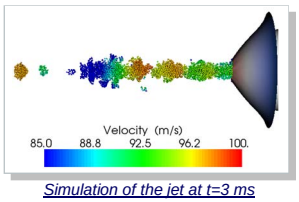

Simulation of the jet at t=3 ms

→ **Comparison** simulation/experiment

- **patterns** in the jet
- **ejection speed** of the fluid
- **peak** and **variation** of **pressure** after impact

- **overestimation of pressure** and its variation beyond 2 ms
  - state equation slightly compressible
  - SPH discretisation too coarse in the fluid
  - too rigid idealised model

⇨ **Predictive simulation** of response just **after impact**
Model is inaccurate once the flow develops

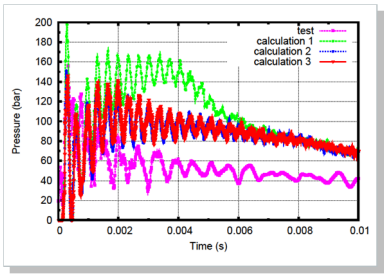

Pressure in the cylinder

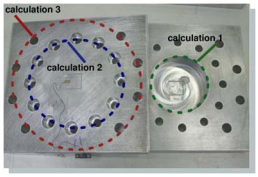

Influence of boundary conditions

103

Results for Thin Plate with U-Notch

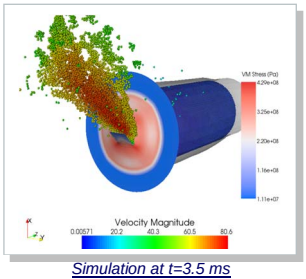

Simulation at t=3.5 ms

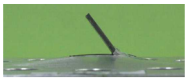

Experimental deformation α~50°

Numerical deform. t=10 ms, α~50°

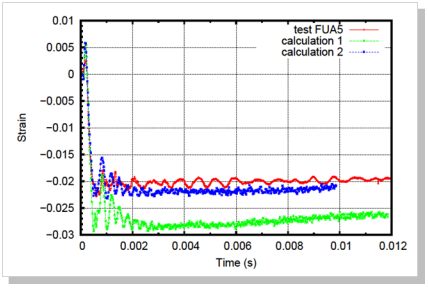

Deformation of the lid

→ **Comparison** simulation/experiment

- **ejection speed** of the fluid
- **opening** of the lid
- **peak** and **variation** of **pressure** after impact
- **variations of deformation**

- **overestimation of pressure** and its variation beyond 2 ms

⇨ **FSI** is treated correctly

104

Results for Badly Designed Specimen

→ Rupture by **stress concentration**: erosion & debris

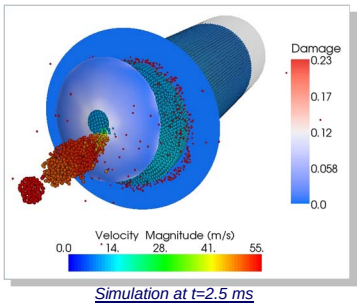

Simulation at t=2.5 ms

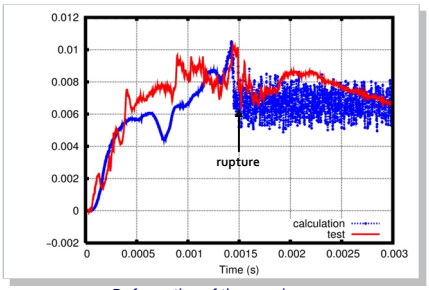

Deformation of the specimen

→ **Comparison** simulation/experiment

- **rupture mode**
- **pressure peak** and **variation**
- **rupture time**
- **variations** of **deformation**

Rupture mode

⇨ **Predictive simulation** of impacted tank **rupture**

105

Results for Thin Plate with X-Notch

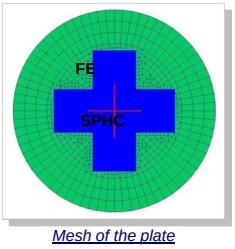

Mesh of the plate

→ **Crack propagation:** SPHC model

→ **Comparison** simulation/experiment

- **ejection speed** of the fluid
- **rupture mode**
- **crack propagation**
- **parasitic ruptures**
- **overestimation of the length** of cracks
- **bifurcation** of cracks

⇨ **The simulation of crack propagation with FSI is feasible**

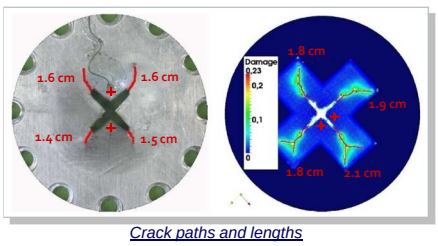

Crack paths and lengths

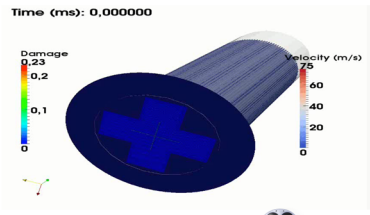

Simulation

106

Towards Industrial Simulations

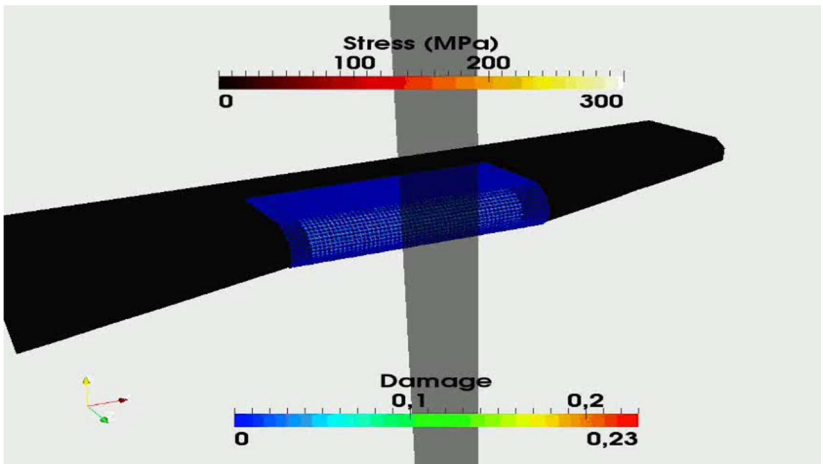

Simplified plane wing (P.Yard)

107

DEM (Courtesy of EDF)

- "Discrete Element" Method from L3S-R UJF Grenoble, implemented in EUROPLEXUS by EDF (J. Rousseau)

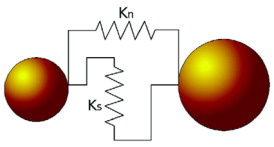

Interactions between "elements"

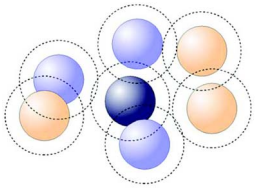

Interaction radius

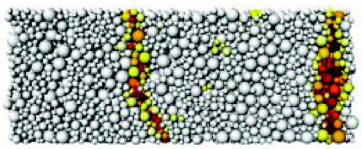

"Specimen" in traction

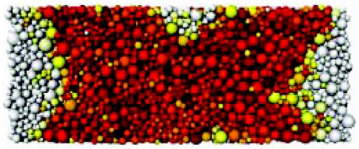

"Specimen" in compression

108

DEM : Pull-out tests

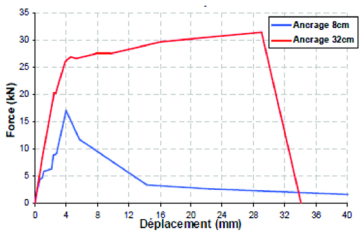

Experimental force

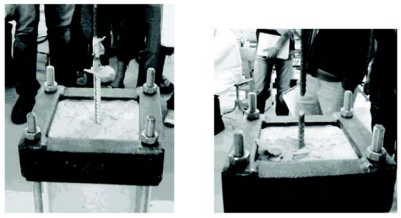

"Short" vs. "long" pull-out

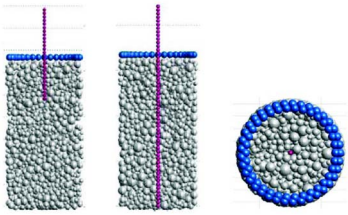

Numerical "specimens"

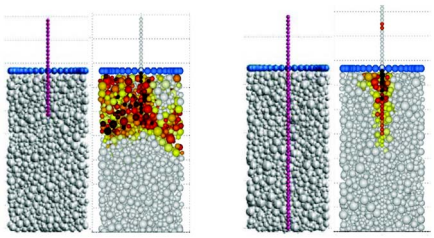

Numerical results

109

DEM : Impact tests on R/C plate

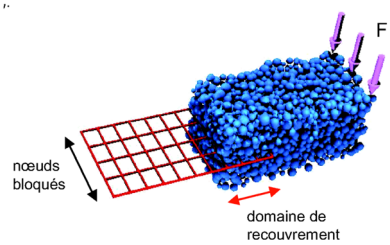

DEM-FE (shell) coupling

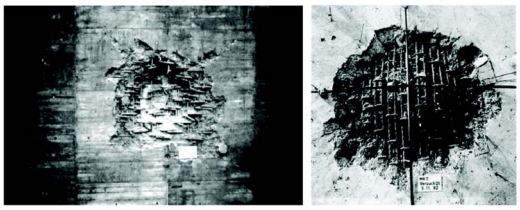

Plate impact experiment

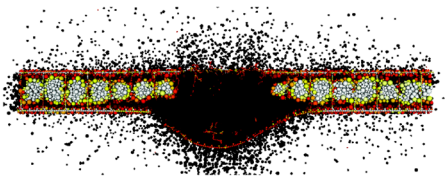

Numerical result

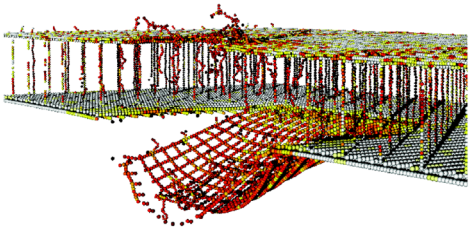

Detail of reinforcement

110

DEM : Impact tests on R/C beam

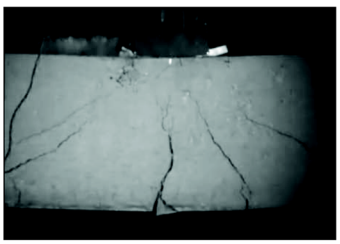

"Long" beam

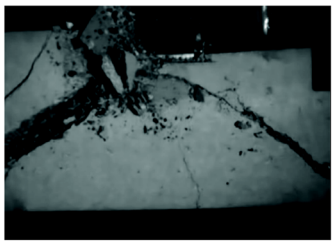

"Short" beam

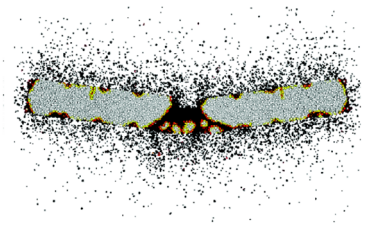

Numerical result (excessive spalling)

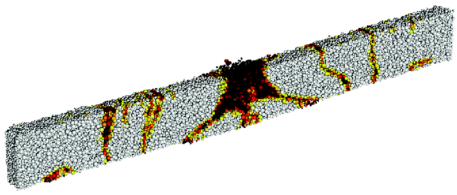

Without reinforcement

111

Simulation of the Meppen Test

(Courtesy of CEA / EDF)

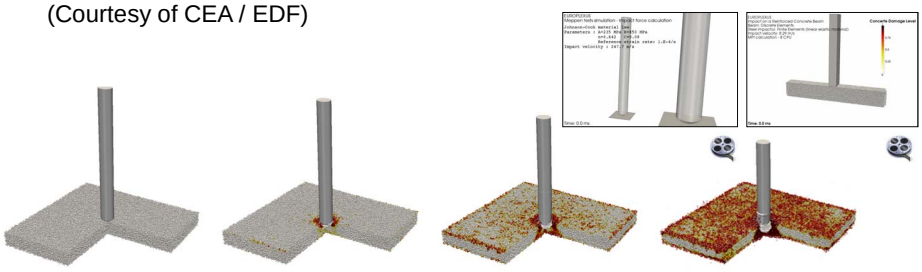

(a) t = 0 ms *(b) t = 2 ms* *(c) t = 5 ms* *(d) t = 10 ms*

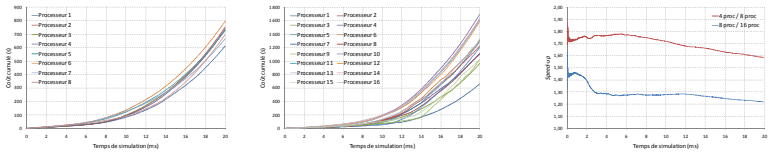

(e) Cost of identifying the global links *(f) Evolution of the speed-up*

Interpretation:

- **Bad distribution of entities** (cf. Ponderation of domain decomposition)
- **Evolution of costs during the run** with loss of structure of the plate
- **Progressive degradation of the *speed-up***

112

Spectral Elements

- Motivation: locally linear wave propagation (no singularities)

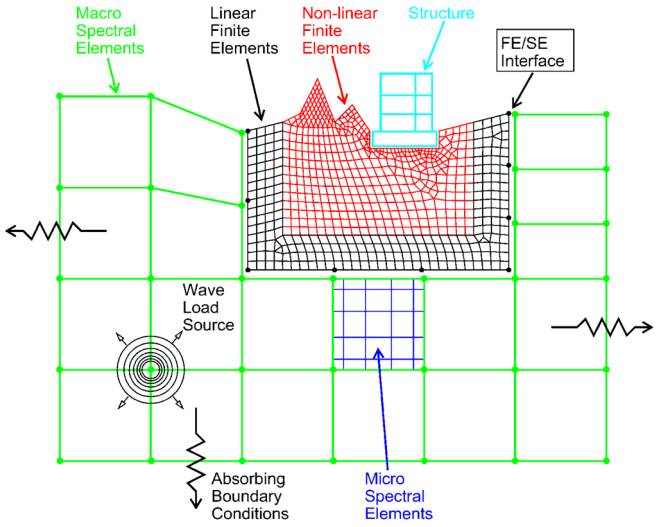

113

Spectral Elements (2)

Various approaches for numerical solution of PDEs :

- Finite-element methods:
  - Discrete approximating function is a polynomial of low degree
  - Well suited to complex geometry and full non-linearities
  - Accuracy limited by low degree of polynomials
- Spectral-type methods:
  - Discrete approximating function is a polynomial of high degree
  - Very accurate ("spectral" accuracy) when exact solution is smooth
  - Currently limited to linear problems (and no singularities)
  - Difficult to treat complicated boundaries: use domain decomposition
- *p*-version of FEM:
  - Shape functions are polynomials of high degree
  - Bases & quadrature formulas completely different from spectral methods

114

Spectral Elements (3)

- To obtain spectral convergence, nodes are placed at special Legendre-Gauss-Lobatto (LGL) positions ξ_P:

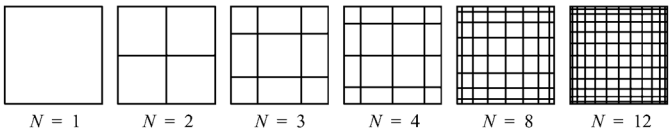

$N \doteq$ degree of polynomial

- These correspond, in 1-D, to the zeroes of L_N', the first space derivative of L_N, the Legendre polynomial of degree N:

$$\{\xi_P\} = \{\text{zeroes of } L_N'\} \cup \{-1,1\}$$

$N+1$ points

115

Spectral Elements (4)

- Solution is then interpolated by Lagrange polynomials through the LGL points:

$$\psi_I = \frac{(\xi-\xi_1)\cdots(\xi-\xi_{I-1})(\xi-\xi_{I+1})\cdots(\xi-\xi_{N+1})}{(\xi_I-\xi_1)\cdots(\xi_I-\xi_{I-1})(\xi_I-\xi_{I+1})\cdots(\xi_I-\xi_{N+1})} \Rightarrow \begin{cases} 1 \text{ in } \xi_I \\ 0 \text{ in } \xi_J, J \neq I \end{cases}$$

- For numerical integrations, use is made of LGL rule instead of the Gauss rule typical of FEM:
  - All quantities, including stresses, are expressed at “nodes”
  - Considerable simplifications in programming: very efficient implementation!
  - For a given accuracy, one more sampling point is needed by LGL rule compared with Gauss rule

116

Spectral Elements (5)

Convergence properties:

- In the FEM, let *h* be the element size and *k* the degree of the piecewise polynomial in each element, then the convergence of the method, obtained for $h \to 0$, is:

$$\|u - u_h\|_{L^2(\Omega)} = Ch^{k+1}$$

- In the SEM, let *N* be the degree of the piecewise polynomial in each element, then the convergence of the method, obtained now for $N \to \infty$, is:

$$\|u - u_N\|_{L^2(\Omega)} = Ce^{-\alpha N}$$

117

Spectral Elements (6)

Generation of spectral mesh and implementation in FEM code

- A dual mesh composed of *macro* and *micro* elements is used:

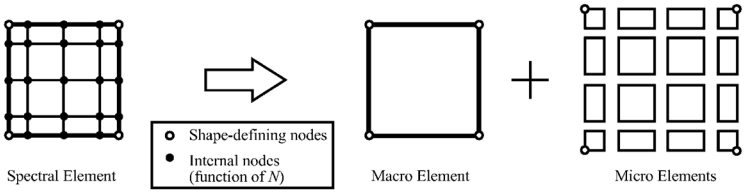

- The macro elements are built first, then the micro mesh is generated according to the chosen N:

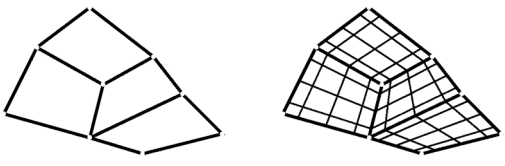

e.g. in Cast3m mesh generator:

```
micro = pxspect2
      macro n tol;
```

118

Spectral Elements (7)

Coupling between FE and SE

- We use an ***integral*** form of continuity condition at the non-conforming FE/SE interface (***mortar*** method):

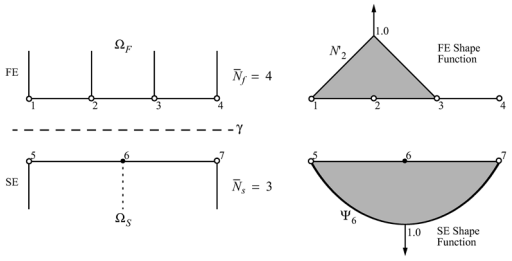

$$\int_{\gamma} (\underline{\dot{u}}_F - \underline{\dot{u}}_S) \cdot N_F' \, d\gamma = 0 \qquad F = 1, \cdots, \bar{N}_F$$

$\gamma \doteq$ FE/SE interface $\qquad \underline{\dot{u}} \doteq$ velocity

$N_F' \doteq$ FE surface shape function $\qquad \bar{N}_F \doteq$ FE nodes on γ

- These conditions are of the usual form $\underline{C}\underline{v} = \underline{b}$ and are solved via the method of Lagrange multipliers.
- More accurate than with ***local*** conditions (node-by-node basis).

119

Spectral Elements (8)

Absorbing boundary conditions (ABCs)

- We use first-order ***Stacey*** ABCs:

$$\frac{\partial}{\partial \underline{n}}(\underline{u} \cdot \underline{n}) = -\frac{1}{\alpha} \cdot \frac{\partial}{\partial t}(\underline{u} \cdot \underline{n}) + \frac{\beta - \alpha}{\alpha} \cdot \frac{\partial}{\partial \tau}(\underline{u} \cdot \underline{\tau})$$

$$\frac{\partial}{\partial \underline{n}}(\underline{u} \cdot \underline{\tau}) = -\frac{1}{\beta} \cdot \frac{\partial}{\partial t}(\underline{u} \cdot \underline{\tau}) + \frac{\beta - \alpha}{\beta} \cdot \frac{\partial}{\partial \tau}(\underline{u} \cdot \underline{n})$$

$\underline{n} \doteq$ normal to boundary

$\underline{\tau} \doteq$ tangent to boundary

$\alpha \doteq$ longitudinal wave speed

$\beta \doteq$ transversal wave speed

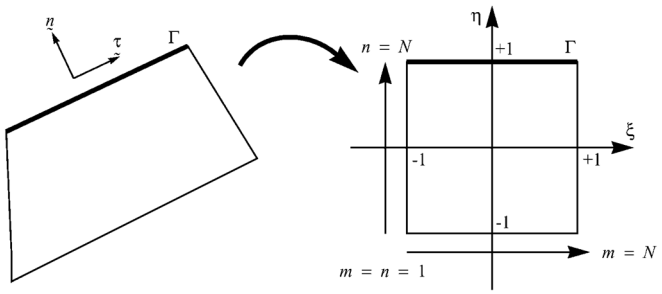

120

Example 9 – Closed FE/SE interface

- Verification of coupling algorithm - closed interface test:

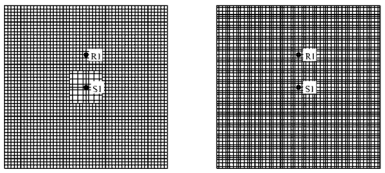

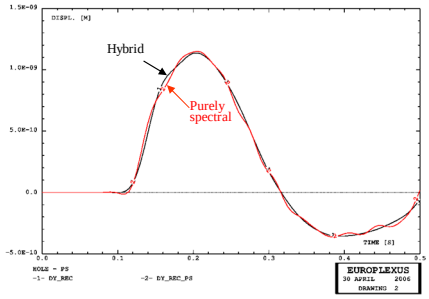

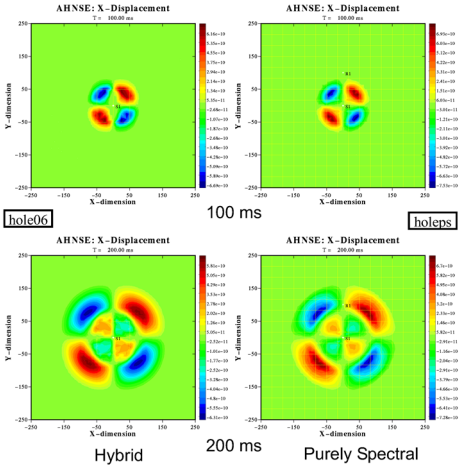

121

Closed FE/SE interface (2)

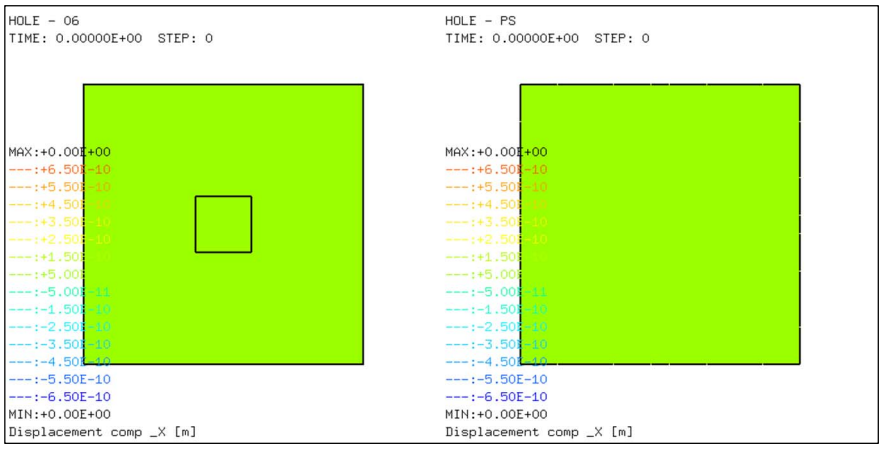

Coupled FE/SE solution

Purely Spectral solution

122

Example 10 – Sediment valley

- Verification of coupling algorithm - sediment valley test:

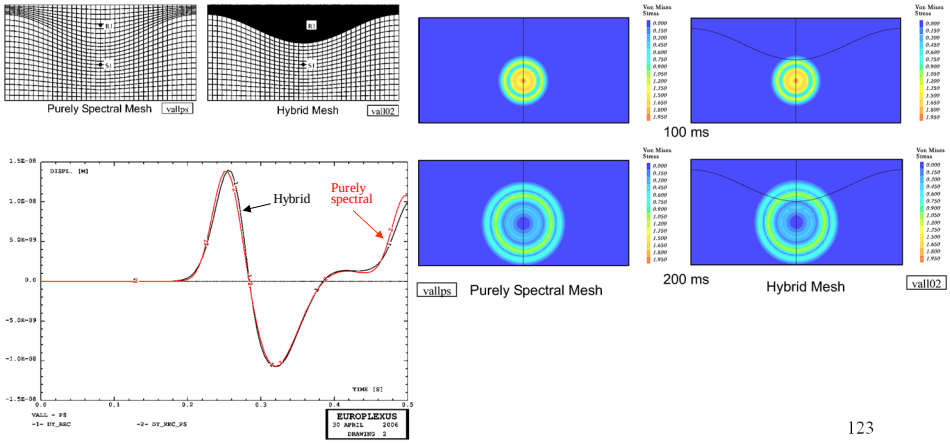

123

Sediment valley (2)

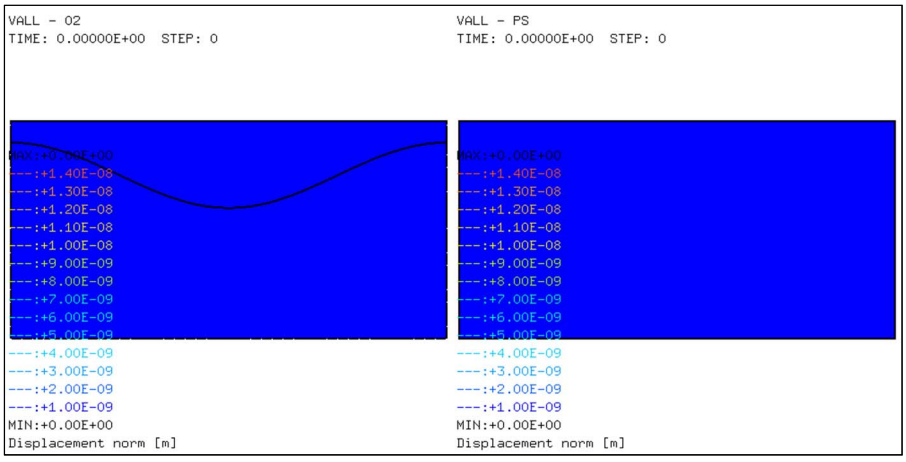

Coupled FE/SE solution

Purely Spectral solution

124

Example 11 - Cylindrical valley

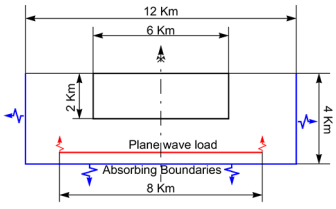

Problem Definition

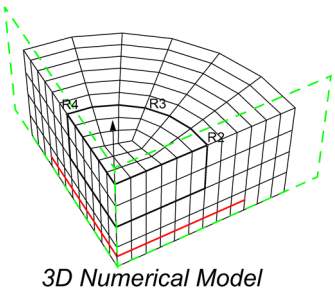

3D Numerical Model

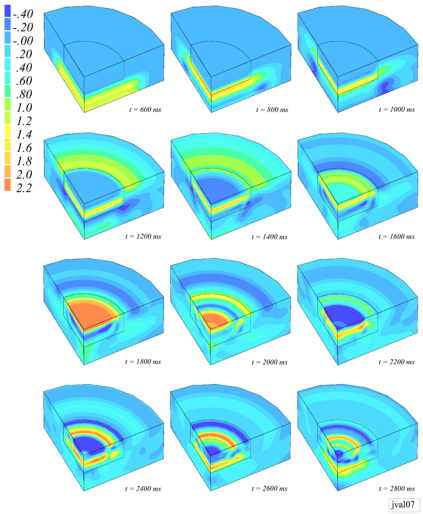

3D Numerical Solution (z-Displacement)

125

Cylindrical valley (2)

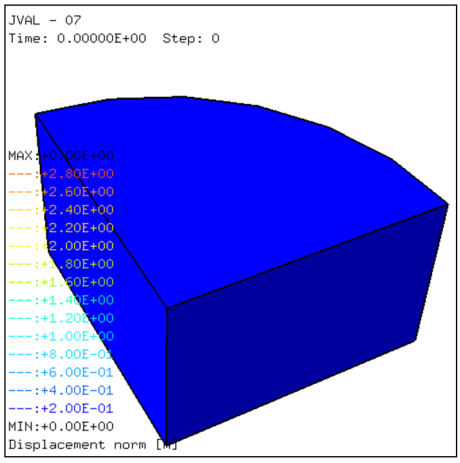

Total displacement

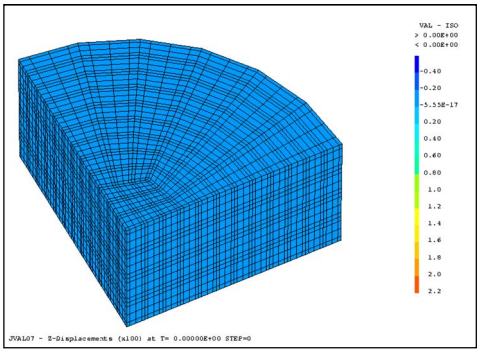

Vertical displacement

126

Example 12 - Matsuzaki valley

- Matsuzaki valley (Japan):

3D computational model (Spectral Elements for the bedrock, coupled with Finite Elements for the heterogeneous valley)

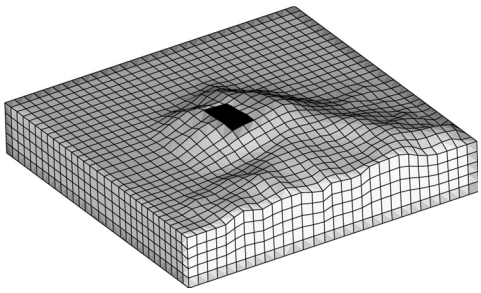

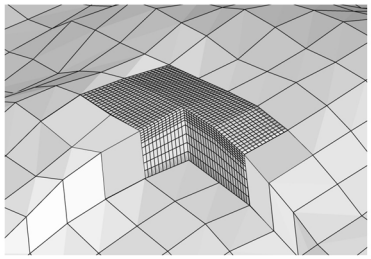

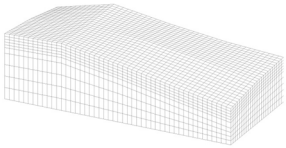

Detail of heterogeneous valley

127

Matsuzaki valley [Courtesy of CRS4]

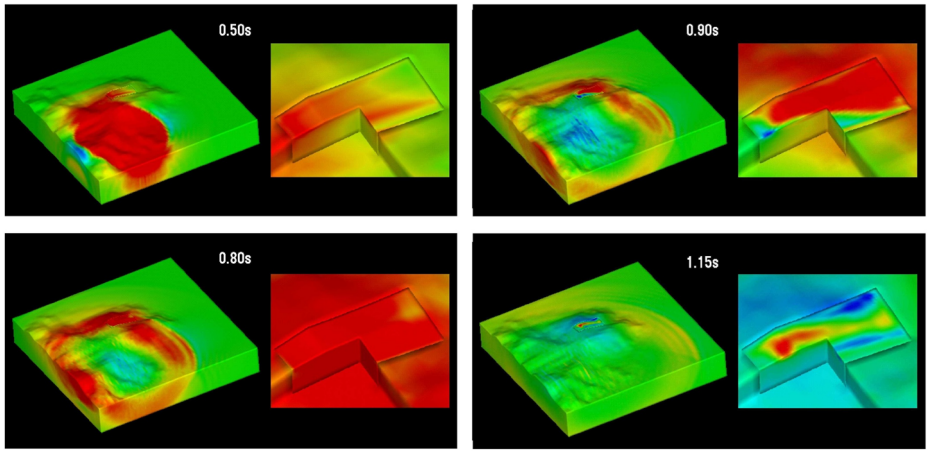

Wave propagation and detailed view of site effects due to localized soil heterogeneity

Numerical Model: 4492 Macro SE, 121284 Micro SE, 11520 FE, 145806 nodes

128

Performance Optimization

- All examples seen so far used the same time increment $\Delta t(t)$ for all elements in the mesh.
- Can be penalizing in explicit methods, especially in 3D when mesh is locally very fine. The smallest element drives the calculation's time increment.

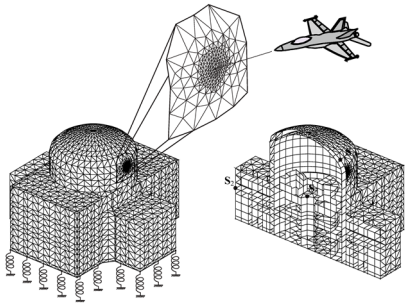

FIGURE [2.3.4.2] : *Ilot nucléaire - Maillage et conditions aux limites*

- Alternative strategies where the step varies both in time and in space: $\Delta t(x,t)$.
  - Spatial time step partitioning
  - Domain decomposition

129

Time Step Partitioning

- Due to J.P. Halleux (1985!)
- Time step is automatically varied in space according to a binary partition (1, ½, ¼, etc.).
- Simple and elegant: activated by **OPTI PART**.
- Each element is integrated with a step much closer to its stability limit than usual (better accuracy!)
- However, difficulties in B.C.s: any nodes subjected to essential conditions are associated with the deepest partition level (smallest step) at the moment.

130

Time Step Partitioning (2)

- Build up partition levels according to binary rule:

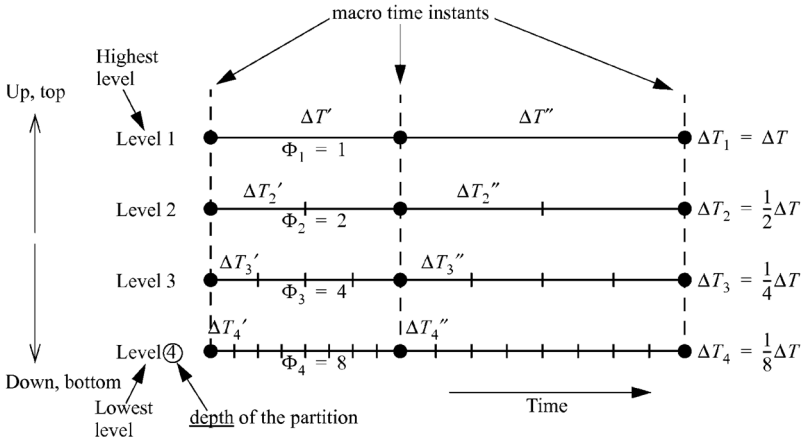

Example of two consecutive macro steps in a binary partition with 4 levels

131

Time Step Partitioning (3)

- Partitioning trivial for unconnected mesh

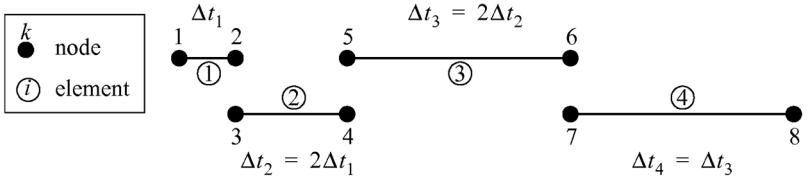

A simple mesh of independent elements

- Complexity arises from element connections through nodes (or from boundary conditions!)

132

Time Step Partitioning (4)

- Intrinsic element frequency:

$$\varphi_i = \Phi_l \quad \text{such that} \quad \Delta T_{l+1} < \Delta t_i \le \Delta T_l \qquad i = 1, \ldots, N_e$$

- Intrinsic node frequency:

$$\psi_k^{\text{free}} = \max\,(\varphi_j) \qquad j = \text{any element sharing node } k \qquad k = 1, \cdots, N_n$$

Used to update *nodal accelerations and velocities*

- Neighbouring element frequency:

$$\bar{\varphi}_i = \max\,(\psi_m) \qquad m = \text{any node of element } i \qquad i = 1, \ldots, N_e$$

Used to update *element quantities*

- Neighbouring node frequency:

$$\bar{\psi}_k = \max\,(\bar{\varphi}_j) \qquad j = \text{any element sharing node } k \qquad k = 1, \cdots, N_n$$

Used to update *nodal configurations*

133

Time Step Partitioning (5)

- Consider following simple example:

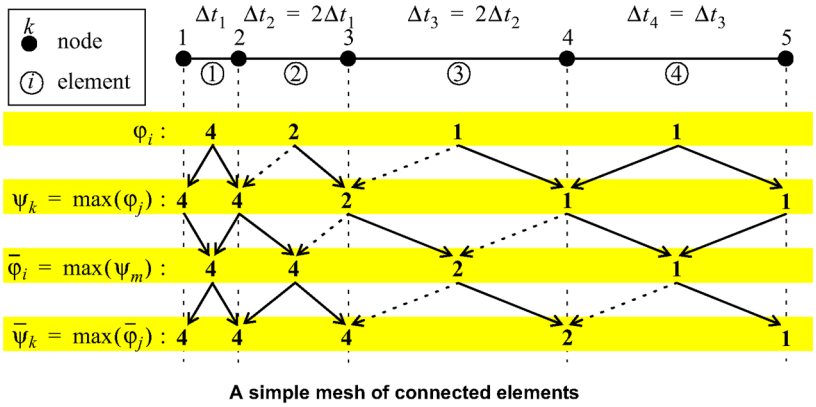

A simple mesh of connected elements

134

Time Step Partitioning (6)

- This leads to the following partition:

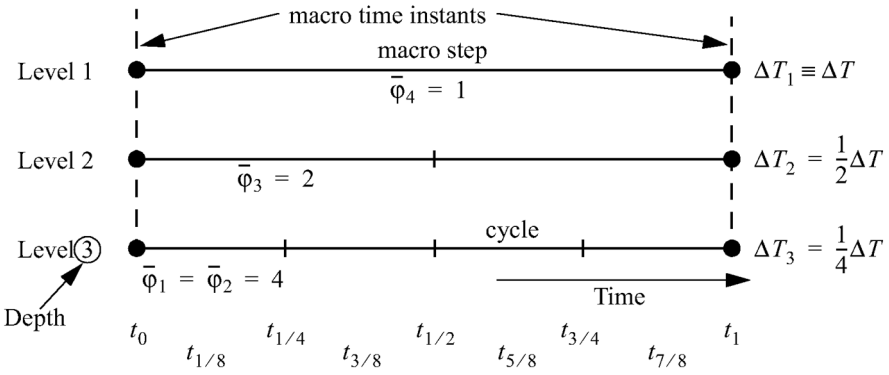

Partition for the mesh shown in the previous Figure

Time Step Partitioning (7)

- Advancing solution in time:

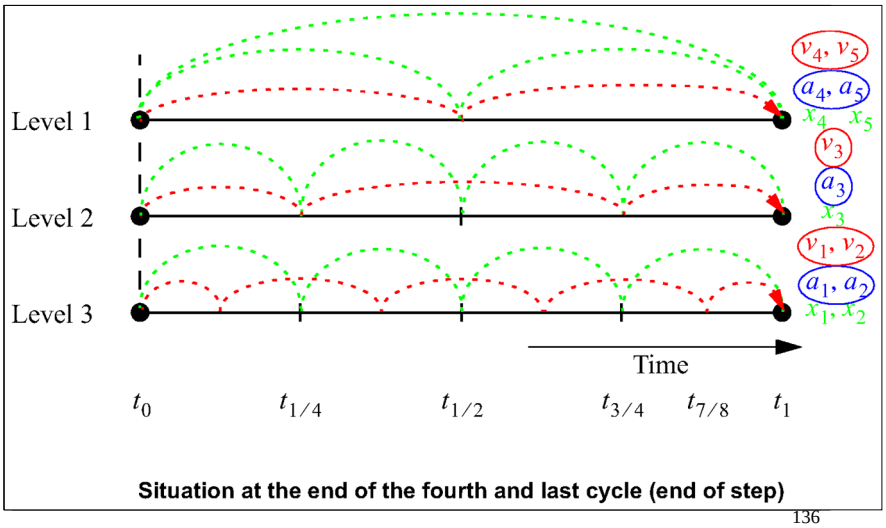

Situation at the end of the fourth and last cycle (end of step)

Time Step Partitioning (8)

- Activity chart:

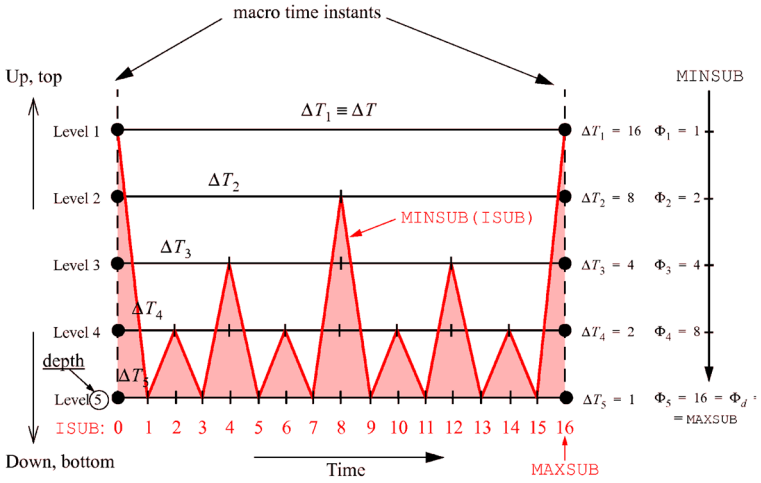

137

Illustration of the meaning of MAXSUB and MINSUB

Treatment of links in partitioning (1)

- First method - assign any linked nodes to lowest partition level:

  $\psi_k^{\text{link}} = \Phi_d \equiv 2^{d-1}$ for any node k subjected to a link

- Then treat by standard Lagrange multipliers technique (recall Part 1)
- Advantages:
  - Extremely simple to implement (if limited to permanent links)
- Drawbacks:
  - Can reduce efficiency if there are many links
  - Deals only with permanent links (synchronization) if search for linked dofs is done just once

138

Treatment of links in partitioning (2)

- Second method (for a permanent link):
  - For nodes *k* subjected to a link compute: $\psi_{\max} = \max_k(\psi_k^{\text{free}})$
  - For the same nodes, set: $\psi_k^{\text{link}} = \psi_{\max}$
  - Consequently, all nodes affected by the link are integrated by the same time increment (synchronized): $\delta t_L = \Delta t_{\max} / \psi_k^{\text{link}} = \Delta t_{\max} / \psi_{\max}$
- Advantages:
  - Fully general (see below for non-permanent links)
  - More efficient than first method, at least potentially
- Drawbacks:
  - More difficult to implement

Treatment of links in partitioning (3)

- For non-permanent links: synchronization issue

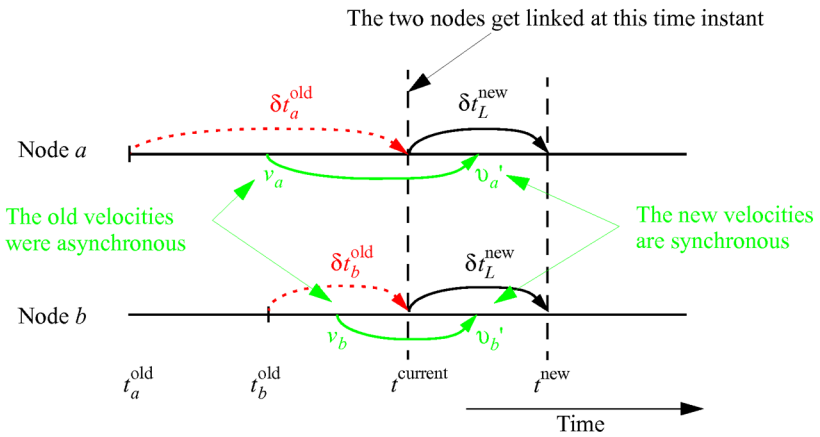

Lack of synchronization in a non-permanent link

Treatment of links in partitioning (4)

- The Lagrange multipliers method (recall Part 1) can be generalized as follows $\underline{C}\underline{v} = \underline{b} \rightarrow \underline{A}\underline{\lambda} = \underline{z}$
- Synchronous case:

$$\underline{A} = \underline{C}\gamma\underline{m}^{-1}\underline{C}^T \qquad \underline{z} = \underline{b} - \underline{C}\underline{v}^{n+1/2} - \underline{C}\gamma\underline{m}^{-1}(\underline{f}^e - \underline{f}^i) \qquad \gamma = \frac{\Delta t^n + \Delta t^{n+1}}{2}$$

- Asynchronous case: just replace the scalar γ by the matrix:

$$\underline{\Gamma} = \text{diag}\,(\gamma_i) \qquad \gamma_i = \frac{\delta t_i^{\text{old}} + \delta t_L^{\text{new}}}{2}$$

- The connections matrix remains symmetric and positive definite like in the synchronous case.

141

Example 12a – Taylor bar impact revisited

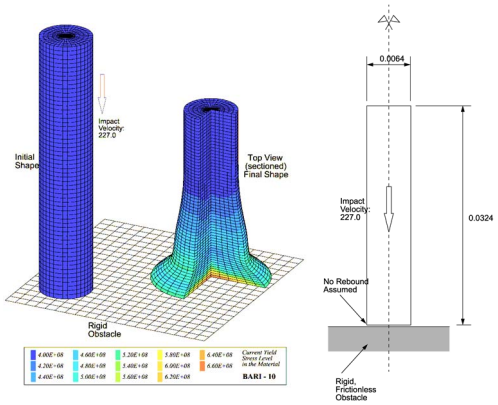

Material Data	
Density	8930
Young's Modulus	1.17×10^{11}
Yield Stress	4.0×10^{8}
Plastic Modulus	1.0×10^{8}
Poisson's Ratio	0.35

- A - Solution with spatially uniform time increment (BAMD01)
- B - Solution with space partitioning (BAMD03)

142

Example 12a – Taylor bar impact revisited (2)

- Comparison of solutions (final yield stress):

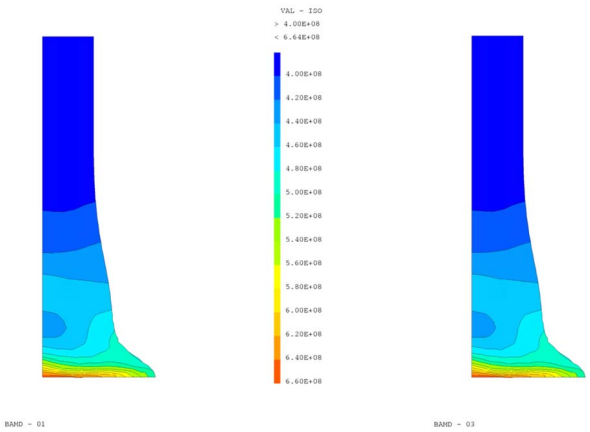

Standard Partition

143

Example 12a – Taylor bar impact revisited (3)

- Comparison of solutions:

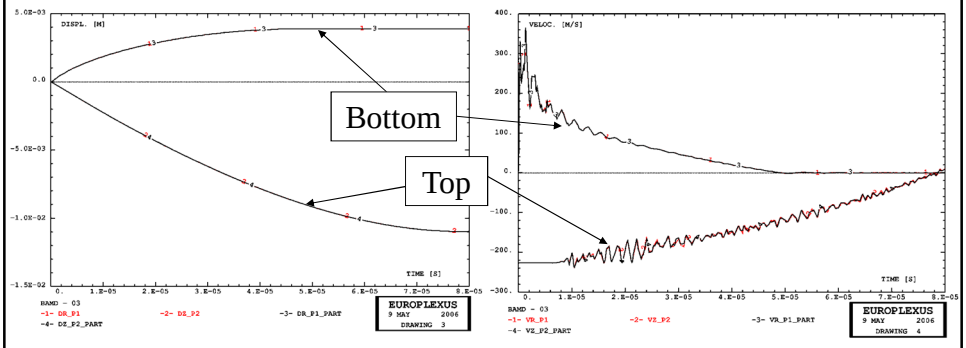

Displacements Velocities

144

Example 12a – Taylor bar impact revisited (4)

- Comparison of solutions (time increments):

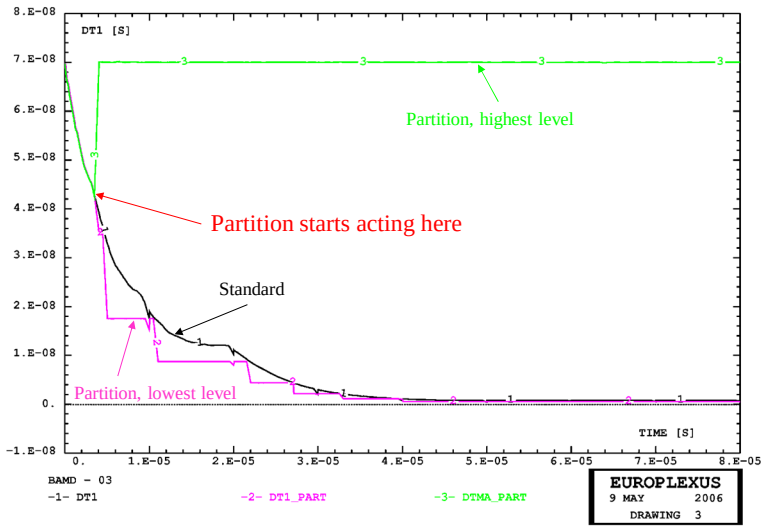

145

The partition at work (final time on initial geom):

Element frequency

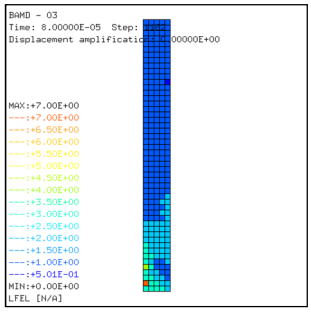

Node frequency

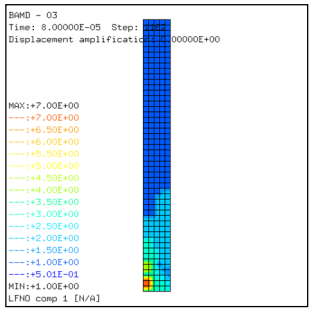

Element neighbour frequency

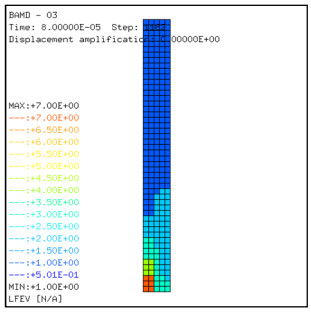

Node neighbour frequency

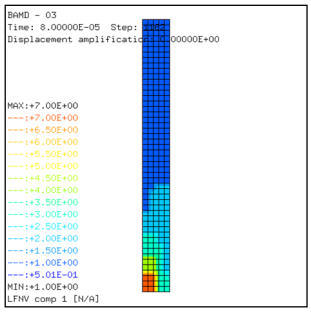

146

Example 12a – Taylor bar impact revisited (6)

- Performance comparison:

Case	Time Integr.	Steps	Cycles	Maximum frequency	Elements * cycles	CPU (s)	Speedup (theor. / actual)
BAMD01	AUTO	59886	—	—	14,971,750	55.7	—
BAMD03	PART	1162	85537	128	1,296,171	6.6	11.6 / **8.4**

- To activate the partition, simply add:

OPTI PART

147

Domain Decomposition

References: see A. Combescure (ENS Cachan), B. Herry, A. Gravouil, N. Bousquet, V. Faucher (2000-2004)

Goal: multi-scale problems in time and space.

- Use appropriate time integration step in each s/d:
  - Couple s/d's with different (and variable) time steps
- Use appropriate time integration scheme in each s/d:
  - Any of the Newmark "beta" time schemes can be coupled
  - Explicit-explicit or explicit-implicit coupling is possible
- Open the way to special techniques:
  - E.g.: combine modal analysis (linear vibrations) with direct time integration
  - Treat vibrating parts in large rotations (rotating machinery)

148

Coupling at the Interfaces

- Two approaches possible: primal or dual

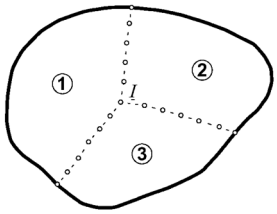

Continuity of kinematic quantities is satisfied *a priori* (same nodes)

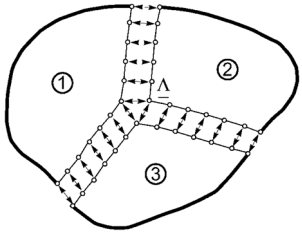

Continuity of kinematic quantities is enforced by suitable conditions (different nodes)

- We use a dual approach:
  - More general also in view of non-conforming interfaces

149

Coupling at the Interfaces (2)

Dual approach (Gravouil & Combescure, 2001)

- Simplest case: 2 S/Ds, conforming interface, same Δt

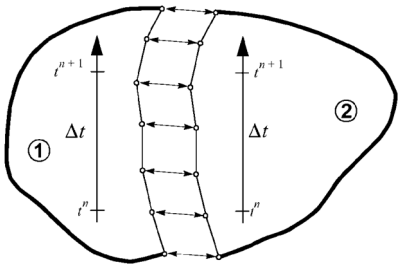

- The coupled problem can be written as:

$$\begin{cases} \underline{M}_1\ddot{\underline{U}}_1 = \underline{F}_1 + \underline{R}_1 \\ \underline{M}_2\ddot{\underline{U}}_2 = \underline{F}_2 + \underline{R}_2 \\ \underline{C}_1\dot{\underline{U}}_1 + \underline{C}_2\dot{\underline{U}}_2 = \underline{0} \end{cases}$$

$\Leftarrow$ equilibrium

$\Leftarrow$ continuity at interface (constraint)

$\underline{F}_i \doteq \underline{F}_i^{\text{ext}} - \underline{F}_i^{\text{int}}$

$i = 1,2$ (sub-domain index)

$\underline{R}_i \doteq$ interface reactions

150

$$\begin{cases} \underline{M}_1\ddot{\underline{U}}_1 = \underline{F}_1 + \underline{R}_1 \\ \underline{M}_2\ddot{\underline{U}}_2 = \underline{F}_2 + \underline{R}_2 \\ \underline{C}_1\dot{\underline{U}}_1 + \underline{C}_2\dot{\underline{U}}_2 = \underline{0} \end{cases}$$

Coupling at the Interfaces (3)

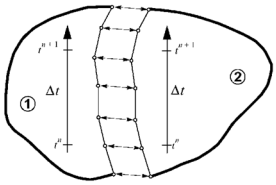

- It can be useful to split the problem into a *free* and a *link* problem by an additive decomposition. Define:

$$\begin{aligned} \ddot{\underline{U}}_{i,\text{free}} &\doteq \underline{M}_i^{-1}\underline{F}_i \\ \ddot{\underline{U}}_{i,\text{link}} &\doteq \underline{M}_i^{-1}\underline{R}_i \end{aligned}$$

so that: $\ddot{\underline{U}}_i = \ddot{\underline{U}}_{i,\text{free}} + \ddot{\underline{U}}_{i,\text{link}}$

- The problem becomes:

Free problem (involves all dofs) $\begin{cases} \underline{M}_1\ddot{\underline{U}}_{1,\text{free}} = \underline{F}_1 \\ \underline{M}_2\ddot{\underline{U}}_{2,\text{free}} = \underline{F}_2 \end{cases}$ + $\begin{cases} \underline{M}_1\ddot{\underline{U}}_{1,\text{link}} = \underline{R}_1 \\ \underline{M}_2\ddot{\underline{U}}_{2,\text{link}} = \underline{R}_2 \\ \underline{C}_1\dot{\underline{U}}_1 + \underline{C}_2\dot{\underline{U}}_2 = \underline{0} \end{cases}$ *Link* problem (involves only dofs on interface)

151

$$\begin{cases} \underline{M}_1\ddot{\underline{U}}_{1,\text{free}} = \underline{F}_1 \\ \underline{M}_2\ddot{\underline{U}}_{2,\text{free}} = \underline{F}_2 \end{cases}$$

Coupling at the Interfaces (4)

$$\begin{cases} \underline{M}_1\ddot{\underline{U}}_{1,\text{link}} = \underline{R}_1 \\ \underline{M}_2\ddot{\underline{U}}_{2,\text{link}} = \underline{R}_2 \\ \underline{C}_1\dot{\underline{U}}_1 + \underline{C}_2\dot{\underline{U}}_2 = \underline{0} \end{cases}$$

- The *free* problem can be solved directly to obtain $\ddot{\underline{U}}_{i,\text{free}}$
- To solve the *link* problem, we introduce as usual Lagrange multipliers and associated reaction (interaction) forces:

$$\underline{R}_i = \underline{C}_i^T\underline{\Lambda}$$

so that:

$$\begin{aligned} \underline{M}_1\ddot{\underline{U}}_{1,\text{link}} - \underline{C}_1^T\underline{\Lambda} &= \underline{0} \\ \underline{M}_2\ddot{\underline{U}}_{2,\text{link}} - \underline{C}_2^T\underline{\Lambda} &= \underline{0} \\ \underline{C}_1\dot{\underline{U}}_1 + \underline{C}_2\dot{\underline{U}}_2 &= \underline{0} \end{aligned}$$

Unknowns: $\ddot{\underline{U}}_{i,\text{link}}$, $\underline{\Lambda}$ and $\dot{\underline{U}}_i$

152

Coupling at the Interfaces (5)

$$\underline{M}_1\ddot{\underline{U}}_{1,\text{link}} - \underline{C}_1^T\underline{\Lambda} = \underline{0}$$
$$\underline{M}_2\ddot{\underline{U}}_{2,\text{link}} - \underline{C}_2^T\underline{\Lambda} = \underline{0}$$
$$\underline{C}_1\dot{\underline{U}}_1 + \underline{C}_2\dot{\underline{U}}_2 = \underline{0}$$

- We express the unknown velocities $\dot{\underline{U}}_i$ in terms of the accelerations. By using CD time integration scheme (recall Part 1)

$$\dot{\underline{U}} = \dot{\underline{U}}^n + \frac{\Delta t}{2}(\ddot{\underline{U}}^n + \ddot{\underline{U}})$$

- By introducing the velocity predictor (or mid-step velocity):

$${}^p\dot{\underline{U}} \doteq \dot{\underline{U}}^n + \frac{\Delta t}{2}\ddot{\underline{U}}^n \equiv \dot{\underline{U}}^{n+1/2}$$

one gets:

$$\dot{\underline{U}} = {}^p\dot{\underline{U}} + \frac{\Delta t}{2}\ddot{\underline{U}}$$

- By splitting the acceleration this becomes:

$$\dot{\underline{U}} = {}^p\dot{\underline{U}} + \frac{\Delta t}{2}\ddot{\underline{U}}_{\text{free}} + \frac{\Delta t}{2}\ddot{\underline{U}}_{\text{link}}$$

153

Coupling at the Interfaces (6)

$$\dot{\underline{U}} = {}^p\dot{\underline{U}} + \frac{\Delta t}{2}\ddot{\underline{U}}_{\text{free}} + \frac{\Delta t}{2}\ddot{\underline{U}}_{\text{link}}$$

$$\underline{M}_1\ddot{\underline{U}}_{1,\text{link}} - \underline{C}_1^T\underline{\Lambda} = \underline{0}$$
$$\underline{M}_2\ddot{\underline{U}}_{2,\text{link}} - \underline{C}_2^T\underline{\Lambda} = \underline{0}$$
$$\underline{C}_1\dot{\underline{U}}_1 + \underline{C}_2\dot{\underline{U}}_2 = \underline{0}$$

- We see therefore that also the velocities can be formally split into a *free* and a *link* part. By defining:

(known) $\rightarrow$ $\boxed{\dot{\underline{U}}_{\text{free}} \doteq {}^p\dot{\underline{U}} + \frac{\Delta t}{2}\ddot{\underline{U}}_{\text{free}}}$ $\qquad$ $\boxed{\dot{\underline{U}}_{\text{link}} \doteq \frac{\Delta t}{2}\ddot{\underline{U}}_{\text{link}}}$

so that:

$$\boxed{\dot{\underline{U}} = \dot{\underline{U}}_{\text{free}} + \dot{\underline{U}}_{\text{link}}}$$

one gets for the link problem:

$$\begin{cases} \underline{M}_1\ddot{\underline{U}}_{1,\text{link}} - \underline{C}_1^T\underline{\Lambda} = \underline{0} \\ \underline{M}_2\ddot{\underline{U}}_{2,\text{link}} - \underline{C}_2^T\underline{\Lambda} = \underline{0} \\ -\frac{\Delta t}{2}\underline{C}_1\ddot{\underline{U}}_{1,\text{link}} - \frac{\Delta t}{2}\underline{C}_2\ddot{\underline{U}}_{2,\text{link}} = \underline{C}_1\dot{\underline{U}}_{1,\text{free}} + \underline{C}_2\dot{\underline{U}}_{2,\text{free}} \end{cases}$$

154

Coupling at the Interfaces (7)

$$\begin{cases} \underline{M}_1\ddot{\underline{U}}_{1,\text{link}} - \underline{C}_1^T\underline{\Lambda} = \underline{0} \\ \underline{M}_2\ddot{\underline{U}}_{2,\text{link}} - \underline{C}_2^T\underline{\Lambda} = \underline{0} \\ -\frac{\Delta t}{2}\underline{C}_1\ddot{\underline{U}}_{1,\text{link}} - \frac{\Delta t}{2}\underline{C}_2\ddot{\underline{U}}_{2,\text{link}} = \underline{C}_1\dot{\underline{U}}_{1,\text{free}} + \underline{C}_2\dot{\underline{U}}_{2,\text{free}} \end{cases}$$

- By condensing on the Lagrange multipliers one obtains formally:

$$\ddot{\underline{U}}_{1,\text{link}} = \underline{M}_1^{-1}\underline{C}_1^T\underline{\Lambda}$$

$$\ddot{\underline{U}}_{2,\text{link}} = \underline{M}_2^{-1}\underline{C}_2^T\underline{\Lambda}$$

$$-\frac{\Delta t}{2}\underline{C}_1\underline{M}_1^{-1}\underline{C}_1^T\underline{\Lambda} - \frac{\Delta t}{2}\underline{C}_2\underline{M}_2^{-1}\underline{C}_2^T\underline{\Lambda} = \underline{C}_1\dot{\underline{U}}_{1,\text{free}} + \underline{C}_2\dot{\underline{U}}_{2,\text{free}}$$

- By posing:

$$\boxed{\underline{H} \doteq \frac{\Delta t}{2}(\underline{C}_1\underline{M}_1^{-1}\underline{C}_1^T + \underline{C}_2\underline{M}_2^{-1}\underline{C}_2^T)} \qquad \text{(Steklov-Poincaré operator)}$$

$$\boxed{\underline{d} \doteq -(\underline{C}_1\dot{\underline{U}}_{1,\text{free}} + \underline{C}_2\dot{\underline{U}}_{2,\text{free}})}$$

one obtains the linear system: $\boxed{\underline{H}\underline{\Lambda} = \underline{d}}$

which upon solution yields the Lagrange multipliers $\underline{\Lambda}$, then the link accelerations $\ddot{\underline{U}}_{i,\text{link}}$

155

Coupling at the Interfaces (8)

Summarizing, the problem can be written in matrix form:

- First, solve the problem <u>without</u> links (*free*). Symbolically:

$$\begin{bmatrix} \underline{M}_1 & 0 & 0 \\ 0 & \underline{M}_2 & 0 \\ 0 & 0 & 0 \end{bmatrix}\begin{bmatrix} \ddot{\underline{U}}_{1,\text{free}} \\ \ddot{\underline{U}}_{2,\text{free}} \\ 0 \end{bmatrix} = \begin{bmatrix} \underline{F}_1 \\ \underline{F}_2 \\ 0 \end{bmatrix}$$

Standard problem! Use single-domain operators.

- Then, solve the problem <u>with</u> links (*link*). Symbolically:

$$\frac{\Delta t}{2}\begin{bmatrix} \underline{M}_1 & 0 & -\underline{C}_1^T \\ 0 & \underline{M}_2 & -\underline{C}_2^T \\ -\underline{C}_1 & -\underline{C}_2 & 0 \end{bmatrix}\begin{bmatrix} \ddot{\underline{U}}_{1,\text{link}} \\ \ddot{\underline{U}}_{2,\text{link}} \\ \underline{\Lambda} \end{bmatrix} = \begin{bmatrix} 0 \\ 0 \\ \underline{C}_1\dot{\underline{U}}_{1,\text{free}} + \underline{C}_2\dot{\underline{U}}_{2,\text{free}} \end{bmatrix}$$

Thanks to diagonal mass matrix, the problem with links is confined only to the interfaces!

156

Coupling at the Interfaces (9)

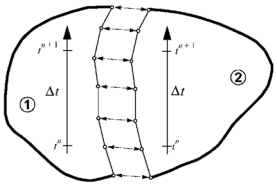

Time integration flowchart is as follows:

- Let complete solution be known at time t^n: $\underline{U}_i^n, \underline{\dot{U}}_i^n, \underline{\ddot{U}}_i^n$
- Compute mid-step velocities (i.e. predictors): ${}^p\underline{\dot{U}}_i \doteq \underline{\dot{U}}_i^n + \frac{\Delta t}{2}\underline{\ddot{U}}_i^n$
- Compute new configurations: $\underline{U}_i = \underline{U}_i^n + \Delta t\, {}^p\underline{\dot{U}}_i$
- Solve *free* problem for accelerations: $\underline{\ddot{U}}_{i,\text{free}} = \underline{M}_i^{-1}\underline{F}_i$
- Compute new free velocities: $\underline{\dot{U}}_{i,\text{free}} \doteq {}^p\underline{\dot{U}}_i + \frac{\Delta t}{2}\underline{\ddot{U}}_{i,\text{free}}$
- Compute: $\underline{H} \doteq \frac{\Delta t}{2}(\underline{C}_1\underline{M}_1^{-1}\underline{C}_1^T + \underline{C}_2\underline{M}_2^{-1}\underline{C}_2^T)$ and $\underline{d} \doteq -(\underline{C}_1\underline{\dot{U}}_{1,\text{free}} + \underline{C}_2\underline{\dot{U}}_{2,\text{free}})$

157

Coupling at the Interfaces (10)

- Solve linear system for the Lagrange multipliers:

$$\underline{H}\,\underline{\Lambda} = \underline{d} \quad \rightarrow \quad \underline{\Lambda} = \underline{H}^{-1}\underline{d}$$

$\underline{H}$ is diagonal for conforming interface!

- Compute interaction forces: $\underline{R}_i = \underline{C}_i^T\,\underline{\Lambda}$
- Compute link accelerations: $\underline{\ddot{U}}_{i,\text{link}} \doteq \underline{M}_i^{-1}\underline{R}_i$ $\underline{M}$ is diagonal!
- Compute total accelerations: $\underline{\ddot{U}}_i = \underline{\ddot{U}}_{i,\text{free}} + \underline{\ddot{U}}_{i,\text{link}}$
- Compute new velocities: $\underline{\dot{U}}_i = \underline{\dot{U}}_{i,\text{free}} + \frac{\Delta t}{2}\underline{\ddot{U}}_{i,\text{link}}$

158

Multiple scales in time

- Use <u>appropriate</u> time scale in each S/D
- Simplest case: <u>constant</u> steps, <u>hierarchic</u> case (exact multiples: $\Delta t_1 = m\Delta t_2$)
- Enforce continuity on <u>finest</u> time scale:

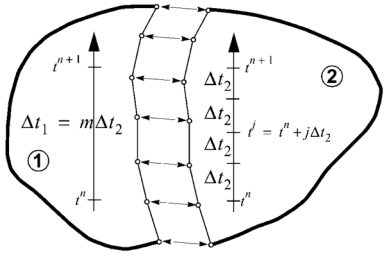

$$\boxed{\underline{C}_1\dot{\underline{U}}_1^j + \underline{C}_2\dot{\underline{U}}_2^j = 0}$$ at generic instant $t^j = t^n + j\Delta t_2$

- By decomposing the velocities this becomes:

$$\underline{C}_1\dot{\underline{U}}_{1,\text{link}}^j + \underline{C}_2\dot{\underline{U}}_{2,\text{link}}^j = -(\underline{C}_1\dot{\underline{U}}_{1,\text{free}}^j + \underline{C}_2\dot{\underline{U}}_{2,\text{free}}^j)$$

159

Multiple scales in time (2)

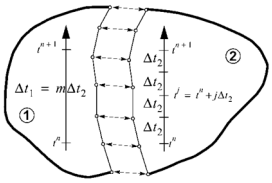

- Solve *free* problem for both S/Ds:

$$\boxed{\underline{M}_1\ddot{\underline{U}}_{1,\text{free}} = \underline{F}_1}$$ for S/D 1 at time t^{n+1} $\qquad$ $$\boxed{\underline{M}_2\ddot{\underline{U}}_{2,\text{free}}^j = \underline{F}_2^j}$$ for S/D 2 at time t^j $\qquad$ $\Rightarrow \dot{\underline{U}}_{1,\text{free}}$ and $\dot{\underline{U}}_{2,\text{free}}^j$

- Estimate free velocity of S/D 1 at t^j by <u>linear interpolation</u>:

$$\boxed{\dot{\underline{U}}_{1,\text{free}}^j = (1-\alpha_j)\dot{\underline{U}}_{1,\text{free}}^n + \alpha_j\dot{\underline{U}}_{1,\text{free}}}$$ with $\alpha_j \doteq j/m$

- Same thing can be done for link velocity:

$$\boxed{\dot{\underline{U}}_{1,\text{link}}^j = (1-\alpha_j)\dot{\underline{U}}_{1,\text{link}}^n + \alpha_j\dot{\underline{U}}_{1,\text{link}}}$$

160

Multiple scales in time (3)

- Express link velocities via link accelerations (multipliers).
  For S/D 2: $\boxed{\underline{\dot{U}}^{j}_{2,\text{link}} = \frac{\Delta t_2}{2} \underline{M}_2^{-1} \underline{C}_2^T \underline{\Lambda}^{j}}$

- For S/D 1: $\underline{\dot{U}}^{n}_{1,\text{link}} = \frac{\Delta t_1}{2} \underline{M}_1^{-1} \underline{C}_1^T \underline{\Lambda}^{n}$ at time t^n

  $\underline{\dot{U}}_{1,\text{link}} = \frac{\Delta t_1}{2} \underline{M}_1^{-1} \underline{C}_1^T \underline{\Lambda}$ at time t^{n+1}

- This, replaced into previous linear interpolation, yields:

$$\boxed{\underline{\dot{U}}^{j}_{1,\text{link}} = \frac{\Delta t_1}{2} \underline{M}_1^{-1} \underline{C}_1^T \underbrace{[(1-\alpha_j)\underline{\Lambda}^{n} + \alpha_j \underline{\Lambda}]}_{\underline{\Lambda}^{j}}}$$

161

Multiple scales in time (4)

- This corresponds to assuming that the <u>interface stresses vary linearly</u> between any two "coarse" instants t^n and t^{n+1}.

- Finally we obtain the linear system:

$$\boxed{\underline{H}\,\underline{\Lambda}^{j} = \underline{B}^{j}}$$

$$\boxed{\begin{aligned} \underline{H} &\doteq \frac{\Delta t_2}{2}(m\underline{C}_1\underline{M}_1^{-1}\underline{C}_1^T + \underline{C}_2\underline{M}_2^{-1}\underline{C}_2^T) \\ \underline{B}^{j} &\doteq -(\underline{C}_1\underline{\dot{U}}^{j}_{1,\text{free}} + \underline{C}_2\underline{\dot{U}}^{j}_{2,\text{free}}) \end{aligned}}$$

162

Multiple scales in time (5)

- The process can be generalized similarly to the case of fully variable and independent time scales:

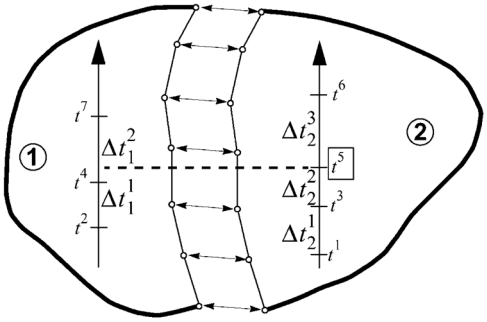

- Enforce continuity on union of the two time scales. E.g:

$$\underline{C}_1\dot{\underline{U}}_1^5 + \underline{C}_2\dot{\underline{U}}_2^5 = 0$$ at generic instant t^5

Multiple scales in time (6)

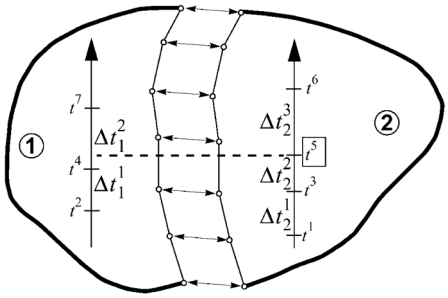

- We obtain the linear system:

$$\underline{H}\,\underline{\Lambda}^5 = \underline{B}^5$$

$$\underline{H} \doteq \frac{\Delta t_1^2}{2}\underline{C}_1\underline{M}_1^{-1}\underline{C}_1^T + \frac{\Delta t_2^2}{2}\underline{C}_2\underline{M}_2^{-1}\underline{C}_2^T$$

$$\underline{B}^5 \doteq -(\underline{C}_1\dot{\underline{U}}_{1,\text{free}}^5 + \underline{C}_2\dot{\underline{U}}_{2,\text{free}}^5) - \underline{C}_1(1-\alpha_5)(\beta_5 - 1)\frac{\Delta t_1^2}{2}\ddot{\underline{U}}_{1,\text{link}}^4$$

$$\alpha_5 \doteq \frac{t_5 - t_4}{t_6 - t_4} \qquad \beta_5 \doteq \frac{\Delta t_1^1}{\Delta t_1^2}$$

Multiple scales in space

- Further gains can be obtained by allowing non-conforming meshes at the interfaces:

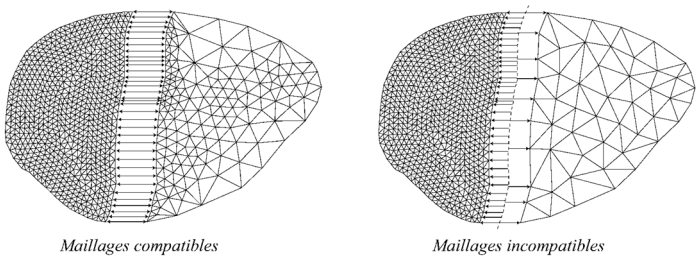

FIGURE [1.2.4.1] : *Maillages non-conformes - Découplage de la taille des éléments*

- Kinematic continuity has to be imposed on the interface I . At the continuous level in space (i.e. before discretization):

$$\boxed{\underline{\dot{U}}_1\big|_I = \underline{\dot{U}}_2\big|_I}$$

165

Multiple scales in space (2)

- We impose continuity on the discrete mesh by means of Lagrange multipliers.
- Several alternatives are possible, depending on spatial location (support) of multipliers.
- LBB condition must be satisfied!
  - Space of multipliers should not be too rich
  - Number of conditions < than total number of concerned dofs
  - Too few conditions: loose coupling
  - Too many conditions: singular problem or spurious "locking" of the interface

166

Multiple scales in space (3)

- "Optimal" method [Herry *et al.*, 2002]: support is union of interface nodes. Exact in 2D plane linear.
- Perfect coupling can be overconstraining (locking) if common nodes are scarce.
- Alternative: the "mortar" method [Bernardi *et al.*, 1990]: support is one of the two meshes, usually finest one.

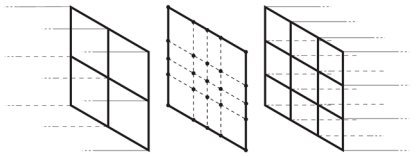

FIGURE [1.2.4.2] : *Méthode optimale - Support des multiplicateurs*

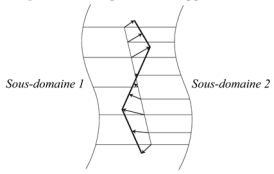

FIGURE [1.2.4.3] : *Méthode optimale 2D - Déformation possible de l'interface*

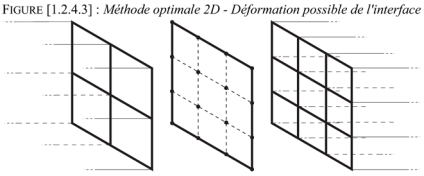

FIGURE [1.2.4.4] : *Méthode mortar - Support des multiplicateurs*

Solution of the interface problem

- In all cases we obtain a linear problem to be solved at the interfaces, of the form:

$$\underline{H}\,\underline{\Lambda} = \underline{B}$$

$\underline{H}$ ≐ interface operator
$\underline{\Lambda}$ ≐ Lagrange multipliers

- $\underline{H}$ is diagonal in the case of conforming interface, but not in the non-conforming case.
- In the presence of *cross points* $\underline{H}$ becomes singular! Suitable treatment is then needed for the solution of the system.

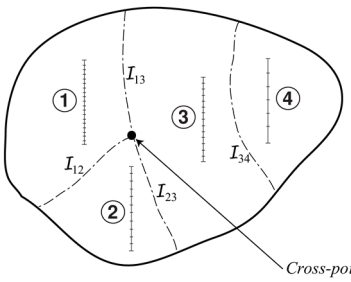

FIGURE [1.3.2.1] : *Interfaces et plusieurs échelles de temps*

168

Multiple scales in frequency

- Some large (CPU!) problems contain multiple frequency scales.
- Impact raises high frequencies and non-linear effects *locally*.
- However, the bulk structure has low-frequency vibratory behaviour (linear).
- Fine FE discretization (to fit complex geometry) is too detailed to describe linear vibrations.

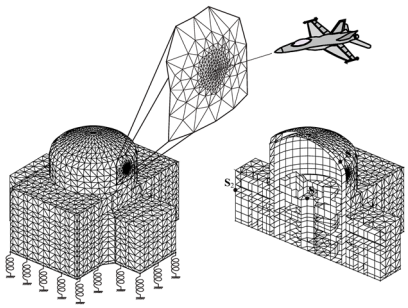

FIGURE [2.3.4.2] : *Ilot nucléaire - Maillage et conditions aux limites*

- Use modal projection: replace FE unknowns (dofs) by less numerous ones, specific to the chosen frequency spectrum.

169

Multiple scales in frequency (2)

- Domain decomposition allows to separate the frequency scales.
- How can one suitably couple a linear, "modal" S/D with a non-linear, "direct" one? One arrives to a form (S/D 1 is modal):

$$\begin{bmatrix} \frac{\Delta t}{2}\hat{\underline{M}}_1 & 0 & -\frac{\Delta t}{2}\hat{\underline{C}}_1^T \\ 0 & \frac{\Delta t}{2}\underline{M}_2 & -\frac{\Delta t}{2}\underline{C}_2^T \\ -\frac{\Delta t}{2}\hat{\underline{C}}_1 & -\frac{\Delta t}{2}\underline{C}_2 & 0 \end{bmatrix} \begin{bmatrix} \ddot{\underline{\alpha}}_1 \\ \ddot{\underline{U}}_2 \\ \underline{\Lambda} \end{bmatrix} = \begin{bmatrix} \frac{\Delta t}{2}\hat{\underline{K}}_1\underline{\alpha}_1 \\ \frac{\Delta t}{2}\underline{F}_2 \\ \hat{\underline{C}}_1\,{}^p\dot{\underline{\alpha}}_1^n + \underline{C}_2\,{}^p\dot{\underline{U}}_2^n \end{bmatrix}$$

$\underline{\alpha}_1 \doteq$ generalized unknowns:

$$\begin{cases} \underline{U}_1 = \underline{\Phi}_1\underline{\alpha}_1 \\ \dot{\underline{U}}_1 = \underline{\Phi}_1\dot{\underline{\alpha}}_1 \\ \ddot{\underline{U}}_1 = \underline{\Phi}_1\ddot{\underline{\alpha}}_1 \end{cases}$$

linear behaviour:

$$\underline{F}_1 = \underline{K}_1\underline{U}_1 = \underline{K}_1\underline{\Phi}_1\underline{\alpha}_1$$

"projected" operators:

$$\begin{cases} \hat{\underline{M}}_1 \doteq \underline{\Phi}_1^T\underline{M}_1\underline{\Phi}_1 \\ \hat{\underline{K}}_1 \doteq \underline{\Phi}_1^T\underline{K}_1\underline{\Phi}_1 \\ \hat{\underline{C}}_1 \doteq \underline{C}_1\underline{\Phi}_1 \end{cases}$$

- This coupling is totally independent from the nature of the base used for modal reduction (free choice!).
- This is possible thanks to dual approach: interface dofs don't need to remain "visible" after reduction.

170

Example: simplified engine

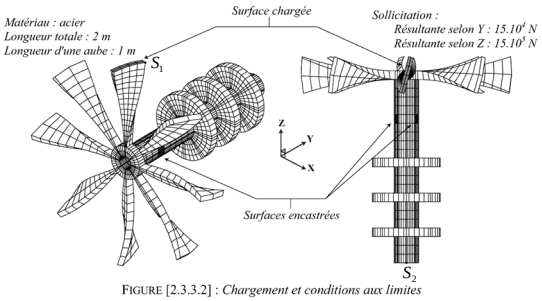

FIGURE [2.3.3.2] : *Chargement et conditions aux limites*

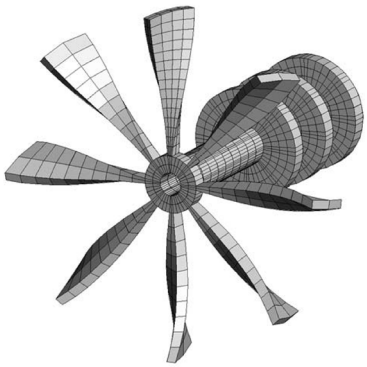

FIGURE [2.3.3.1] : *Structure 3D massive - Maillage*

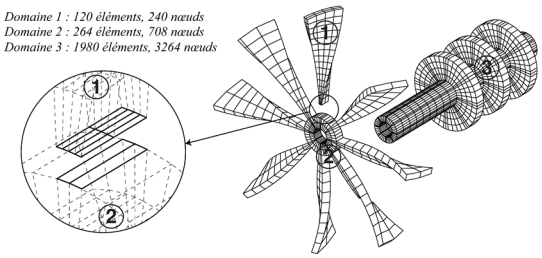

FIGURE [2.3.3.3] : *Décomposition en sous-domaines*

171

Example: simplified engine (2)

	No S/Ds	3 S/Ds	3 S/Ds (#3 modal)
dofs S/D 1	720	720	720
dofs S/D 2	2124	2124	2124
dofs S/D 3	12636	12636	50 free modes
dofs total	12636	12636	2894
Δt^{crit} S/D 3 [µ s]	0.97	**0.97**	**80.**
CPU [s]	4630	3383	693
CPU %	**100**	**73**	**14**

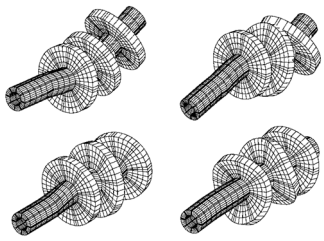

FIGURE [2.3.3.4] : *Modes propres libres sur le sous-domaine 3*

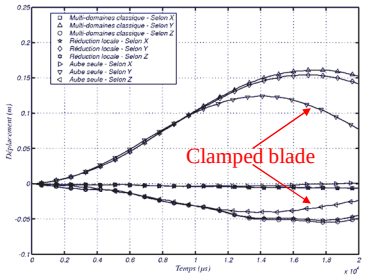

FIGURE [2.3.3.5] : *Déplacement au point* $\mathbf{S}_1$

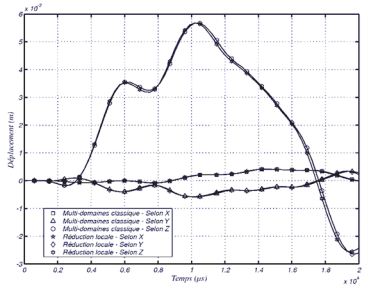

FIGURE [2.3.3.6] : *Déplacement au point* $\mathbf{S}_2$

172

Example: power plant

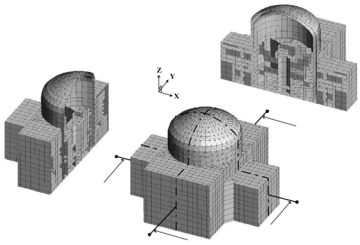

FIGURE [2.3.4.1] : *Structure 3D coque – Ilot nucléaire*

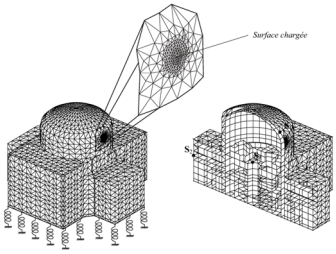

FIGURE [2.3.4.2] : *Ilot nucléaire - Maillage et conditions aux limites*

Domaine 1 : 6609 éléments à 3 nœuds et 5806 éléments à 4 noeuds
Domaine 2 : 158 éléments à 3 nœuds
Domaine 3 : 204 éléments à 3 nœuds

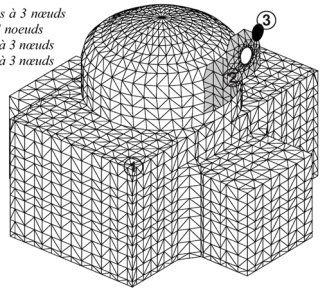

FIGURE [2.3.4.4] : *Décomposition en sous-domaines*

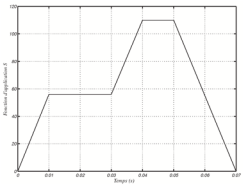

FIGURE [2.3.4.3] : *Fonction d'application temporelle du chargement*

173

Example: power plant (2)

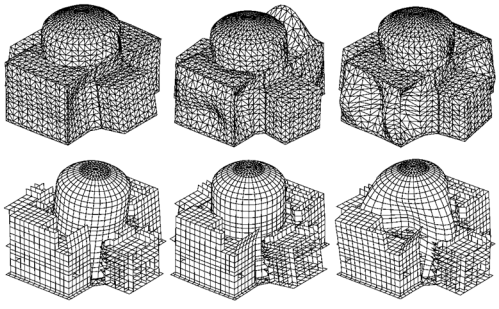

FIGURE [2.3.4.5] : *Modes de vibration encastrés (internes et externes)*

	No S/Ds	3 S/Ds	3 S/Ds (#1 modal)
dofs S/D 1	40338	40338	84 static + 150 clamped modes = 234
Δt^{crit} S/D 1 [μs]	26	**26**	**132**
CPU [s]	22722	3766	853
CPU %	**100**	**17**	**3.7**

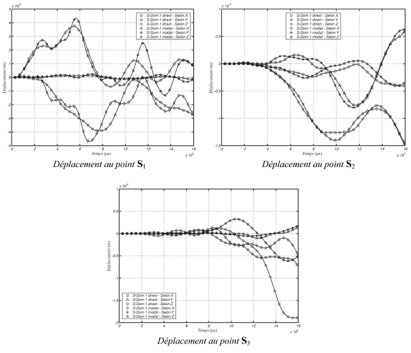

FIGURE [2.3.4.6] : *Déplacements aux points* S_1, S_2 *et* S_3

Bad results at S_3 due to wrong modeling of soil conditions (successively corrected)

174

Example: aircraft

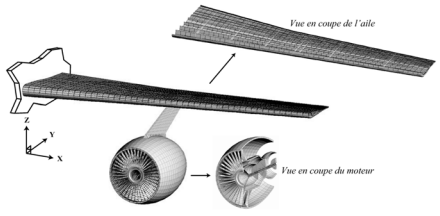

FIGURE [3.6.3.1] : *Impact sur un moteur d'avion - Maillage et conditions aux limites*

Material is linear elastic in S/Ds 1, 5 and 6, elasto-plastic in S/Ds 2, 3 and 4

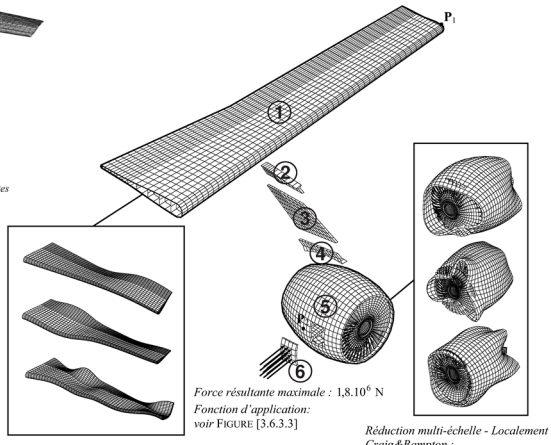

Force résultante maximale : $1{,}8.10^6$ N
Fonction d'application: voir FIGURE [3.6.3.3]

Réduction linéaire Craig&Bampton :
78 modes statiques
100 modes propres à interface fixe

Réduction multi-échelle - Localement Craig&Bampton :
189 modes statiques
150 modes propres à interface fixe

FIGURE [3.6.3.2] : *Chargement, sous-domaines et modèles réduits*

175

Example: aircraft (2)

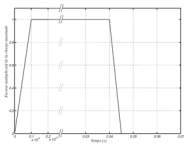

FIGURE [3.6.3.3] : *Fonction d'application temporelle du chargement*

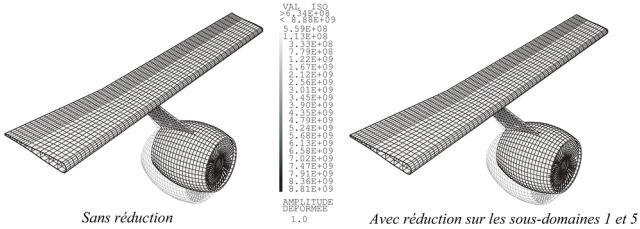

Sans réduction — *Avec réduction sur les sous-domaines 1 et 5*

FIGURE [3.6.3.4] : *Comparaison des déformées et des contraintes de Von Mises au temps final*

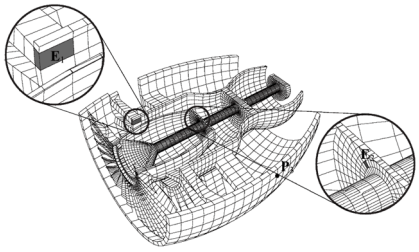

FIGURE [3.6.3.5] : *Coupe horizontale du moteur*

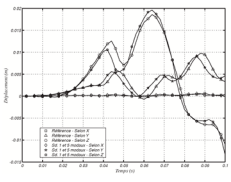

FIGURE [3.6.3.6] : *Déplacement au point* $\mathbf{P}_1$

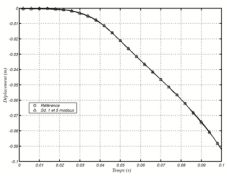

FIGURE [3.6.3.7] : *Déplacement relatif selon* x *entre les points* $\mathbf{P}_2$ et $\mathbf{P}_3$

176

Example: aircraft (3)

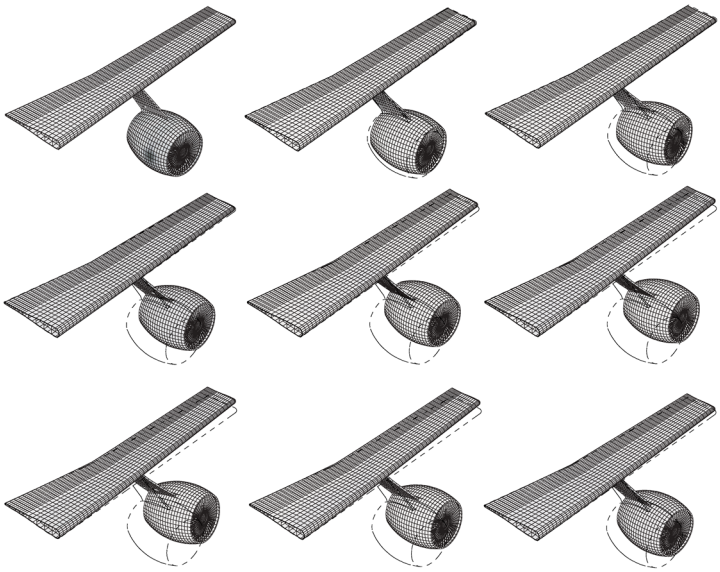

Thanks to CPU gain with modal S/Ds it was possible to pursue calculation for the whole first vibration mode of the wing

177

FIGURE [3.6.3.10] : *Simulation prolongée et premier mode d'ébranlement de l'aile*

Example 13 – Domains in 2D

- Thick plane strain beam under bending:

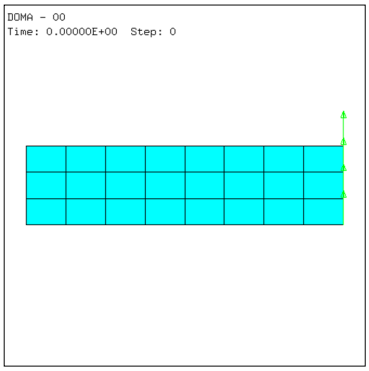

Reference Case (no decomposition)

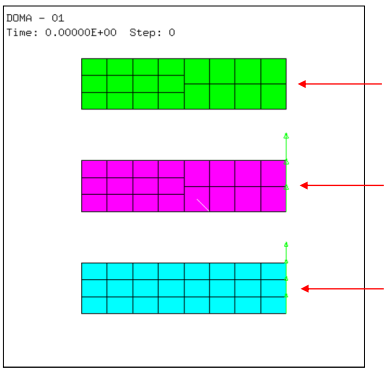

Case with various decompositions

Two non-conforming subdomains (second one is modal)

Two non-conforming subdomains

Two conforming subdomains

178

Example 13 – Domains in 2D (2)

- Tip displacement:

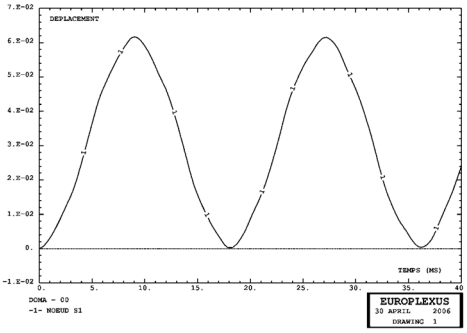

Reference Case (no decomposition)

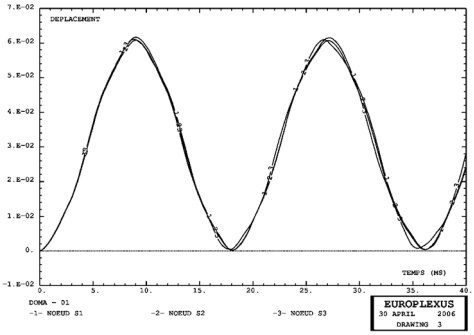

Case with various decompositions

179

Example 13 – Domains in 2D (3)

- Displacement norm field:

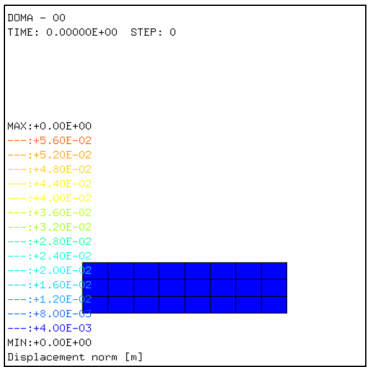

Reference Case (no decomposition)

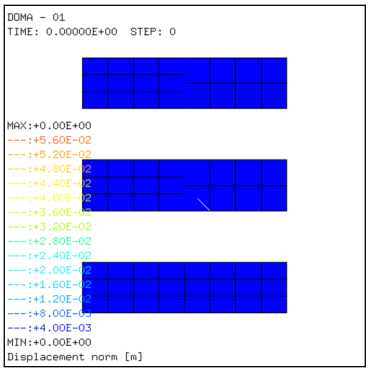

Case with various decompositions

Compare

180

Example 14 – Domains in 3D

- Thick 3D beam under bending:

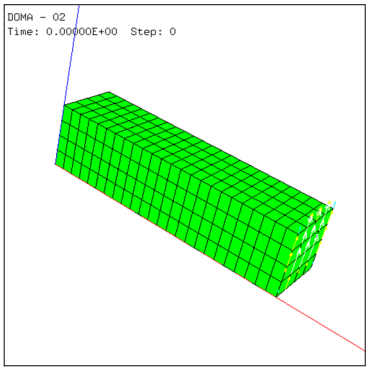

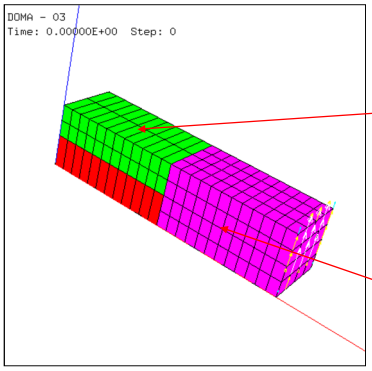

Subdomains 1 and 2 are conforming

Subdomains 1 (or 2) and 3 are non-conforming

Reference Case (no decomposition)

Case with domain decomposition

181

Example 14 – Domains in 3D (2)

- Tip displacement:

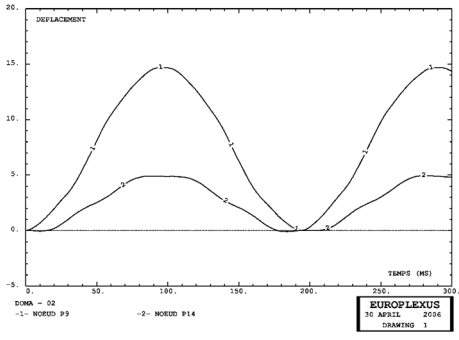

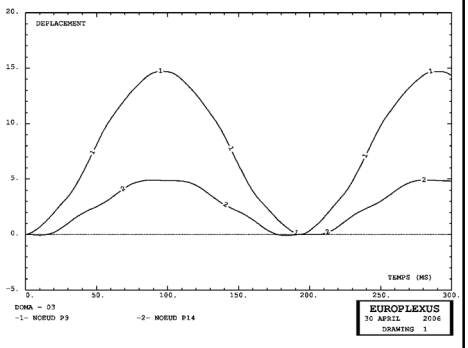

Reference Case (no decomposition)

Case with domain decomposition

182

Example 14 – Domains in 3D (3)

- Displacement norm field:

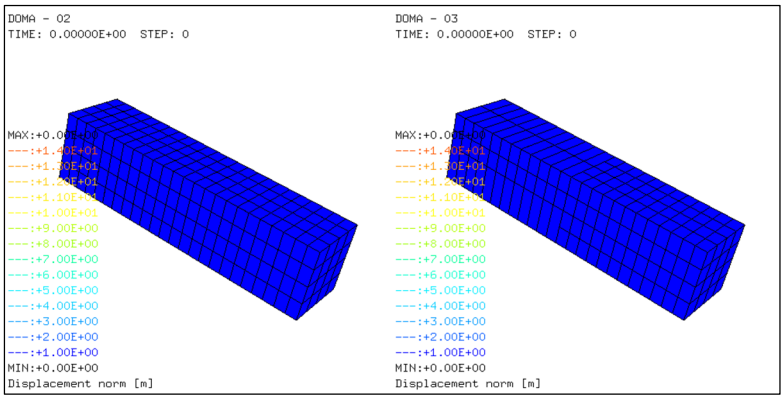

Reference Case (no decomposition)

Case with domain decomposition

183

Example 15 – Bar Impact Revisited

- Taylor bar impact test:

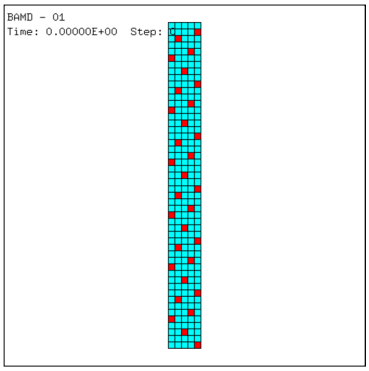

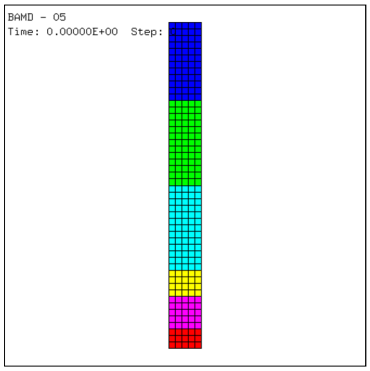

Reference Case (no decomposition)

Case with time step partitioning (OPTI PART)

Case with domain decomposition (colors indicate sub-domains)

184

Example 15 – Bar Impact Revisited (2)

- Displace-ments:

Case	Description	Time Steps	Time stations	CPU (s)
bamd01	Reference	59886	N/A	99.5
bamd03	OPTI PART	1165	N/A	13.3
bamd05	6 s/d, unequal size	1152	78948 [65246, 7545, 6218, 3265, 2303, 2303]	12.2

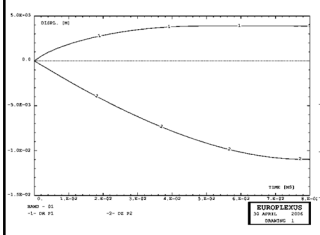

Reference Case (no decomposition)

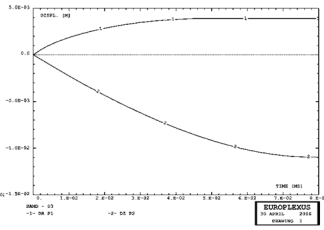

Case with time step partitioning (OPTI PART)

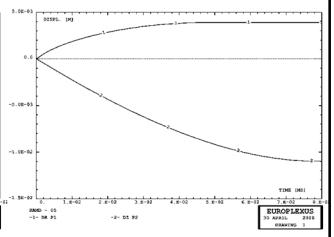

Case with domain decomposition

185

Example 15 – Bar Impact Revisited (3)

- Current yield stress (plastic strain):

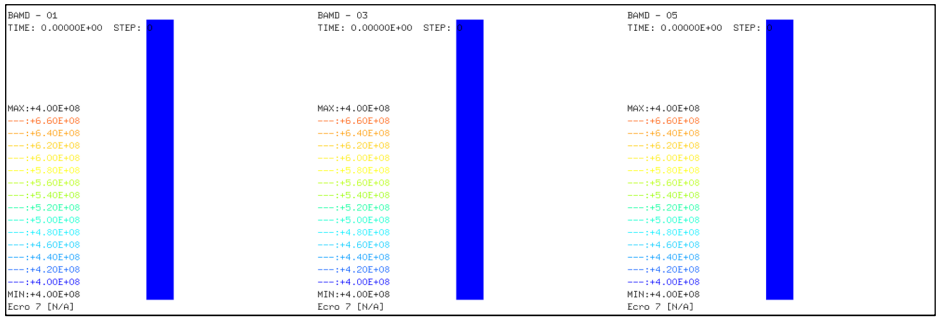

Reference Case (no decomposition)

Case with time step partitioning (OPTI PART)

Case with domain decomposition

186

Potential benefits of **Adaptivity**

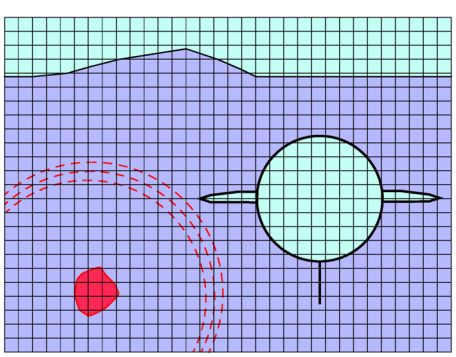

A) without adaptivity

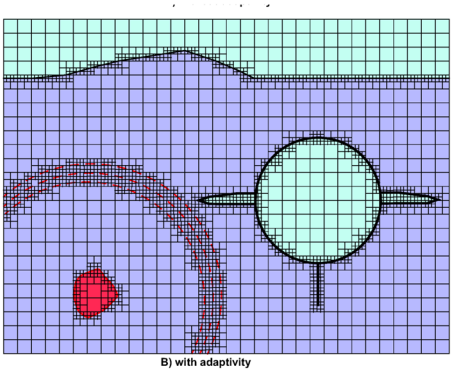

B) with adaptivity

Increase accuracy at :

- Wavefronts
- Material Interfaces (including FSI!!!)
- Free surfaces
- ...

187

Adaptivity : Element Splitting

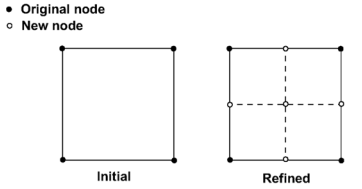

Figure 4 - Refinement of a quadrilateral in 2D

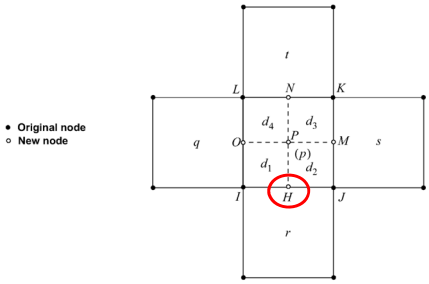

Figure 5 - Refinement of a quadrilateral in 2D with hanging nodes

- Chosen strategy for quadrilateral
- "Hanging" nodes

188

Adaptivity : Element Splitting (2)

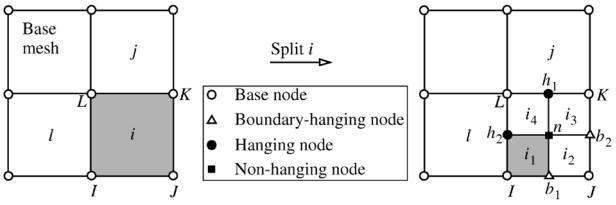

Fig. 1. Splitting a QUA4.

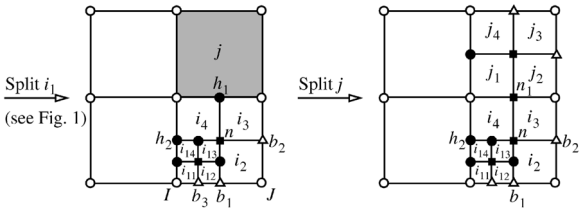

Fig. 2. Further splitting.

189

Adaptivity : Nodes Classification

Table 1. A classification of nodes.

Node type	Location	Classification	Interface
Base	Internal	—	—
	Boundary	—	—
Descendent	Internal	Non-hanging	Conforming
		Hanging	Non-conforming
	Boundary	Hanging (3D only)	Non-conforming (internally)
		B-hanging	—

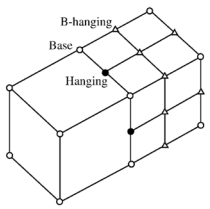

Example of hanging nodes on 3D boundary

190

Adaptivity : Data Structure

Challenge : EUROPLEXUS is a “fixed-memory” code

Solution : over-allocation (base mesh + extension), needs user-given dimensioning of extension zones

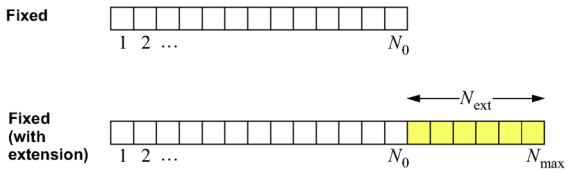

Figure 1 - Data structure without and with extension

191

Adaptivity : Data Structure (2)

- Tree-like organization of elements

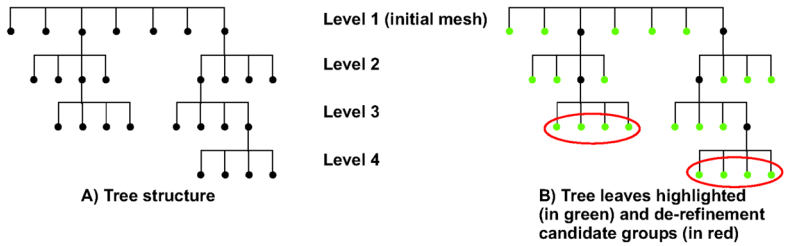

192

Adaptivity : Data Structure (3)

- Tree-like organization of elements

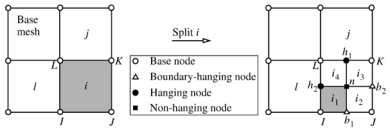

Fig. 1. Splitting a QUA4.

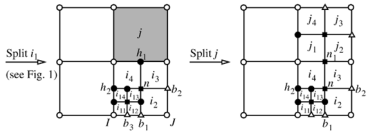

Fig. 2. Further splitting.

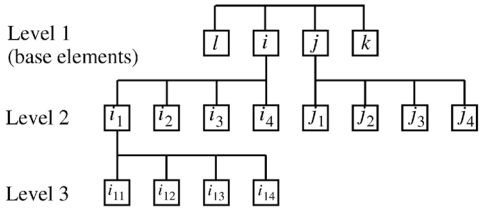

Fig. 3. Tree data structure for the elements.

193

Adaptivity : Boundary Conditions

1. Applied pressures : **automatic** if represented by CLxx element (split/unsplit **together** with companion element)
2. Essential BCs (LINKs, by Lagrange Multipliers) : simple strategy is to inherit the BCs (e.g. blockages) from **parent nodes**

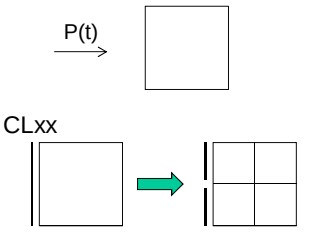

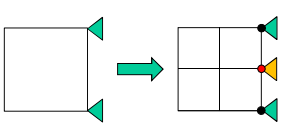

194

Example : wave in a slab

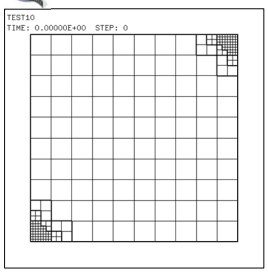

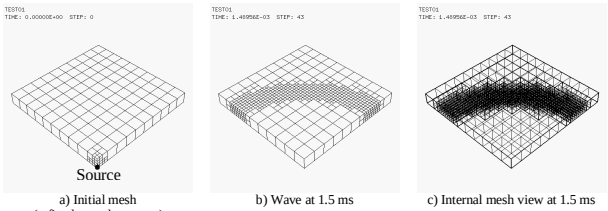

a) Initial mesh (refined near the source) | b) Wave at 1.5 ms | c) Internal mesh view at 1.5 ms

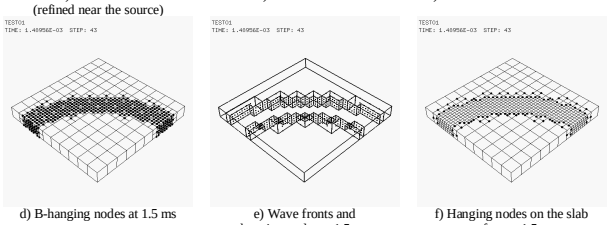

d) B-hanging nodes at 1.5 ms | e) Wave fronts and hanging nodes at 1.5 ms | f) Hanging nodes on the slab surface at 1.5 ms

Figure 9. Spherical wave propagating in a 3D slab.

2D *3D*

195

Wave in an elastic bar

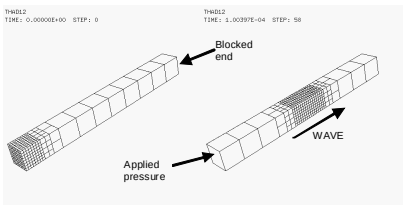

a) Initial mesh and adapted mesh at 10 µs

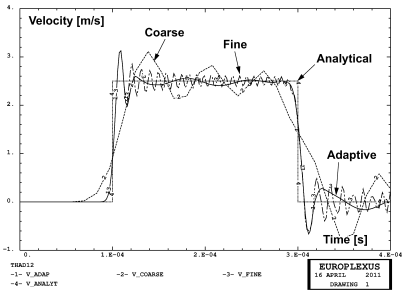

b) Comparison of velocities at bar mid-point

Figure 10. Plane step wave in an elastic bar.

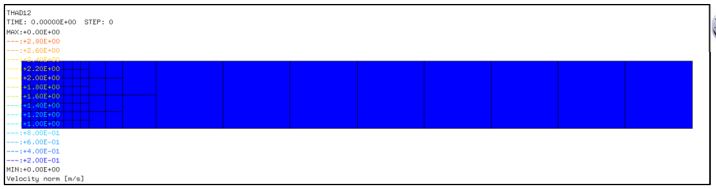

196

Adaptivity in fluids : transport

- Introduce concept of **p-neighbor** at non-conforming element-to-element interface

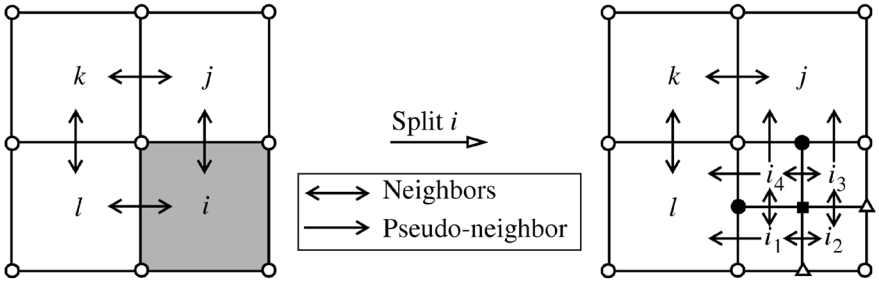

Fig. 4. Neighbors and pseudo-neighbors.

197

Shock tube : adaptive

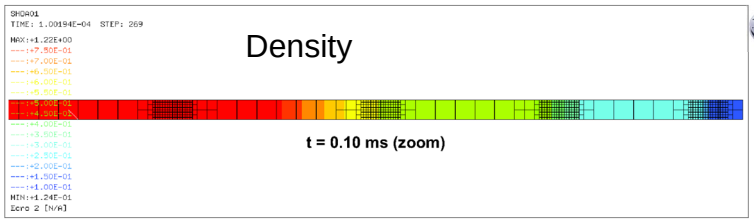

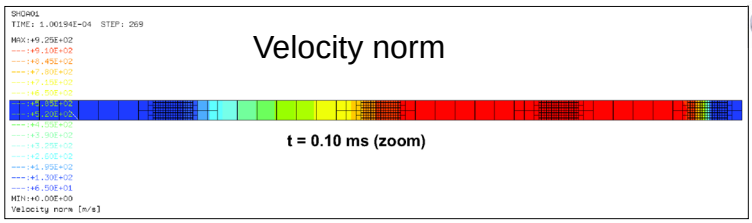

198

Shock tube

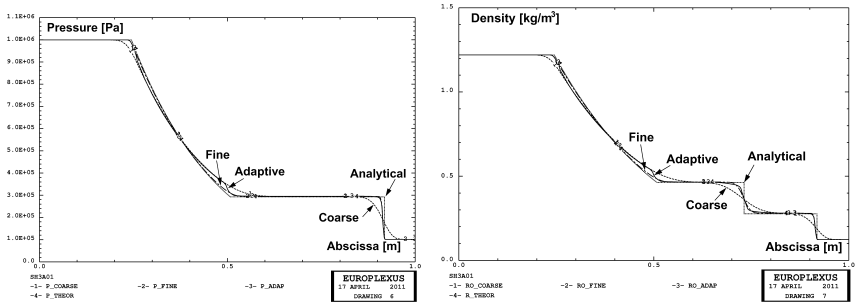

a) Pressure along the tube at 0.25 ms b) Density along the tube at 0.25 ms

Figure 11. Shock tube.

199

Shock tube : CPU

Name	Base mesh	Extensions	Wave(s)	Steps	CPU [s]	Elements * steps
SHOR01	100 FL24	—	—	122	0.34	12,300
SHOR02	200 FL24	—	—	238	0.37	47,800
SHOR03	400 FL24	—	—	471	1.00	188,800
SHOR04	800 FL24	—	—	937	3.42	750,400
SHOA00	6,400 Q41L	—	—	937	23.81	6,003,200
SHOA04	6,400 Q41L	—	—	937	23.52	6,003,200
SHOA01	100 Q41L	NPOI 669 NDDL 1338 FL24 760	4 PLAN MAXL 4 H1 0.015 H2 0.05	899	4.06	556,026
SHOA03	100 Q41L	NPOI 669 NDDL 1338 FL24 760	4 PLAN MAXL 4 H1 0.015 H2 0.05	901	4.09	557,291

Table 1 - Numerical solutions of the shock tube problem

200

Towards “real” ADAP : Error Indicators

- Work is ongoing on **curvature-** or **gradient-based error indicators** with various types of (**node-** or **element-based**) quantities :

*Error indicator based on **velocity curvature** only captures shock*

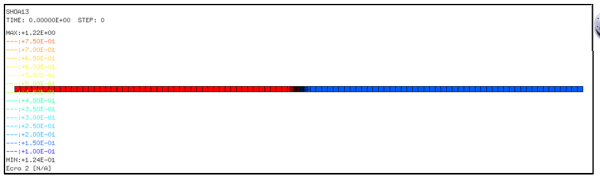

*Error indicator based on **density gradient** captures both shock and contact discontinuity*

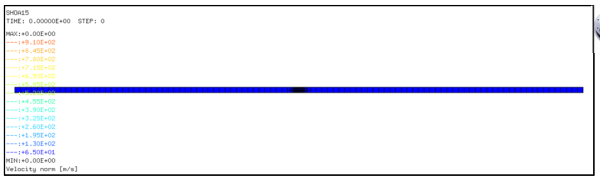

201

Example of “smart” use of ADAP

- Bomb explosion : ADAP is used to **initially refine** the bomb region. **After** bomb fragmentation and pressure wave expansion the fluid mesh is **unrefined** to increase computation efficiency!

Pressure

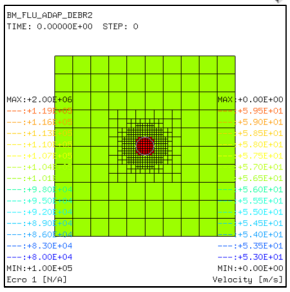

Compressed gas charge

Pressure

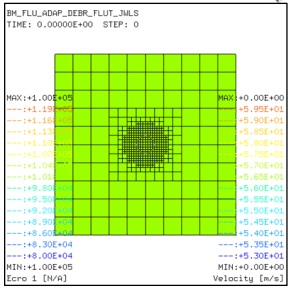

Solid explosive charge (JWLS)

Solid fraction

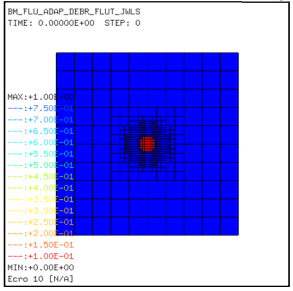

202

Perspectives for Fluids

- Continue development of CCFV models:
  - Improve source term for explosions : **detonation** / **deflagration** …
  - Chemistry
  - Combustion
  - Improve **multi-phase** flow (VOFIRE ?)
- Full Navier-Stokes (incompressible or quasi-) with **deformable** structures
  - PFEM ?

203

Perspectives for Solids / Structures)

- Improve damage and failure description:
  - Concrete (unreinforced / reinforced)
  - Glass
  - Composites
  - Soils and other geotechnical materials
  - Fracture mechanics (XFEM etc.)
  - Meshless methods (SPH etc.)
- Improve contact / impact and perforation:
  - DEM coupling with FE
  - “Generalized” pinball contact model

204

Perspectives for FSI

- Completion / improvement of FSI models battery (ongoing work):
  - Strong / Weak coupling
  - FE / FV (NC, CC) modeling of fluids
  - Conforming / non-conforming
  - "Embedded"-like techniques (FLSR, FLSW, …)
  - "Adaptivity" to increase accuracy of FLSR / FLSW
  - Combine ADAP with PART or/and S/D to increase calculation efficiency
- Towards fully automatic FSI (industrial production)
  - See example …

205

FLSW + Adaptivity + VOFIRE

- Towards fully automatic FSI (industrial production):
  - **Only structure** is modelled "intelligently"
  - Eulerian "background" fluid mesh (automatic, highly optimized) with **FLSR / FLSW** (very fine mesh locally to enhance precision)
  - **Adaptivity** of fluid mesh on **shock fronts** + **FS interface** + **PART**
  - **Multi-phase / multi-component** techniques (+ VOFIRE)

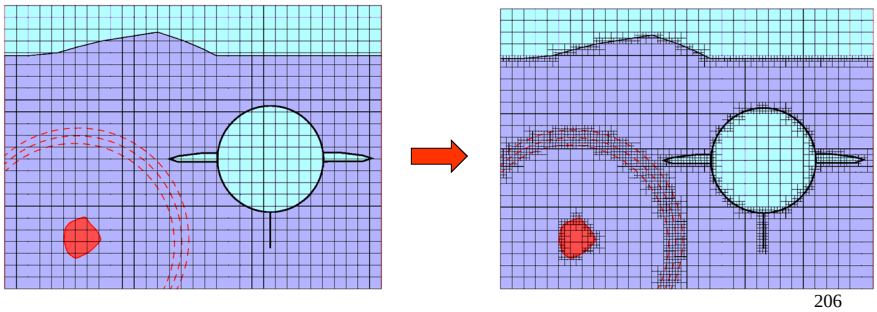

206